

**DIRECTED EVOLUTION AND CHARACTERISATION OF AN  
ANG2-SELECTIVE LIGAND TRAP**

Thesis submitted for the degree of  
Doctor of Philosophy  
at the University of Leicester

by

Teonchit Nuamchit

Department of Cardiovascular Sciences

University of Leicester

November 2014

Teonchit Nuamchit

**DIRECTED EVOLUTION AND CHARACTERISATION OF AN ANG2-  
SELECTIVE LIGAND TRAP**

**Abstract**

The angiopoietin (Ang) ligands and their Tie2 receptor play a role in vascular growth, maintenance of adult vasculature and vascular remodelling. Many studies showed that Ang1 ligand has a protective effect for controlling of vascular morphogenesis and homeostasis whereas excess Ang2 has more deleterious effect on the vascular system. Upregulated expression of Ang2 is associated with several pathologies such as inflammation and tumour angiogenesis, and blocking Ang2 with antibodies or using transgenic approaches has been shown to improve outcomes in preclinical models of these conditions. Ang2 inhibitors therefore have significant potential as therapeutics. Ligand traps are alternatives to antibodies for blocking the action of ligands. This study aims to use directed evolution to modify Tie2 extracellular domain to a form that selectively binds Ang2 binding, and test its ability to suppress Ang2-mediated effects. Such a selective ectodomain would be a candidate Ang2 ligand trap. Directed evolution was attempted using a method that combines in-cell mutagenesis, utilizing somatic hypermutation, with cell surface display. Despite several attempts evolution was not successful. However, an evolved ectodomain was produced by others. This evolved ectodomain was analysed for binding specificity, cellular, *in vivo* effects. The ectodomain was found to be selective for Ang2 binding, and unable to bind Ang1 and Ang4. Furthermore, the evolved ectodomain was found to inhibit the antagonistic and agonistic effects of Ang2 on endothelial cell Akt signalling. Studies were also found that the evolved ectodomain was able to inhibit endothelial cell migration in response to high concentrations of Ang2. Preliminary *in vivo* work showed that the ectodomain was able to block localized oedema in a mouse model of lipopolysaccharide-induced inflammation. These findings suggest the evolved ectodomain would be a good candidate for development into an Ang2-ligand-trap.

## **Acknowledgements**

First of all I am greatly indebted to my supervisor, Professor Nick Brindle for his constant guidance and encouragement. This thesis would not have been possible without his efforts.

I would like to thank the Brindle group for their technical assistance and understanding during this period of research. In particular, I must mention Kathryn Steele, Tariq Tahir, Harprit Singh, Djalil Baiou and Nisha Patel.

I would like to express my gratitude to my sponsor, Thai government, for giving me a great opportunity to study in the UK, my colleagues in Faculty of Allied Health Sciences, Naresuan University, and my friends who always support me.

Finally, I would like to thank my family and my best friend for supporting and understanding me throughout my study.

# List of Contents

## Contents

<b>ABSTRACT .....</b>	<b>II</b>
<b>ACKNOWLEDGEMENTS.....</b>	<b>III</b>
<b>LIST OF CONTENTS.....</b>	<b>IV</b>
<b>LIST OF FIGURES .....</b>	<b>VIII</b>
<b>LIST OF TABLES .....</b>	<b>XI</b>
<b>LIST OF ABBREVIATIONS.....</b>	<b>XII</b>
<b>CHAPTER 1: INTRODUCTION .....</b>	<b>1</b>
1.1 ANGIOPOIETIN-TIE SYSTEM .....	1
1.1.1 <i>Tie</i> receptors .....	1
1.1.2 <i>Angiopoietin</i> Family.....	4
1.1.3 <i>Angiopoietin–Tie</i> interaction.....	5
1.1.4 <i>Ang1</i> effects .....	9
1.1.5 <i>Angiopoietin2</i> in pathology.....	12
1.1.6 <i>Ang2</i> and <i>Integrins</i> .....	14
1.2 LIGAND TRAPS.....	16
1.2.1 <i>Protein Engineering</i> .....	16
1.2.2 <i>Somatic Hypermutation</i> .....	20
1.2.3 <i>Cell Surface Display</i> .....	24
1.3 AIMS AND HYPOTHESES.....	24
<b>CHAPTER 2: MATERIALS AND METHOD.....</b>	<b>26</b>
2.1 MATERIALS .....	26
2.1.1 <i>Buffers</i> .....	26
2.1.3 <i>Commercial Kits</i> .....	27
2.1.2 <i>Culture media</i> .....	28
2.2 PREPARATION & STORAGE OF PLASMID DNA.....	29
2.2.1 <i>Total RNA isolation (RNeasy Minikit, Qiagen)</i> .....	29
2.2.2 <i>Genomic DNA isolation sorted DT40 cells (Generation Capture Column Kit, Qiagen)</i> .....	29
2.2.3 <i>NEB Turbo Competent E. coli (New England Biolabs)</i> .....	29
2.2.4 <i>Transformation of TOP10 chemically competent cells (Invitrogen)</i> .....	30

2.2.5 Plasmid DNA preparation: Miniprep (Qiagen).....	30
2.2.6 Plasmid DNA preparation: Maxiprep (Qiagen).....	30
2.2.7 DNA quantification: absorbance.....	31
2.2.8 Agarose gel electrophoresis.....	31
2.2.9 Purification of DNA: gel extraction .....	32
2.2.10 Purification of DNA: chloroform phenol extraction .....	32
2.2.11 Purification of DNA: ethanol precipitation .....	32
2.2.12 Glycerol stocks.....	33
<b>2.3 PCR &amp; CLONING .....</b>	<b>33</b>
2.3.1 PCR: plasmid DNA.....	33
2.3.2 Reverse transcription .....	34
2.3.3 TA cloning for sequencing (TOPO TA cloning®Kit for sequencing Invitrogen) .....	34
2.3.4 TA cloning into the PEF6/V5 His TOPO® expression vector.....	35
2.3.5 Site directed mutagenesis to produce introduce F/I mutation.....	35
2.3.6 Site directed mutagenesis to produce RH mutation.....	35
2.3.7 Restriction digestion of DNA .....	36
2.3.8 Sequencing .....	36
<b>2.4 CELL CULTURE, TRANSFECTION AND PROTEIN PRODUCTION.....</b>	<b>36</b>
2.4.1 Tie expressing DT40 cells and Culture .....	36
2.4.2 Stable non-targeted transfection of DT40 cells.....	37
2.4.3 Freezing and storage of DT40 cells .....	37
2.4.4 Chinese Hamster Ovary cells (CHO) .....	38
2.4.5 Transfection for CHO cell line by Lipofectamine.....	38
2.4.6 Culture of HUVEC .....	38
2.4.7 Culture of EA.hy926 cells.....	39
2.4.8 Culture of HEK293 cells .....	39
<b>2.5 PROTEIN PRODUCTION.....</b>	<b>40</b>
2.5.1 Expression of Soluble Ectodomains.....	40
2.5.2 Large-scale transient transfection of HEK 293 cells for protein production .....	40
2.5.3 Protein Purification .....	40
2.5.4 Exchanging the elution buffer.....	41
2.5.5 Bradford assay for Protein quantification .....	41
<b>2.6 ANALYSIS OF ANG1 ANG2 AND ANG4 BINDING TO WILD-TYPE OR EVOLVED ECTODOMAIN-FC BY BIOLAYER INTERFEROMETRY.....</b>	<b>41</b>
<b>2.7 BINDING ASSAYS .....</b>	<b>42</b>
<b>2.8 PROTEIN .....</b>	<b>42</b>
2.8.1 Preparation of whole cell lysates for SDS-PAGE.....	42
2.8.2 SDS-polyacrylamide gel electrophoresis (PAGE).....	43
2.8.3 Western blotting .....	43

2.8.4 Immunoblotting.....	44
2.8.5 Cellular Assays.....	44
2.8.6 ImageJ analysis.....	46
2.8.7 Immunoprecipitation: Ang2 integrin binding Western blot analysis in a cell-free system.....	46
2.9 MIGRATION ASSAY .....	46
2.10 FLOW CYTOMETRY & FLORESCENCE ACTIVATED CELL SORTING (FACS).....	47
2.10.1 Binding and fluorescent cell labelling reagents.....	47
2.10.2 On-cell binding and labelling procedure.....	47
2.10.3 Flow cytometry .....	47
2.10.4 Competitive equilibrium Ang1 and Ang2.....	48
2.10.5 Fluorescence Activated Cell Sorting (FACS).....	48
2.11 METHOD FOR IN VIVO EXPERIMENTS .....	50
<b>CHAPTER 3: EVOLUTION OF TIE2 ECTODOMAIN .....</b>	<b>51</b>
3.1 ESTABLISHING FACS.....	51
3.2 DNA RECOVERY AND SEQUENCING FROM SORTED CELLS.....	58
3.3 CLONING AND EXPRESSION OF AID IN THE CELLS TO MAXIMIZE MUTATIONS.....	60
3.4 AID TRANSFECTION INTO TIE2-DT40 CELLS .....	64
3.5 SELECTION OF TIE2-DT40 FOR PREFERENTIAL ANG2 BINDING .....	69
3.6 ITERATIVE SORTS TO SELECT FOR PREFERENTIAL ANG2 BINDING .....	71
3.7 DISCUSSION.....	73
<b>CHAPTER 4: CHARACTERISATION OF EVOLVED ECTODOMAIN .....</b>	<b>77</b>
4.1 EXPRESSION OF SOLUBLE WILD-TYPE AND R3 ECTODOMAIN IN HEK293 CELLS .....	79
4.2 BINDING KINETICS OF THE R3-Fc AND Wt-Fc ECTODOMAIN TO ANG1 AND ANG2 .....	81
4.3 QUANTITATIVE ANALYSIS OF BINDING OF THE EVOLVED AND WILD-TYPE ECTODOMAIN TO ANG1 AND ANG2 USING ELISA.....	87
4.4 QUANTITATIVE ANALYSIS OF BINDING OF THE F161I SUBSTITUTION AND DOUBLE R167, H168 DELETION TO ANG1 AND ANG2 USING ELISA .....	87
4.5 EFFECT OF EVOLVED ECTODOMAIN ON ANGIOPOIETINS SIGNALLING IN ENDOTHELIAL CELLS .....	93
4.6 EFFECT OF EVOLVED ECTODOMAIN ON ENDOTHELIAL FUNCTION REGULATED BY ANGIOPOIETIN .....	98

4.7 DISCUSSION.....	101
<b>CHAPTER 5: MODIFICATION OF R3, INTEGRIN BINDING AND <i>IN VIVO</i> ACTIVITY.....</b>	<b>104</b>
5.1 DECREASING R3 SIZE.....	104
5.2 THE EFFECTS OF R3 ON ANG2 INTEGRIN BINDING.....	105
5.2.1 <i>Effects of pH on ectodomain Ang2 binding</i> .....	107
5.2.2 <i>Ang2 integrin binding</i> .....	107
5.3 TEST OF R3 ACTIVITY <i>IN VIVO</i> .....	116
5.3.1 <i>Effects on local oedema</i> .....	116
5.3.2 <i>Effects on Factor B</i> .....	121
5.3.3 <i>Effects on Mast cell degranulation</i> .....	121
5.4 DISCUSSION.....	127
5.4.1 <i>Producing 1-210 R3</i> .....	127
5.4.2 <i>Ang2 integrin binding</i> .....	127
5.4.3 <i>In vivo activity studies</i> .....	129
<b>CHAPTER 6: GENERAL DISCUSSION.....</b>	<b>132</b>
6.1 EVOLUTION OF TIE2 ECTODOMAIN.....	132
6.2 CHARACTERISATION OF EVOLVED TIE2 ECTODOMAIN.....	133
6.3 MODIFICATION OF R3, INTEGRIN BINDING AND <i>IN VIVO</i> ACTIVITY.....	135
6.3.1 <i>Decreasing R3 size</i> .....	135
6.3.2 <i>Ang2 integrin binding</i> .....	136
6.3.3 <i>In vivo activities study</i> .....	137
6.4 CONCLUSION.....	138
<b>APPENDICES.....</b>	<b>139</b>
<b>BIBLIOGRAPHY.....</b>	<b>151</b>

## List of Figures

FIGURE 1.1 TIE RECEPTORS AND ANGIOPOIETINS.....	3
FIGURE 1.2 ANGIOPOIETIN-TIE SYSTEM.....	6
FIGURE 1.3 CRYSTAL STRUCTURE OF THE ANG2–TIE2 BINDING INTERACTION.....	7
FIGURE 1.4 TIE2 SIGNAL TRANSDUCTION .....	11
FIGURE 1.5 DIRECTED EVOLUTION .....	19
FIGURE 1.6 THE ROLE OF ACTIVATION-INDUCED CYTIDINE DEAMINASE (AID) IN SOMATIC HYPERMUTATION (SHM) .....	23
FIGURE 3.1 REPRESENTATIVE DOT PLOT SHOWING THE POPULATION OF LIVE CELLS IN THE SQUARE P1.....	53
FIGURE 3.2 REPRESENTATIVE DOT PLOT SHOWING THE SIGNAL FOR FLAG AND ANG2 IN UNSTAINED CELLS.....	54
FIGURE 3.3 REPRESENTATIVE DOT PLOT SHOWING THE SINGLE STAINED CONTROL...	54
FIGURE 3.4 DUAL STAINING DOT PLOTS SHOWING THE SIGNAL OF ANGIOPOIETIN2 BINDING CELL SURFACE EXPRESSED TIE2 ECTODOMAIN.....	55
FIGURE 3.5 DOT PLOT AND HISTOGRAM COMPARING THE FLUORESCENCE SIGNAL OF STREPTAVIDIN-PE/CY5 BETWEEN CELLS INCUBATED BIOTINYLATED-ANG2 AND CELLS WITHOUT ANG2. ....	57
FIGURE 3.6 DUAL STAINING DOT PLOTS SHOWING THE SORTED CELLS.....	59
FIGURE 3.7 SCHEMATIC DEPICTING CLONING STRATEGY OF HUMAN AID INTO PEF6/V5-HIS-TOPO®.....	61
FIGURE 3.8 RESTRICTION DIGEST FOR AID POSITIVE CLONE. ....	62
FIGURE 3.9 EXPRESSION OF AID IN CHO CELLS.....	63
FIGURE 3.10 LINEARISATION OF AID-BLAST <sup>R</sup> -TOPO.....	65
FIGURE 3.11 ELECTROPORATED CIRCULAR AND LINEARISED TRANSFECTION OF THE AID IN DT40 EXPRESSING TIE2 CELL LINE.....	67
FIGURE 3.12 ELECTROPORATED CIRCULAR TRANSFECTION OF THE AID IN DT40 EXPRESSING TIE2 CELL LINE.....	68
FIGURE 3.13 COMPETITIVE EQUILIBRIUM OF ANG1 VERSUS ANG2.....	70
FIGURE 3.14 SORTING FOR HIGH AFFINITY ANG2 BINDERS.....	72
FIGURE 4.1 THREE AMINO ACID CHANGES SWITCH BINDING SPECIFICITY OF TIE2.....	78
FIGURE 4.2 COOMASSIE STAINED SDS GEL OF R3 ELUATE FROM NICKEL COLUMN. ..	80
FIGURE 4.3 WESTERN BLOT OF R3-FC PROBED FOR TIE2. ....	80

FIGURE 4.4 SENSORGRAM FOR BINDING OF ANG1 TO THE WT-Fc MEASURED BY BLI. .....	82
FIGURE 4.5 SENSORGRAM FOR BINDING OF ANG1 TO THE R3-Fc MEASURED BY BLI. .....	83
FIGURE 4.6 SENSORGRAM FOR BINDING OF ANG2 TO THE WT-Fc MEASURED BY BLI. .....	84
FIGURE 4.7 SENSORGRAM FOR BINDING OF ANG2 TO THE R3-Fc MEASURED BY BLI. .....	85
FIGURE 4.8 SENSORGRAM FOR BINDING OF ANG4 TO THE R3-Fc AND WT-Fc MEASURED BY BLI.....	86
FIGURE 4.9 BINDING OF WT-Fc AND R3-Fc TO ANG1. ....	88
FIGURE 4.10 BINDING OF WT-Fc AND R3-Fc TO ANG2. ....	89
FIGURE 4.11 BINDING OF F/I AND $\Delta$ RH MUTANTS TO ANG1.....	90
FIGURE 4.12 BINDING OF F/I AND $\Delta$ RH MUTANTS TO ANG2.....	91
FIGURE 4.13 EVOLVED ECTODOMAIN BLOCKS THE ANTAGONISTIC EFFECTS OF ANG2 IN THE ENDOTHELIAL CELLS LINE EA.HY926. ....	94
FIGURE 4.14 EVOLVED ECTODOMAIN BLOCKS THE ANTAGONISTIC EFFECTS OF ANG2 IN HUVECS. ....	95
FIGURE 4.15 EVOLVED ECTODOMAIN BLOCKS THE AGONISTIC EFFECTS OF ANG2 IN HUVECS. ....	96
FIGURE 4.16 EFFECT OF R3-Fc AND WT-Fc ON ANG1-ACTIVATION OF AKT PHOSPHORYLATION IN HUVECS. ....	97
FIGURE 4.17 EFFECT OF EVOLVED ECTODOMAIN ON MIGRATION INDUCED BY ANGIOPOIETINS IN THE ENDOTHELIAL CELLS LINE EA.HY926. ....	99
FIGURE 4.18 EXAMPLE OF EFFECTS OF EVOLVED ECTODOMAIN ON MIGRATION INDUCED BY ANGIOPOIETINS IN THE ENDOTHELIAL CELLS LINE EA.HY926.....	100
FIGURE 5.1 COOMASSIE STAINED SDS GELS OF PROTEIN FRACTION OF SOLUBLE R3- 210. ....	106
FIGURE 5.2 BLOT EXPRESSIONS OF PROTEIN FRACTION OF SOLUBLE R3-210 PROBED FOR TIE2.....	106
FIGURE 5.3 THE ABILITY OF R3 TO BIND ANG2 IN PH 4.5 AND PH 7.5.....	108
FIGURE 5.4 THE ABILITY OF ANG2 TO BIND AVB3 INTEGRIN IN PH 7.5. ....	110
FIGURE 5.5 THE ABILITY OF ANG2 TO BIND AVB3 INTEGRIN IN PH 4.5. ....	111

FIGURE 5.6 THE ABILITY OF ANG2 TO BIND AVB3 INTEGRIN IN IMMUNOPRECIPITATION ASSAY FOR ANG2 IN A CELL-FREE SYSTEM.....	112
FIGURE 5.7 THE ABILITY OF ANG2 TO BIND AVB3 INTEGRIN IN IMMUNOPRECIPITATION ASSAY FOR AVB3 INTEGRIN IN A CELL-FREE SYSTEM. ....	114
FIGURE 5.8 THE ABILITY OF ANG2 TO BIND AVB3 INTEGRIN IN IMMUNOPRECIPITATION ASSAY FOR AVB3 INTEGRIN IN A CELL-FREE SYSTEM. ....	115
FIGURE 5.9 EXAMPLES OF MEASUREMENT OF SUBCUTIS THICKNESS IN VARIOUS MICE HOCK SECTIONS. ....	117
FIGURE 5.10 QUANTITATIVE ANALYSIS OF LOCAL OEDEMA FORMATION IN MICE AFTER 1 HOUR INJECTION. ....	118
FIGURE 5.11 QUANTITATIVE ANALYSIS OF LOCAL OEDEMA FORMATION IN MICE AFTER 2 HOUR INJECTION. ....	119
FIGURE 5.12 EVOLVED ECTODOMAIN SUPPRESSES LOCALIZED OEDEMA IN VIVO. ....	120
FIGURE 5.13 THE ABILITY OF R3-Fc FOR INHIBITING COMPLEMENTS FACTOR B THAT WAS ACTIVATED BY LPS. ....	122
FIGURE 5.14 SECTION OF HISTOLOGICAL ANALYSIS OF MAST CELLS.....	123
FIGURE 5.15 SECTION OF HISTOLOGICAL ANALYSIS FOR NEUTROPHILS.....	123

## List of Tables

TABLE 2.1 PCR REACTION COMPONENTS FOR 50 $\mu$ L REACTION VOLUME .....	33
TABLE 2.2 PCR CONDITION .....	34
TABLE 2.3 SDS-PAGE COMPOSITION.....	43
TABLE 2.4 DETAILS OF CONDITIONS USED FOR SPECIFIC ANTIBODIES IN WESTERN BLOTTING .....	45
TABLE 2.5 FLUORESCENCE SPECTRA .....	48
TABLE 2.6 ANTIBODIES USED FOR FACS.....	49
TABLE 3.1 FLUORESCENCE INTENSITY BY ANG2 CONCENTRATION .....	51
TABLE 4.1 RELATIVE BINDING OF ECTODOMAIN MUTANTS .....	92
TABLE 5.1 THE PERCENTAGE OF DEGRANULATED MAST CELLS RELATE TO THE TREATMENT (R3) FOR THE ONE-HOUR GROUP.....	125
TABLE 5.2 THE PERCENTAGE OF DEGRANULATED MAST CELLS RELATE TO THE TREATMENT (R3) FOR THE TWO-HOUR GROUP. ....	126

## List of Abbreviations

A	Adenine
AAV	Adeno-associated virus
AHC	Anti-hlgG Fc Capture
AID	Activation induced cytidine deaminase
Alpha-MEM	Alpha-Minimum essential medium
AMPK	5' AMP-activated protein kinase
Ang	Angiopoietin
ANOVA	Analysis of variance
APS	Ammonium persulphate
ARDS	Adult respiratory distress syndrome
Arg	Arginine
BBB	Blood brain barrier
BER	Base excision repair
BLI	Bio layer interferometry
bp	Base pair
BSA	Bovine serum albumin
C	Cytosine
CAM	Chorioallantoic membrane assay
cDNA	complementary DNA
CHO	Chinese hamster ovary
CMV	Cytomegalovirus
CPD	Computational protein design
CSR	Class switch recombination
C-terminus	Carboxy-terminus
dC	deoxycytidine
ddH <sub>2</sub> O	Double-distilled water
DEPC	Diethyl pyrocarbonate
DMEM	Dulbecco's modified eagle medium
DMSO	Dimethyl sulfoxide
DNA	Deoxyribonucleic acid
dNTP	Deoxyribonucleotide
Dok-R	Docking protein

dsDNA	Double-stranded DNA
DTT	Dithiothreitol
EB	Elution buffer
E.coli	Escherichia coli
ECD	Extracellular domain
ECL	Electrogenerated chemiluminescence
ECM	Extracellular matrix
ECs	Endothelial cells
EDTA	Ethylenediaminetetraacetic acid
eEF1 $\alpha$	Eukaryotic translation elongation factor 1 $\alpha$
EGF	Epidermal growth factor
eGFP	enhanced green fluorescent protein
EGTA	Ethylene glycol tetraacetic acid
ELISA	Enzyme linked immunosorbent assay
Erk	Extracellular-signal-regulated kinases
eNOS	Endothelial nitric oxide synthase
Exo 1	Exonuclease 1
F	Phenylalanine
FACS	Fluorescence activated cell sorting
FAK	Focal adhesion kinase
Fc	Fragment crystallizable
FCS	Foetal calf serum
FITC	Fluorescein isothiocyanate
FN	Fibronectin
FOXO	Forkhead transcription factor
FSC	Forward scatter
Fv	Antibody variable domain
G	Guanine
GFP	Green fluorescence protein
GC	Gene conversion
GRB2	growth factor receptor-bound protein 2
GTP	Guanosine-5'-triphosphate
H	Histidine

HEK	Human embryonic kidney
HRP	Horseradish peroxidase
HUVEC	Human umbilical vascular endothelial cell
I	Isoleucine
ICAM	Intercellular adhesion molecule
Ig	Immunoglobulin
Ile	Isoleucine
ILK	Integrin-linked kinase
<i>K<sub>d</sub></i>	Dissociation constant
kDa	Kilo Dalton
LB	Luria Bertani
LPS	Lipopolysaccharide
LMW	Low molecular weight
MAPK	Mitogen-activated protein kinase
MFI	Mean Fluorescence intensity
MMR	Mismatch Repair
MMLV-RT	Moloney Murine Leukemia Virus Reverse Transcriptase
mRFP	Monomeric red fluorescence protein
mRNA	Messenger ribonucleic acid
MSH	MutS homologue
MSH2	MutS homolog 2
MSH6	MutS homolog 6
Nck	Non-catalytic region of tyrosine kinase adaptor protein 1
NF- $\kappa$ B	Nuclear factor- $\kappa$ B
Ni-NTA	Nitrilotriacetic acid
N-terminus	Amino-terminus
OD	Optical density
PAGE	Polyacrylamide gel electrophoresis
Pak	P21-activating kinase
PBS	Phosphate Buffer Saline
PCAM	Platelet endothelial cell adhesion molecule

PCR	Polymerase chain reaction
PDGF	Platelet derive growth factor
PE	Phycoerythrin
PE/Cy5	Phycoerythrin/Cy5
PEI	Polyethylenimine
Phe	Phenylalanine
PKB	Protein kinase B
PNCL	Protein and Nucleic Acid Chemistry Laboratory
PI3K	Phosphatidyl-inositol-3 kinase
R	Arginine
Ras	Rat sarcoma
RasGAP	Ras GTPase activating protein
RFP	Red fluorescence protein
RNA	Ribonucleic acid
RT	Room temperature
RT-PCR	Reverse transcriptase polymerase chain reaction
RTKs	Receptor tyrosine kinases
SDS	Sodium dodecyl sulphate
SD	Standard deviation
SEM	Standard error of mean
SHM	Somatic hypermutation
SOC	Super optimal broth with catabolite repression
SPR	Surface plasmon resonance
SSC	Side scatter
ssDNA	Single strand DNA
T	Thymine
TAE	Tris-acetate-EDTA
TBS	Tris-buffered saline
TE	Trypsin –EDTA
TEM	Tie2 expressing monocyte
TEMED	Tetramethylethylenediamine
Tie	Tyrosine kinase with immunoglobulin-like and EGF-like domain
TNF	Tumour necrosis factor

U	Uracil
UNG	Urasil DNA-glycosylase
VCAM	Vascular cell adhesion molecule
VEGF	Vascular endothelial growth factor
WinMDI	Windows multiple document interafce for flow cytometry
Wt	Wild-type

## **Chapter 1: Introduction**

The Tie family are one of two family of receptor tyrosine kinases (RTKs) expressed mainly in endothelial cells and the receptors plays a pivotal role in controlling vascular stability, maturation, remodelling and endothelial cell survival (Augustin et al., 2009, Yuan et al., 2009). Tie family receptor tyrosine kinases, comprising Tie1 and Tie2, are principally expressed on endothelial cells and early haematopoietic cells (Puri and Bernstein, 2003). The angiopoietins (Ang) are a family of growth factor ligands that activate the Tie2 receptor. Ang1 and Ang2 are characterised as agonist and antagonist ligand of Tie2, respectively (Davis et al., 1996, Maisonpierre et al., 1997) that bind to the Tie2 receptor and activate a range of signalling pathways (Bogdanovic et al., 2006). Tie receptors and the angiopoietins are involved in several disease processes, such as cardiovascular disease and tumour angiogenesis (Chong et al., 2004). Many studies showed that excess Tie2 signalling as well as the loss of Tie2 function have deleterious effect on the vascular system (Thomas and Augustin, 2009).

### **1.1 Angiopoietin-Tie System**

#### ***1.1.1 Tie receptors***

Tie1 is an orphan endothelial receptor that is expressed on endothelial cells (Partanen et al., 1992, Dumont et al., 1992, Sato et al., 1993, Maisonpierre et al., 1993). Tie1 and Tie2 form heteromeric complexes on the cell surface (Marron et al., 2000, Marron et al., 2007, Hansen et al., 2010, Seegar et al., 2010). Tie1 occludes the ligand binding site on Tie2 when the receptors are complexed, thereby inhibiting Tie2-driven signalling and endothelial survival (Marron et al., 2007, Yuan et al., 2007). Ang1 is able to disrupt the Tie1-Tie2 complex, resulting in Tie2 activation, whereas Ang2 has no effect on that the Tie1-Tie2 complex (Hansen et al., 2010, Seegar et al., 2010). Although Tie1 is required for embryonic vessel development, it is not essential for the maintenance of vascular integrity in adult vasculature (Puri et al., 1995). Under pathological conditions,

Tie1 expression is often increased (Kaipainen et al., 1994). A study of Tie1 expression showed that Tie1 attenuation could decrease atherosclerosis progression in a dose dependent under circumstance of shear stress (Woo and Baldwin, 2011).

Tie2 is expressed on endothelial cells and non-endothelial cells both in normal tissue and diseases including tumour cells, fibroblast, monocytes and synovial lining cells (Makinde and Agrawal, 2008). Ang1 and Ang2 are able to bind Tie2 in a very similar manner (Yu et al., 2013). The Tie2 receptor tyrosine kinase has a role in maintenance of adult vasculature and maturation of embryonic vasculature (Peters et al., 2004). Mice lacking either Ang1 or Tie2 show embryonic lethality due to defect of cardiovascular system development (Felmeden et al., 2003).

Tie1 and Tie2 receptors are highly conserved in their amino-acid sequences. There is 76% amino acid identity overall, but only 33% in the extracellular domain (Schnurch and Risau, 1993). The extracellular domain of both receptors is composed of two immunoglobulin (Ig)-like domains, three tandem epidermal growth factor (EGF)-like modules, a third immunoglobulin and three fibronectin type III (FNIII) repeats. The intracellular domain contains a tyrosine kinase domain, which is split by a kinase insert sequence, and followed by the carboxy-terminal tail (Dumont et al. 1992, Barton et al. 2006) (Figure 1.1). The Ang-binding site of Tie2 is located on the N-terminal pair of Ig-like domains, predominantly in the second Ig-like domain (Macdonald et al., 2006).

**Figure removed for copyright reasons**

**Figure 1.1 Tie receptors and Angiopoietins**

Schematic diagram depicting structure of Tie receptors and angiopoietins (Huang *et al.*, 2010).

### **1.1.2 Angiopoietin Family**

Angiopoietins are ligands for receptor tyrosine kinase Tie2 which are required for controlling vascular morphogenesis and homeostasis (Thomas and Augustin, 2009). To date, four angiopoietins, Ang1, Ang2, Ang3 and Ang4, have been identified. Ang3 is identified as the mouse ortholog of human Ang4 and antagonist of Tie2 (Valenzuela et al., 1999). Unlike Ang3, Ang4 has been identified as agonist of Tie2 (Lee et al., 2004). However, the biological roles of Ang3 and Ang4 are still unclear and require further elucidation. Since Ang1 and Ang2 are the best characterised among the angiopoietin family, this review will focus on Tie2 receptor and their ligands Ang1 and Ang2.

Ang1 and Ang2 share approximately 60% amino acid sequence similarity (Davis et al., 1996, Maisonpierre et al., 1997). They also share a similar structure and the same binding domain for the Tie2 receptor. Their structures comprise an amino-terminal superclustering domain that is responsible for forming higher order multimers of ligands, a coiled-coil domain that mediates dimerization, a short linker peptide and a carboxy-terminal fibrinogen-like domain which contains a so-called P domain that acts as the receptor recognition for Tie2 binding (Figure 1.1). The P domain contains a calcium binding site (Barton et al., 2005, Macdonald et al., 2006).

Ang1 contains 498 amino acids and is a secreted 70 kDa glycoprotein (Davis et al., 1996). It is produced constitutively by smooth muscle cells and pericytes at a low level in healthy adults (Augustin et al., 2009). Ang1 is essential for controlling vascular quiescence (Fiedler and Augustin, 2006) and maintaining resting endothelial cells, anti-plasma leakage, anti-thrombotic effects and inhibiting vascular inflammation (Brindle et al., 2006).

Ang2 is a secreted protein containing 480 amino acid residues and mainly produced by endothelial cells where it is stored in Weibel-Palade bodies (Augustin et al., 2009). There are numerous substances which induce the secretion of Ang2 from Weibel-Palade bodies in seconds to minutes, including hypoxia, shear stress, thrombin and VEGF (Fiedler and Augustin, 2006, Dixit et

al., 2008). It has been reported the up-regulated Ang2 expression serves as the initiation of inflammation, resulting in the recruitment of myeloid cells to activate inflammation (Kim and Koh, 2011).

Ang2 is a partial agonist for Tie2 (Bogdanovic et al. 2006, Yuan et al. 2009). Ang2 counteracts Ang-1/Tie2 signalling by displacing binding of Ang1 for Tie2. In contrast, high concentration of Ang2 can act as a Tie2 agonist when in the absence of Ang1 (Yuan et al., 2009) or with prolonged exposure of endothelial cells to the ligands (Maisonpierre et al., 1997). However, the mechanisms of the paradoxical agonist activity of Ang2 depending on local condition remain unclear and require to further define in the future (Hashimoto and Pittet, 2006).

### ***1.1.3 Angiopoietin–Tie interaction***

Angiopoietin ligand-receptor interaction of the Ang-Tie family are shown in Figure 1.2.

Crystal structure analysis of the Ang2-Tie2 interaction indicates that the Tie2 ectodomain beyond residues 210 or the first two Ig-like domains are sufficient for angiopoietin binding (Macdonald et al., 2006). The Tie2 Ig2 domain is the only part of Tie2 that contacts Ang2 during binding (Barton et al., 2006) (Figure 1.3). Ang2 binds at the tip of arrowhead-shaped Tie2 (Barton et al., 2006). The arrowhead-shaped structure of Tie2 contains the Ig and EGF-like domain folded together into a compact structure (Barton et al., 2006). The structure of the Ang2-Tie2 complex displays an elongated shape with overall dimension of 130 Å 65 Å 50 Å (Barton et al., 2006). The C terminus of Ang2 binds the N terminus of Tie2 without major conformational changes or domain rearrangement in either receptor or ligand. Ang2 recognizing Tie2 receptor utilizes lock and key mechanism via the best-fit in shape and chemical recognition. Thus Ang2-Tie2 recognition is similar to the antigen-antibody interaction.

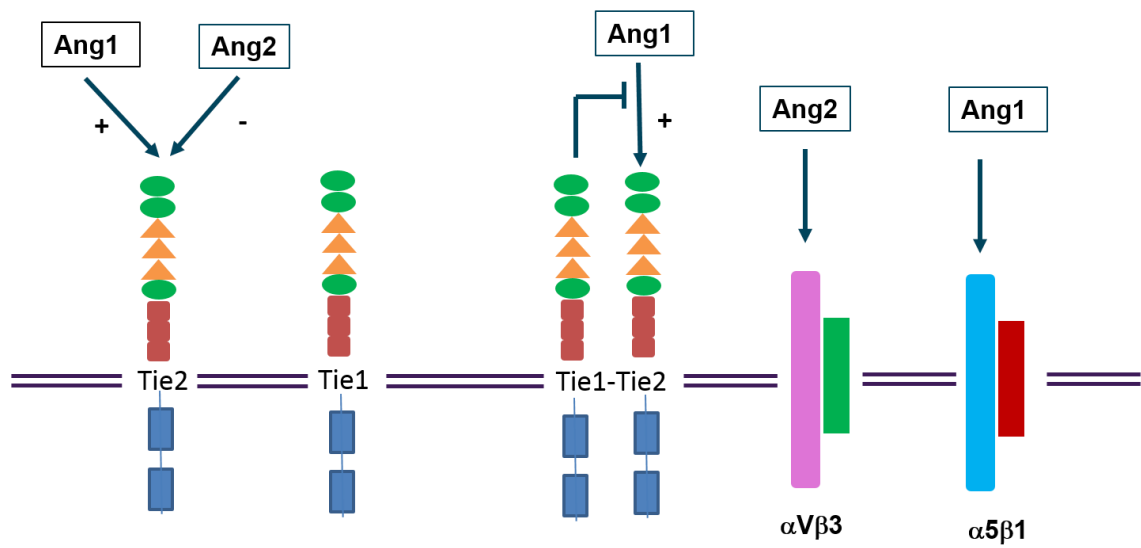


**Figure 1.2 Angiopoietin-Tie system**

Schematic diagram depicting the interaction of Ang1 and Ang2 with Tie receptor as well as integrins. Arrow indicates interaction, + and – indicates agonist or antagonist respectively.

**Figure removed for copyright reasons**

**Figure 1.3 Crystal structure of the Ang2–Tie2 binding interaction.**

Illustrates the Ang2/Tie2 complex. Yellow, P domain of Ang2; red, the rest of Ang2; green, Tie2 Ig2; blue, the rest of Tie2; black sphere, bound  $\text{Ca}^{2+}$ . The 13<sup>th</sup> Tie2-contacting residues (right low), 6 residues conservation between Ang1 and Ang2 are shown in black. The seven differences between Ang1 and Ang2 are shown in red (Barton et al. 2006).

The crystal structure of Ang1 bound to Tie2 has also been solved and indicates that the overall structure of Ang1 and Ang2 are very similar. The Ang1/Tie2 interface is also similar to the Ang2/Tie2 interface (Yu et al., 2013). The interacting regions of Ang2 and Tie2 in the absence of Ang2 coiled-coil and superclustering motifs form a complex with a 1:1 stoichiometry, resulting a heterodimer ligand-receptor assembly (Barton et al., 2006). Likewise, the stoichiometry of Ang1 receptor binding domain and Tie2 Fc *in vitro* studies form a complex with a 1:1 stoichiometry (Davis et al., 2003).

Oligomerization is crucial for angiopoietin to activate the Tie2 receptor. Native Ang1 forms higher order oligomers with basic trimeric, tetrameric, and pentameric oligomers, Ang2 also forms lower order oligomer with more than 80% native Ang2 being tetramer. The binding and activation of Tie2 requires at least Ang1 tetramers, formed by intermolecular disulfide linkage involving cysteines 41 and 54 positions in the superclustering domain of Ang1 (Kim et al., 2005).

Maisonpierre (Maisonpierre et al., 1997) demonstrated Ang1 and Ang2 have similar binding affinities to Tie2-Fc with  $K_d \sim 3\text{nM}$  by Scatchard analysis. Similarly, Fiedler (Fiedler et al., 2003) using a competition ELISA-based assay reported binding of immobilised myc-tagged human Ang1 and Ang2 to soluble Tie2-Fc with  $IC_{50}$  of Ang1  $2.2 \pm 1.1$  pmol, whereas  $IC_{50}$  of Ang2 to soluble Tie2-Fc was  $3.3 \pm 1.1$  pmol.

In addition measurement of the interaction between native Ang1 and Tie2 receptor was performed using biosensor of surface plasmon resonance (SPR) and the binding affinity estimated at 7.5 nM (Cho et al., 2004). A binding study of recombinant Ang1 and Ang2 with sTie2 demonstrated Ang2 bound Tie2 with lower affinity than Ang1. Fifty percent of saturation for Ang1 was achieved at 1.9nM, while Ang2 was achieved at 40.2nM, suggesting under these conditions Ang2 binds Tie2 with lower affinity than Ang1 around 20 folds (Yuan et al., 2009).

#### **1.1.4 Ang1 effects**

Binding of angiopoietins to the Tie2 receptor leads to receptor oligomerization and phosphorylation of specific tyrosine residues in the receptor intracellular domain that serve as binding sites for a number of effector molecules. The downstream signalling pathway of angiopoietin-Tie2 system leads to cellular responses, including cell survival, migration, proliferation and extracellular matrix interaction (Brindle et al., 2006) (Figure 1.4).

##### *1.1.4.1 EC survival and maintenance:*

Ang1 stimulates vessel survival through activation of PI3K that has a major role in cell survival (Brindle et al., 2006). Ang1-induced Tie2 activation results in phosphorylation the tyrosine residue 1101 of Tie2, which leads to recruitment of adaptor proteins such as growth factor receptor-bound protein 2 (GRB2) and the p85 subunit of phosphatidylinositol-3 kinase (PI3-K), which subsequently activates Akt/PKB pathway, a process linked to EC survival, activation of endothelial nitric oxide synthase and inhibition of the apoptotic pathway (Kim et al., 2000a, Papapetropoulos et al., 2000). Furthermore, Akt also signals to inactivate the forkhead transcription factor FKHR1 (FOXO1) causing suppression of Ang2 expression (Daly et al., 2004, Brindle et al., 2006, Tsigkos et al., 2006, Augustin et al., 2009). Inhibition of FOXO1 may contribute to endothelial cell survival and vascular stability by down-regulating expression of genes associated with endothelial cell apoptosis following suppression of Ang2. Endothelial Ang2 production can be controlled by Ang1-Tie2 signalling which drives a negative feedback loop via the PI3K-Akt pathway (Daly et al., 2004, Tsigkos et al., 2006, Augustin et al., 2009).

##### *1.1.4.2 Anti-inflammatory effect*

Ang1 acts as anti-inflammatory molecule which suppresses inflammatory nuclear factor- $\kappa$ B (NF- $\kappa$ B), resulting in inhibition of expression of cell adhesion molecules, including vascular cell adhesion molecule-1 (VCAM-1) and intercellular adhesion

molecule-1 (ICAM-1). Ang1 also attenuates tumour necrosis factor- $\alpha$  (TNF- $\alpha$ ) and VEGF induced tissue factor expression in HUVECs (Brindle et al., 2006).

#### *1.1.4.3 Anti-apoptotic effect*

Ang1 can inhibit endothelial cell apoptosis from serum deprivation in a variety of different endothelial cell types, including human umbilical vein endothelial cells (HUVECs), and aortic endothelial cells. Ang1 also prevents apoptosis in some nonendothelial cells, including mouse cardiac and skeletal myocytes (Dallabrida et al., 2005). Ang1/Tie2 signalling is able to promote its anti-apoptotic effect through the PI3K/AKT pathway, which recruits the regulatory p85 subunit of PI3K to phosphorylated tyrosine residue 1102 in the intracellular domain of Tie2.

#### *1.1.4.4 EC migration*

Ang1 stimulates endothelial cell migration through activation of the PI3K-Akt and Dok-R/Nck/Pak pathways. Dok-R is recruited to bind Tie2 via binding to phosphorylated tyrosine, which leads to tyrosine phosphorylation of Dok-R recruited to Tie2, serving as binding sites for the small GTPases-activating proteins for Ras, p120RasGAP (RasGAP) and adaptor protein Nck (Master et al., 2001). Nck is recruited and phosphorylated following binding of Dok to the receptor. Then P21-activating kinase (Pak) binds to Nck, resulting in increased Ang1-mediated cell motility (Master et al. 2001). The recruitment of adaptor protein ShcA to Tie2 also appears to have a roles in migration and organization (Audero et al., 2004). The GTPases RhoA and Rac1 are also involved in Ang1-mediated endothelial motility (Brindle et al., 2006). Furthermore, Ang-1 may elicit cell migration by modulating phosphorylation of ERK1/2 and p38MAPK through activation of PI3K (Makinde and Agrawal, 2008).

#### *1.1.4.5 EC permeability*

Ang1 functions as a potent anti-permeability factor for in endothelial monolayer (Gamble et al., 2000).

**Figure removed for copyright reasons**

**Figure 1.4 Tie2 signal transduction**

Schematic diagram depicting Tie2 signal transduction. The angiopoietins bind to Tie2 receptors and activate a range of signaling pathways including endothelial cell proliferation, inflammation and endothelial cell survival (Huang et al. 2010).

It has been found Ang1 attenuates the phosphorylation of vascular endothelial cadherin and platelet endothelial cell adhesion molecule (PECAM) that is involved in vascular permeability (Gamble et al., 2000). Ang1 can also counteract the permeability effect following activation with thrombin, VEGF or TNF  $\alpha$  (Kim et al., 2001, Puri and Bernstein, 2003).

Overall therefore Ang1 has broadly protective effects on the vasculature and is required to maintain normal vessel function.

### ***1.1.5 Angiopoietin2 in pathology***

#### *1.1.5.1 Vascular development and angiogenesis*

Ang2 is important for developmental vascularization where it destabilizes endothelial cells allowing vessel growth. A number of studies have indicated the involvement of Ang2 in the pathophysiology of vascular and inflammatory diseases. High levels of Ang2 have been found in acute lung injury and adult respiratory distress syndrome (ARDS), arteriosclerosis, hypertension, congestive heart failure, and type 2 diabetes (Chong et al., 2004, Nadar et al., 2005, Gallagher et al., 2008, Rasul et al., 2011).

#### *1.1.5.2 Inflammation*

Ang2 plays a role in vascular inflammatory responses. In a model of hyperoxia-induced acute lung injury, Ang2 deficient mice respond to hyperoxia with reduced oxidant-induced injury, cell death, inflammation, permeability alterations and mortality (Bhandari et al., 2006). During inflammation, mice deficient in Ang2 cannot elicit a rapid inflammatory response and do not induce adhesion molecule expression in response to the potent mediator of inflammation, tumour necrosis factor alpha (TNF- $\alpha$ ). Recombinant Ang2 alone has no effect on the proinflammatory programme of ECs but is involved the later steps of leukocyte adhesion, including firm adhesion and leukocyte transmigration. Ang2 restores the inflammation defect in Ang2 deficient mice (Fiedler et al., 2006). These findings reveal that Ang2 potentiates the effect of TNF on the induction of

inflammatory gene transcription, such as the expression of the cytokine-inducible adhesion molecules ICAM1 and VCAM1 (Augustin et al., 2009).

#### *1.1.5.3 Tumour angiogenesis*

Increasing evidence demonstrate that Ang2 plays an important role in tumour angiogenesis. Ang2 is highly expressed in several types of tumours, including gastric cancer, glioma and prostate cancer and hepatocellular carcinoma (Tanaka et al., 1999, Lind et al., 2005, Gu et al., 2006). Increased Ang2 expression at sites of tumour promotes vessel destabilization and regression during the earliest stages of tumour angiogenesis, resulting in transient tumour hypoxia (Ellis et al., 2001, Daly et al., 2013). Systemic overexpression of Ang2 was found to induce massive tumour vessel regression in 24 hours, even without the concomitant inhibition of VEGF (Cao et al., 2007). Hypoxia in tumour induces overexpression of VEGF, along with that of Ang2, allowing robust angiogenesis (Horner et al., 2001, Chen et al., 2014). Many studies reported the levels of circulating Ang2 was high during tumour progression and transcription of Ang2 marked upregulated in the tumour associated endothelium. Recent evidence suggested Ang2 has a more complicated role in angiogenesis with invasive tumour and metastasis cancer. In vivo study studies, the administration of selective Ang2 inhibitors can inhibit tumour growth such as reduction in tumour vascularity and inhibition of metastasis (Falcon et al., 2009, Holopainen et al., 2012). Additionally, tumour-derived Ang2 enhances tumour infiltration with Tie2-expressing monocytes (TEMs) which induce tumour angiogenesis (Coffelt et al., 2010). The upregulation of Tie2 expression in TEM was reduced by Ang2 antagonist, thereby inhibiting their proangiogenic activity. Therefore, the Ang2-TEM axis may exhibit as a novel target for cancer therapy.

#### *1.1.5.4 Ang2 is a biomarker*

Ang2 also serves as a circulating biomarker in many diseases. Increased plasma levels of Ang2 has been reported in diabetic retinopathy, inflammatory bowel disease, congestive heart failure, liver cirrhosis (Chong et al., 2004, Lip et al., 2004, Koutroubakis et al., 2006, Scholz et al., 2007). Clinical studies have

confirmed the elevation of Ang2 in severe sepsis patients which is correlated with disease severity. The effect of sepsis-related inflammatory mediators on Ang-2 production by lung endothelium in vitro was investigated. The results demonstrated the strong relationship of serum Ang2 with serum tumour necrosis factor-alpha (Orfanos et al., 2007). Another study reported elevation of plasma Ang2 with septic shock compared to healthy subjects. The levels of Ang2 appeared to correlate with the severity of disease and prognosis (Giuliano et al., 2007).

With regard to glomerular diseases using a Podocin-driven Ang-2 transgenic mice model, up-regulated Ang2 expression destabilized glomerular endothelial cells, causing glomerular endothelial apoptosis, downregulated nephrin expression, increased albuminuria, hyperglycemic and immune-mediated glomerulopathies. More pericytes around kidney cortical peritubular capillaries were observed in Ang2 null mice (Woolf et al., 2009). In glomerulo nephritis mice, loss of glomerular capillary was associated with decreased in Ang1 and with up-regulation of Ang2 (Yuan et al., 2002).

These data demonstrated a critical role of Ang2 signalling in pathological diseases, suggesting Ang2 target for treatment of tumour angiogenesis and other diseases.

### **1.1.6 Ang2 and Integrins**

Integrins are a family of transmembrane receptor protein that connects cell adhesion to the extracellular matrix (ECM) and to other cells (Weber et al., 2011). They consist of 18 $\alpha$  subunits and 8 $\beta$  subunits, which dimerize non-covalently to form 24 different heterodimers (Campbell and Humphries, 2011). Integrin extracellular domains are generally large structures, a proximately 80–150 kDa in size (Kalli et al., 2010). The extracellular domains of integrins can bind to extracellular matrix glycoproteins including collagens, fibronectins, laminins, and to cellular receptors such as ICAM, and VCAM. Several ligands result in cellular responses to the extracellular matrix and growth factor signalling. The

cytoplasmic domains are able to link the cytoskeleton proteins that regulate in response to changes in the environment for cell survival (Alberts et al., 2002). Such linkage between the cell exterior and interior allows for transducing signal in both direction. Integrins generally transduce signals through activation of focal adhesion kinase (FAK) to regulate cytoskeletal organization, cell motility, cell survival, cell proliferation, cell shape, and angiogenesis (Zhao and Guan, 2009).

In addition, Tie receptor angiopoietins have been found to interact with integrins. Ang1 binds  $\alpha 5\beta 1$  integrin via the receptor binding fibrinogen-like domain of Ang1 (Weber et al., 2005). Ang1-driven angiogenesis using the chorioallantoic membrane assay (CAM) was inhibited completely by anti- $\alpha 5\beta 1$  and partly by anti- $\alpha \nu\beta 3$  antibodies (Reynolds et al., 2005). Recombinant Ang1 monomer binds to integrin  $\alpha 5\beta 1$  in heart tissue leading to activation of pro-survival signalling and AMPK<sub>T172</sub> (master regulator of cardiac energetics and metabolism), and integrin-linked kinase (ILK), resulting in reduction of cardiac hypertrophy in mice (Dallabrida et al., 2008). Moreover, Ang2 has been found to bind directly to  $\alpha \nu\beta 3$  integrin (Felcht et al., 2012) and to induce  $\alpha \nu\beta 3$  integrin internalization and degradation following stimulation of endothelial cells (Thomas et al., 2010). Ang2 and integrins are involved in mediating tumour angiogenesis. However, Ang2 was observed to bind to integrins with lower affinity compared to Tie2 receptor. It is known that these integrins as well as Ang2 are up-regulated upon blood vessel angiogenesis and may enhance angiogenesis. Ang2 and integrin expression are associated with tumour growth and metastasis (Scholz et al., 2011).

Taken together, the data above supports the idea that high expression of Ang2 is associated with many disease processes. Therapeutic blocking of Ang2 signalling in pathological diseases is currently being pursued through the use of Ang2 inhibitors. Ang2 inhibitors have been proposed to act as a candidate for suppressing tumour growth. Moreover, these agents would be beneficial in inflammatory diseases associated overexpression of Ang2. Inhibitors of Ang2 include aptamers and antibodies. A complementary approach to inhibitory Ang2 is by use of an Ang2 specific ligand trap.

## **1.2 Ligand traps**

Receptor ectodomain-based ligand traps are regarded as novel therapeutic molecules because of high affinity biological blockers while minimizing one or more disadvantages of other drugs (Economides and Stahl, 2013). A soluble native receptor ectodomain is utilised as a ligand trap that acts to sequester the elevated levels of the target ligand. Both receptor ectodomain-based ligand traps and monoclonal antibodies have similar mode of actions that bind and sequester ligands away from their target receptors. However, ligand traps have some pharmaceutical advantages over antibodies in term of reduced immunogenicity and improved specificity profile. Ligand traps have better tissue penetration due to smaller size while antibodies are larger molecule thus limiting tissue penetration (Zwaagstra et al., 2012).

An Ang2-specific ligand trap would be an attractive potential therapeutic for diseases in which Ang2 has a significant role. However, the Tie2 ectodomain binds both Ang1 and Ang2. As Ang1 is protective of the vasculature, the use of the native ectodomain would also block normal vascular protective mechanism and could exacerbate the pathology as well as disrupting normal vascular function. Creation of a form of Tie2 ectodomain specific for only Ang2 binding would be a major step forward in generating an Ang2-ligand trap. The focus of this thesis is the use of protein engineering to change the binding specificity of Tie2 in order to create an Ang2-ligand trap.

### ***1.2.1 Protein Engineering***

Protein engineering is the methods of design and construction a novel useful protein with desired functions (Blundell et al., 1989). These can be achieved by manipulation of protein structure and function using computational protein design (CPD), X-ray crystallography, site-directed mutagenesis to recombinant DNA technology. Rational design and directed evolution are commonly strategies to engineer new proteins with desired phenotype (Hellinga, 1997). Often, researchers combine these two strategies to accomplish goals.

In rational design, the aim is to use knowledge of protein sequence and structure data as well as functional information to determine and modify the primary amino acid sequence for engineering the novel protein with defined properties. Several computational algorithms combined with the protein structure and functional information can be developed to predict globally correctly folded forms for mutation of the residues (Tiwari et al., 2012). An optimized sequence that folds with desired structure is selected to create a protein design with the desired changes (Koga et al., 2012). Although they have been some successes, the complexity of protein structure-function relationship makes it difficult to predict folding and stability of proteins based on their amino acid sequences and simulation model, which considerably limits rational protein design.

The Tie2/Ang1 complex is structurally similar to the Tie2/Ang2 complex, suggesting the receptor-binding interface of Ang1 and Ang2 are very similar (Yu et al., 2013). Examination of the Ang1-Tie2 and Ang2-Tie2 structure reveals no clear structural determinant for ligand specificity of Tie2 binding. The possibilities for rational engineering of Tie2 for Ang2-specific binding are therefore limited. The crystal structure of the Ang2/Tie2 complex (Figure 1.3) reveals that there are thirteen Tie2 contacting residues (Barton et al., 2006). Of the thirteen Tie2-contacting residues, six are conserved between Ang1 and Ang2. The conserved Ang2 residues F469L, K473K, Y476Y have been identified by mutagenesis as important for Tie2 binding (Barton et al., 2005). Of the seven differences, two residues (I434M and F469L) are unique to Ang1, however, conservative substitutions of hydrophobic residues do not significantly affect the ligand-receptor interaction (Yu et al., 2013). Two other residues are likely to have little effect on the ligand-receptor interaction (Barton et al., 2006). Thus, it is possible that three Tie2-contacting residues (N467G, S417I and S480P) are likely to be responsible for the different properties of both ligands.

#### *1.2.1.1 Directed Evolution*

Directed evolution is a method in protein engineering which is similar to the process of natural selection but in a much shorter timescale. The principle of this method utilizes the natural process of evolution by mutation and selection of

mutant with desired phenotype. Evolved protein is generated by random mutations and proteins with desirable properties can be selected by efficient screening techniques (Yuan et al., 2005). This technology has been developed to overcome the limitation of rational design of protein function as directed evolution provides the selection of evolved molecules without the necessity for detailed structural and mechanism information.

The initial step of directed evolution is the generation of mutant gene library. The generation of mutant library can be achieved by using several methods such as the error-prone polymerase chain reaction (Mullis and Faloona, 1987) and DNA shuffling (Stemmer, 1994). Clones of the mutant library are expressed and the encoded mutant proteins with desirable functional fitness can then be selected by a high throughput assay with sensitive and specific selection. cDNA encoding the selected protein must be linked to the protein to allow recovering of the encoding DNA. DNA from these selected variants are then used to create another mutant library in order to introduce additional mutations onto those already showing in proteins. This library is again screened and the whole cycle of selection and further mutation is re-iterated until the desired phenotype is obtained (Figure 1.5). These methodologies facilitate the identification of mutants with small improvements in desired function. In this way, the best mutants are selected and evolved (Yuan et al., 2005).

Directed evolution has been successful in engineering new properties in many proteins. Example is Humalog (insulin) that has been developed by reversal of Lys and Pro at C terminus of the B chain, resulting in faster onset of action (DiMarchi et al., 1994). Another example is directed evolution of novel adeno-associated virus (AAV) vectors that crosses the seizure-compromised blood brain barrier (BBB) and transduce cells (Gray et al., 2010). There are significant limitations to directed evolution, notably the process of generating a mutant library, recovering DNA-encoding desirable phenotypes and growth of another library from it can be very time consuming and laborious.

**Figure removed for copyright reasons**

**Figure 1.5 Directed evolution**

Schematic diagram depicting the principle of directed evolution process. The first step is to select gene of interest. Secondly, the gene library of variants is created by random mutation such as shuffling technique. In the next step, the libraries of DNA sequences are inserted into a bacterial host which produce variants. Then, screenings of colonies are performed for the property of interest. Improved genes are isolated and the process repeated using a wide array of high-throughput analytical devices until the protein mutant with desired function is evolved (Weissman et al. 2004).

Furthermore, most methods for directed evolution are *in vitro*, or in prokaryotic expression systems making it difficult to use for coupled mammalian proteins such as Tie2 that require evolution of coupled extracellular proteins based on somatic hypermutation (SHM) in B cells.

### **1.2.2 Somatic Hypermutation**

Somatic hypermutation (SHM) is the primary mechanism for the diversification of the antibody repertoires with refined specificity in man and mouse. The process introduces a point mutation at a frequency of about  $10^{-3}$  per base pair per generation (McKean et al., 1984, Rajewsky et al., 1987, Woo et al., 2003). The generation of antibody diversity in mammalian B lymphocytes occurs by the process of SHM of the variable (V) region, generating high-affinity antigen binding sites (Li et al., 2004). SHM offers a possible approach to generate diversity of sequence that could be exploited in mammalian cells for directed evolution. If it is possible to replace an exogenous non-immunoglobulin (Ig) gene encoding the protein in the rearranged immunoglobulin genes which are the target for directed evolution, then it may be that SHM could introduce mutations into the genes in the same way as are the immunoglobulin genes. As in the SHM of immunoglobulins, each B cell would therefore express copies of mutated target proteins and the population of cells would constitute a library. This library could then be screened to select the cell expressing the protein with desired properties.

Recent reports indicate that insertion of non-immunoglobulin genes into the Ig locus in B cells is tolerated and that such genes are mutated by SHM and this approach can be used to evolve non-fluorescent proteins in directed protein evolution. Wang et al. (2004) used a fluorescent protein as a reporter gene and established an evolutionary model in hypermutating cells line. They demonstrated the variants of the green fluorescent protein (GFP) were able to diversify by SHM following transfected in Ramos B cells, a cell line derived from Burkitt's lymphoma. Following one month of culture and selection the mutant GFP gene were able to generate new variants with novel properties such as changed emission spectra (Wang et al., 2004a, Wang et al., 2004b).

In another study Wang et al. (2004) used SHM in Ramos cells to produce a mutant mPlum with far-red emission from a monomeric red fluorescent protein (mRFP) following iterative round of sorting (Wang et al., 2004b), using the process of SHM together with the enzyme activation-induced cytidine deaminase (AID). These cells introduce point hypermutation into the rearranged V regions of Ig with a rate of mutation between  $2 \times 10^{-5}$  per bp per generation. However, Ramos cells do not sustain mutations over prolonged culture (Sale and Neuberger, 1998, Zhang et al., 2001).

Directed evolution in a chicken B cell line has been proposed by Arakawa (Arakawa et al., 2008). DT40 cells can use SHM and gene conversion to mutate Ig genes. However, modified DT40 cells have been established by deletion of pseudo V donors or RAD 51 paralogues to abolish gene conversion, enhancing AID-dependent Ig hypermutation. Modified DT40 mutate their Ig V at rates of  $2.4 \times 10^{-5}$  per bp per generation (Sale et al., 2001, Arakawa et al., 2004). Arakawa engineered a GFP transgene in the DT40 cell line, allowing gene diversified by SHM. The genes with improved phenotype were selected by iterative FACS. In the end, this strategy produced GFP variants with higher fluorescence intensity following three rounds of iterative sorting as compared with the GFP-derived from bio-imaging of vertebrate cells (Arakawa and Buerstedde, 2009).

The enzyme Activation-Induced cytidine Deaminase (AID) is essential to initiate somatic hypermutation, generating high-affinity antibody responses to protein antigen by diversification of Ig genes in germinal center-B cells (Muramatsu et al., 1999). AID-mediated SHM in B cells introduces point mutations into the variable region of Ig heavy and light chain genes. AID is transported into the nucleus and deaminates cytosine (C) on single-stranded DNA (ssDNA) to generate uracil (U) producing a G-U mismatch (Maul, Gearhart 2010). The G-U mismatch is then replicated to produce a C-to T mutation or G-to A mutation on the other strand. Alternatively, the G-U mismatch may be removed by uracil-DNA-glycosylase (UNG) to create an abasic site on DNA (Di Noia, Neuberger 2007). The abasic site can be converted to a single-stranded nick by AP-endonuclease and then repaired by base excision repair without generating mutation (Li et al., 2004). Additional mutation or mutations on A-T base pairs may

be generated by the recruitment of mismatch repair proteins MSH2 and MSH6 as well as error-prone DNA polymerase to bind G-U mismatches or G abasic mismatches, which are then excised and replaced by re-synthesis with error-prone polymerase (Figure 1.6).

SHM of the H chain V region produces mostly single base substitutions with occasionally insertions and deletions, starting around 100 to 200 bp downstream of the promoter and ending around 1.5 to 2.0 kb downstream (Li et al., 2004). In mouse and human, the frequency of V region mutation occurs at rates of  $10^{-5}$  to  $10^{-3}$  mutations per base pair per generation in B cells (Kocks and Rajewsky, 1989). The mutation rate of Ig is around 1 million-fold higher than the spontaneous rate of mutation in most other genes (Li et al., 2004). There are more transition mutations such as C to T, G to A than transversion mutation such as C to A or G; G to C or T (Peled et al., 2008). Additionally, the deoxycytidines (dC) within WRCY/RGYW motifs (where R = purine, Y = pyrimidine and W = A or T) are the most common target of mutation (Schrader et al., 2003). WRCY/RGYW sequence motifs referred to as hot-spots for SHM. Arakawa et al. reported mutations within the RGYW/WRCY hotspot motifs account for 51.9% of all mutations from their sequencing of the Ig light chain of pseudo V donors knockout DT40 clones cultured for 5-6 weeks (Arakawa et al., 2004).

As reviewed above DT40 is able to diversify exogenous transgenes to generate libraries of mutant proteins. Furthermore, DT40 is able to manipulate the expression of exogenous AID, which can be controlled by an inducible promoter, or Cre recombinase system (Arakawa et al., 2002). Overexpression of AID is likely to induce SHM and maximize mutation. Therefore, it is possible to exploit the platform of gene diversification in B cell for evolution of non-fluorescent proteins with distinct functions. This can be performed by using SHM in B cells coupled with cell surface display for generating and expressing a library of mutants on the surface of B cells. After that such mutants with desired function, such as specific binding activity, could be screened and selected using FACS.

**Figure removed for copyright reasons**

**Figure 1.6 The role of activation-induced cytidine deaminase (AID) in somatic hypermutation (SHM)**

SHM is initiated by AID. AID deaminates cytidine (C) nucleotides to uridine (U)-guanosine (G) mismatch on single-stranded DNA. Three mismatch pathways exist to repair this mismatch. The U:G mismatch mutation can be fixed at the site of deamination by recruitment of the mismatch repair machinery, resulting in mutation at A:T base pairs adjacent to the initiating U:G lesion. If the mismatch were left unrepaired, DNA polymerases will create C>T and G>A transition mutations. In base-excision repair (BER), an abasic site formed by uracil-DNA glycosylase (UNG) will give rise to both transition and transversion mutations (Odegard and Schatz, 2006)

### **1.2.3 Cell Surface Display**

Cell surface display is carried out by expressing the protein of interest as a fusion to a transmembrane anchor on a cell surface (Lee et al., 2003). Cells produce and display the mutant protein with the desired functional characteristics such as, for example, improved protein-binding affinity. Cells expressing desired mutants can then be selected by FACS following binding of fluorescently-labelled binding protein.

The cell surface technique has been applied most extensively in yeast and bacteria. However, the expression of mammalian proteins in bacterial host cells has some drawbacks in term of differences in protein folding and post-translational modification, resulting in non-functional proteins (Boder and Wittrup, 1997). The misfolding of protein influences its properties. Alternatively, yeast surface display has become the possibility for expressed extracellular eukaryotic proteins (Blagodatski and Katanaev, 2011), providing many advantages compared to other prokaryotic cells display. This system allows quantitative discrimination between mutants, eukaryotic expression and processing (Colby et al., 2004). However, this technique still requires multiple transfection and recovery steps to obtain the desired protein variant.

### **1.3 Aims and hypotheses**

Ang2 is increased in a range of diseases where it drives pathological changes. This study seeks to use SHM combined with cell surface display to create a novel variant of the Tie2 ectodomain specific for Ang2 binding, and test this protein in cellular and *in vivo* assays for suppression of Ang2-mediated effects.

In this study the following hypotheses will be tested.

1. Somatic hypermutation combined with cell surface display can generate an evolved form of Tie2 ectodomain with Ang2-specific binding.
2. Soluble evolved Tie2 ectodomain will exhibit specific Ang2 binding and suppress Ang2 effects in cellular assay.
3. Soluble Ang2-specific Tie2 ectodomain will inhibit Ang2-mediated effects *in vivo*.

## Chapter 2: Materials and Method

All reagents were of analytical reagent grade and supplied by Sigma-Aldrich (Poole, UK) or Fischer Scientific (Loughborough, UK) unless otherwise stated. Experiments were conducted at room temperature (RT) except where indicated. Solutions were made with double-distilled water (ddH<sub>2</sub>O) and pH was adjusted to the desired value with concentrated HCl or NaOH.

### 2.1 Materials

#### 2.1.1 Buffers

Sample buffer (2X) with DTT: 50mM Tris (pH 6.8), 10% (v/v) glycerol, 2% (w/v) SDS, 0.1% (w/v) bromphenol blue, 5mM EDTA, 100mM DTT

Lysis buffer: 50mM Tris-HCl (pH 7.4), 50mM NaCl, 1mM NaF, 1mM EGTA, 1mM NA Orthovanadate, 1% (v/v) TritonX-100, complete protease inhibitor cocktail (1 protease tablet in 10 ml solution)

Running buffer (10X): 2.5mM Tris (pH 8.3), 192mM glycine, 30mM SDS made up to 1 litre in dH<sub>2</sub>O then this 10X solution was diluted in dH<sub>2</sub>O to make 1X Running buffer

Transfer buffer (1X): 25mM Tris-HCl (pH 8.3), 192mM glycine, 20% (v/v) methanol

TBS-TX-100: 50mM Tris, 150mM NaCl, 0.1% (v/v) TritonX-100

Blocking buffer: 5% (w/v) non-fat dried milk in TBS-TX-100

Developer: 198µM p-Coumaric acid in DMSO, 1.25mM Luminol (5-amino-2,3-dihydro-1,4-phthalazinedione) in DMSO, 1:3333 H<sub>2</sub>O, 0.1M Tris-HCl (pH 8.5)

PBS: 140mM NaCl, 2.7mM KCl, 10mM Na<sub>2</sub>HPO<sub>4</sub>, 1.8mM KH<sub>2</sub>PO<sub>4</sub> (pH 7.4)

1XTAE (Tris-acetate-EDTA) : 40mM Tris-Acetate, 1 mM EDTA, 2.85ml Glacial acetic acid diluted in 50ml dH<sub>2</sub>O

DNA loading buffer (6x): 0.25% (w/v) each bromophenol blue and xylene cyanol, 40% (w/v) sucrose in water

TE buffer: 10mM Tris-HCl, 1mM EDTA (pH7.5)

EB buffer: 10mM Tris-HCl (pH 8.5)

RNase-free H<sub>2</sub>O: 0.1% (v/v) Diethyl pyrocarbonate (DEPC)

10X Kinetic buffer: 10mM phosphate, 150mM NaCl, 0.02% (v/v) Tween 20, 0.05% (w/v) sodium azide, 1 mg/ml BSA (pH 7.4)

NP40 buffer (100mM Tris-HCl, 300mM NaCl, 10% (v/v) NP40 solution, 10% (v/v) glycerine)

Conditioning/Regeneration solution: 10mM Glycine pH 1.7

### **2.1.3 Commercial Kits**

BIOTAQ™ DNA Polymerase (Bioline; London, UK)

Finnzymes Phusion™ High Fidelity DNA Polymerase (NEB; Hitchin, UK)

Ambion® RETROscript®(Invitrogen; Paisley, UK)

QIAquick® Gel Extraction Kit (Qiagen; Crawley, UK)

RNeasy® Mini Kit (Qiagen; Crawley, UK)

QIAprep® Spin Miniprep kit (Qiagen; Crawley, UK)

HISpeed® Plasmid Maxi kit (Qiagen; Crawley, UK)

pcDNA™3.1 Directional TOPO® Expression Kit (Invitrogen; Paisley, UK)

TOPO®TA Cloning® Kit for sequencing (Invitrogen; Paisley, UK)

Lipofectamine™2000 transfection reagent (Invitrogen; Paisley, UK)

Qiagen hispeed maxiprep kit (Qiagen; Crawley, UK)

Zeba spin desalting column and devices

Octet Biosensors for Label-Free Detection of protein binding (ForteBio, USA)

### **2.1.2 Culture media**

All media were provide as sterile solutions or autoclaved at 120°C for 20 minutes at 15-lb/in<sup>2</sup>.

LB: 1% (w/v) Tryptone, 0.5% (w/v) Yeast Extract, 200mM NaCl (pH7.4)

LB Agar: 1% (w/v) Tryptone, 0.5% (w/v) Yeast Extract, 200mM NaCl, 2% (w/v) agar (pH7.4)

SOC: 2% (w/v) Tryptone, 0.5% (w/v) Yeast Extract, 10mM NaCl, 2.5mM KCl, 10mM MgCl<sub>2</sub>, 10mM MgSO<sub>4</sub>, 20mM glucose

CHO complete media: Alpha-MEM (Life Technologies, UK), 2mM L-glutamine, 10% (v/v) FCS

DT40 complete media: RPMI 1640 7% (v/v) fetal bovine serum (FCS), 3% (v/v) chicken serum

HUVECs complete media: Medium 200 (Life Technologies, UK), 10ml Low Serum Growth Supplement (LSGS)

EA.hy926 complete media: DMEM (Life Technologies, UK), 10% (v/v) FCS

HEK293 complete media: Freestyle 293 Expression medium (Life Technologies, UK)

## **2.2 Preparation & Storage of plasmid DNA**

### **2.2.1 Total RNA isolation (RNeasy Minikit, Qiagen)**

Between  $1 \times 10^6$  and  $5 \times 10^6$  cells were centrifuged at 250g for 5 minutes and washed once with PBS. RNA isolation was carried out as per the manufacturer's instructions. RNA was resuspended in RNase-free water and assessed by absorbance. RNA was generally used immediately for downstream application, but if storage was required 1:50 RNase inhibitor (Ambion) was added prior to freezing at  $-80^\circ\text{C}$ .

### **2.2.2 Genomic DNA isolation sorted DT40 cells (Generation Capture Column Kit, Qiagen)**

After many rounds of sorting, genomic DNA were recovered from the highest Ang2 binding population to determine which DNA sequence variants are responsible for the displayed phenotype.  $1 \times 10^6$  cells were harvested to obtain mRNA and used for amplification of DNA encoding Tie2 ectodomain. Ten colonies resulting from transformation as previous described were randomly picked and sent for sequencing (Korea).

### **2.2.3 NEB Turbo Competent *E. coli* (New England Biolabs)**

NEB Turbo Competent *E. coli* cells were thawed on ice for 10 minutes and 1-5 $\mu\text{l}$ , containing 1pg-100ng of plasmid DNA, was added to 100 $\mu\text{l}$  aliquots of *E. coli* cells as supplied by the manufacturer. The mixture was incubated on ice for 30 minutes, followed by a heat shock at exactly  $42^\circ\text{C}$  for exactly 30 seconds and subsequent placed on ice for 5 minutes. 950 $\mu\text{l}$  of room temperature SOC was added into the mixture then incubated at  $37^\circ\text{C}$  for 60 minutes shaking at 250 rpm. Between 50 and 100  $\mu\text{l}$  of each dilution was spread on LB agar plates with 100 $\mu\text{g}/\text{mL}$  Ampicillin. The plates were incubated overnight at  $37^\circ\text{C}$ .

#### **2.2.4 Transformation of TOP10 chemically competent cells (Invitrogen)**

TOP10 competent *E. coli* cells (Invitrogen) were thawed on ice and gently mixed with 2-5µl TA cloning reaction. After incubation on ice for 30 minutes, the cells were heat-shocked at 42°C for 60 seconds prior to transferring to ice for 2 minutes. 250µl room temperature SOC medium was added into the mixture followed by incubation at 37°C for 1 hour with 250rpm shaking. Between 50 and 100 µl of each culture was spread on LB agar plates containing the appropriate antibiotic. The plate were incubated overnight at 37°C and colonies were analysed by plasmid miniprep, restriction analysis and sequencing.

#### **2.2.5 Plasmid DNA preparation: Miniprep (Qiagen)**

Each single colony obtained after transformation was picked with a sterile pipette tip and inoculated into 5-10 ml of LB medium containing 100µg/ml ampicillin and grown overnight at 37°C on a shaker at 225 rpm. The bacterial culture was centrifuged at 3500g for 10 min and plasmid recovered using the QIAprep Mini Prepkit (Qiagen) as per manufacturers' protocol. Finally, the plasmid sample was eluted in 30 µl elution buffer and determined DNA concentration by measuring the absorbance at 260 nm using a Nano-Drop spectrophotometer.

#### **2.2.6 Plasmid DNA preparation: Maxiprep (Qiagen)**

A single colony was picked and inoculated into a starter culture of 5 ml LB medium containing 100µg/ml ampicillin and grown for 8 hours at 37°C on a shaker at 225 rpm. After that the starter culture was diluted in 250 ml of LB medium and grown overnight at 37°C on a shaker at 225 rpm. The bacteria cells were harvested by centrifugation at 6000g 4 °C for 15 min. Plasmids were recovered then carried out by using the HiSpeed® Plasmid Maxi kit (Qiagen) as per manufacturers' protocol. Briefly, the cell pellet was suspended in buffers P1, P2 and P3 supplied with the kit and the lysate formed was poured onto the QIAfilter Cartridge. The lysate was filtered into the equilibrated HiSpeed Tip allowing to flow through by gravity. After the lysate has entered, the HiSpeed Tip

was washed with 60ml Buffer QC. The DNA was eluted with Buffer QF and precipitated with isopropanol followed by incubation for 5 minutes. The eluate-isopropanol mixture was then transferred into the syringe attached to the QIAprecipitator Module outlet nozzle prior to filtering the eluted-isopropanol mixture through the QIAprecipitator using constant pressure. The membrane was dried by forcing air through the QIAprecipitator several times. The QIAprecipitator was attached with the outlet of a 1.5 ml collection tube and the plasmid sample was eluted in 1ml TE buffer. DNA concentration for the plasmid preparation was determined by measuring the absorbance at 260 nm on a spectrophotometer.

### ***2.2.7 DNA quantification: absorbance***

The optical density of DNA at 260 and 280 nm was determined using a Nano-Drop spectrophotometer. This machine automatically determined the nucleic acid concentration using Beer's Law and the mass extinction coefficient of 50 ng/ $\mu$ l  $\text{cm}^{-1}$  for dsDNA. The ratio of absorbance at 260 nm and 280 nm was used to assess the purity of DNA. The A260/A280 ratio should be between 1.8-2.0.

### ***2.2.8 Agarose gel electrophoresis***

Electrophoresis of DNA samples was carried out using 0.5-1% (w/v) agarose TAE gels in TAE buffer. The agarose (Melford, Chelsworth, UK) was heated and dissolved in 1X TAE buffer and the dissolved agarose was allowed to cool to approximately 50°C, then ethidium bromide was added to the gel to a final concentration of 0.2  $\mu$ g/ml. The mixture was poured into a gel tray with comb. After the gel had set, it was immersed in 1X TAE buffer within an electrophoresis tank. The DNA samples were mixed with 6X loading dye depending on volume of sample, and loaded into the wells, alongside a 10 $\mu$ l DNA ladder (TrackIt 1 kb Plus, Invitrogen or Hyperladder IV, Bionline). Electrophoresis was conducted with a constant voltage of 120V until the blue dye reached the bottom of the gel. DNA fragments were separated and then visualized using an ultra violet light transilluminator. Images were captured on Multimage light cabinet (Flowgen,

Shenstone, UK) and determined by comparison with 1 Kb plus DNA ladder run alongside the samples on the same gel.

### ***2.2.9 Purification of DNA: gel extraction***

The DNA fragment was resolved on agarose gel by electrophoresis and excised from the gel using a scalpel blade. The purification of PCR product was performed as per the manufacturer's guidelines (Qiagen). Briefly, 3 volumes of buffer QG was added to 1 volume of gel before incubation at 50°C for 10 minutes. After the gel had completely dissolved, 1 gel volume of isopropanol was added to sample for increasing the yield of DNA fragments. To bind the DNA, the sample was applied to the QIAquick column prior to centrifugation for 1 minute. Following discarded flow-through and placement the column back in the same tube, 0.5ml of buffer QG was added and centrifuged before adding 0.75ml of buffer PE for washing. Finally, DNA was eluted and resuspended in EB buffer or sterile water, depending on downstream application, and assessed by absorbance and agarose gel electrophoresis.

### ***2.2.10 Purification of DNA: chloroform phenol extraction***

An equal volume of Phenol-Chloroform-Isoamyl alcohol was added to the DNA sample then mixed and shaken to produce an emulsion. The mixture yield two phases was centrifuged at 12000g for 15 minutes at 4°C. The upper aqueous phase was transferred to a clean tube and further proceeded to ethanol precipitation.

### ***2.2.11 Purification of DNA: ethanol precipitation***

0.1 volumes of 3M sodium acetate pH 5.2 and 2.5 volumes of 100% ethanol were added to the DNA sample. Following incubation at -20°C overnight, the DNA was centrifuged at 14000g for 30 minutes at 4°C. The supernatant was discarded. The DNA pellet was rinsed with 70% Ethanol and centrifuged again for 15

minutes. The supernatant was discarded and pellet was dissolved in appropriate volume of sterile water.

### **2.2.12 Glycerol stocks**

A single colony of the clone was picked from a plate and grown overnight in LB ampicillin. 0.5ml of the culture was added to 0.5ml of 80% (v/v) sterile glycerol in sterile cryovials. The mixture was vortexed. The glycerol stock was frozen in liquid nitrogen and stored at -80°C.

## **2.3 PCR & Cloning**

### **2.3.1 PCR: plasmid DNA**

PCR was conducted with either BIOTAQ DNA polymerase (Bioline) in the case of analytical applications, or high-fidelity Phusion DNA polymerase (Finnzymes) for cloning and sequencing. The PCR reaction set up is shown in Table 2.1.

**Table 2.1 PCR reaction components for 50µl reaction volume**

<b>Component</b>	<b>Final Concentration or Amount</b>
PCR buffer	1X
dNTP	10mM
Template DNA	10 ng
Forward primer	1 pmol
Reward primer	1 pmol
Enhancer	1µl (optional)
DNA polymerase	1 unit
Nuclease-free water	39 µl
Mineral oil	30 µl

The Perkin Elmer Thermocycler was used for the amplification cycles. Cycling parameters are shown in Table 2.2.

**Table 2.2 PCR condition**

Step	Temperature	Time	Cycles
	92°C	3 min	1
Denaturation	94°C	1 min	25
Annealing	45-60°C	1 min	
Extension	72°C	1 min	
	72°C	10 min	1
Soak	4°C	∞	-

### **2.3.2 Reverse transcription**

Total RNA was reverse transcribed to cDNA using the Ambion RETROscript™ kit. 2µg total RNA was mixed with 2µl total RNA was mixed with 2µl oligo dT or random decamers and made up to 12µl with RNase-free H<sub>2</sub>O. This was incubated at 85°C for 3 minutes followed by immediate cooling on ice. A mastermix was prepared to incorporate 4µl dNTPs, 2µl 10x RT buffer, 1µl RNase inhibitor and 1µl MMLV-RT per reaction. The required 8µl of mastermix was added to each sample, followed by incubation at 50°C for 1 hour and 92°C for 10 minutes. The cDNA product was stored at -20°C if not used directly for PCR.

### **2.3.3 TA cloning for sequencing (TOPO TA cloning®Kit for sequencing Invitrogen)**

PCR was performed using proofreading polymerase. Addition of 3' adenine overhang to the PCR product was achieved using the Biotaq PCR kit (Bioline). 30µl gel-purified PCR product was incubated at 72°C for 15 minutes with 9µl ddH<sub>2</sub>O, 5µl NH<sub>4</sub> buffer, 4µl MgCl<sub>2</sub>, 1µl dNTPs & 1µl Biotaq. The cloning reaction was performed as per the manufacturer's instructions. 4 µl of PCR product was

added to 1µl pCR4-TOPO®vector and 1µl salt solution and incubated at RT for 20 minutes. 2µl of cloning reaction was transformed into TOP10 cells.

#### **2.3.4 TA cloning into the PEF6/V5 His TOPO® expression vector**

PCR products were amplified with designed primers using proofreading polymerase and the product was gel-purified. The cloning reaction was performed as per the manufacturer's instructions. Briefly, 2µl PCR product was typically added to 1µl TA vector, 1µl salt solution and 1µl sterile H<sub>2</sub>O and incubated at RT for 1 hr. Then, 2µl of cloning reaction was transformed into TOP10 chemically competent cells (Section 2.2.2).

#### **2.3.5 Site directed mutagenesis to produce introduce F/I mutation**

To produce soluble Tie2 ectodomain fusion proteins with a single F to I substitution (F/I), site directed mutagenesis was used (Stratagene's QuikChange®, Agilent Technologies). cDNA encoding Wt-Tie2-Fc was amplified with designed primers to introduce F/I substitution (appendix). The reaction conditions are specified in Appendix. The amplified product was cloned as described above to create F/I mutations into Wt-Tie2-Fc. Following temperature cycling, the product is treated with Dpn I to digest the parental DNA template and to select for mutation-containing synthesized DNA. Cloning reaction was transformed into NEB Turbo Competent *E. coli*. Colonies were carried out by plasmid miniprep (Qiagen) and sequenced for confirmation of mutation.

#### **2.3.6 Site directed mutagenesis to produce RH mutation**

To produce soluble Tie2 ectodomain fusion proteins with RH deletion, site directed mutagenesis was used (Stratagene's QuikChange®, Agilent Technologies). To produce soluble RH-Fc fusion proteins, plasmid of Wt-Tie2-Fc was amplified with primers to introduce RH deletion (appendix). The PCR conditions are specified in Appendix. The amplified product was cloned as

described above to create RH mutation. Following treatment with Dpn I, cloning reaction was transformed into NEB Turbo Competent *E. coli*. Colonies were carried out by plasmid miniprep (Qiagen) and sequenced for confirmation of mutation.

### **2.3.7 Restriction digestion of DNA**

Restriction enzymes and appropriate reaction buffers were selected and used as per manufacturers' instruction. Diagnostic restriction was typically digested using 200ng of DNA in the reaction volume with 20 units of enzyme and 1X buffer concentration. The volume of reaction was made up to 10 µl using autoclaved distilled RNase/DNAase free water. The digestion was incubated at 37°C for 180 min. The result of digested product was visualized by conduction of gel electrophoresis.

### **2.3.8 Sequencing**

Purification of plasmid DNA was performed by miniprep and eluted with elution buffer. Sample and primers were sent to the University of Leicester Protein Nucleic Acid Chemistry Sequencing Service for sequencing. Additionally, 96-well plates of individual fresh colony agar stabs were supplied to Macrogen Inc., South Korea for sequencing.

## **2.4 Cell culture, transfection and protein production**

### **2.4.1 Tie expressing DT40 cells and Culture**

The DT40 chicken B cell line 'ψV-AID<sup>R</sup>CI4' was a kind gift from Arakawa et al. (GSF Institute for molecular Radiobiology, Munich, Germany). DT40 cells expressing Tie2 ectodomain on the cell surface was a kind gift of Dr. K. Steele. Briefly, the Tie2 surface expression construct was prepared. Initially, amplification products that consists of cDNA encoding of Tie2 ectodomain

(residues 1-442), platelet-derived growth factor receptor  $\beta$  (residues 514-562 which includes the transmembrane sequence) and with an amino terminal five alanine linker followed by the FLAG epitope were generated before ligating into pcDNA3.1 (Appendix 7.1). The plasmids were then transferred into the vector pHypermur2 (Appendix 7.2) prior to stable integration into the re-arranged immunoglobulin locus of the DT40 cells resulting in generation of Tie2-DT40 cell lines (Dr. K. Steele, University of Leicester). Cells were cultured in T25 and T80 flasks at 37°C in 5% CO<sub>2</sub>. Cells were passaged every 3 days at ratio of 1:3 to 1:30 depending on future application.

#### ***2.4.2 Stable non-targeted transfection of DT40 cells.***

pAIDblast<sup>f</sup> vector was linearised with the EcorR5 and SnaB1 followed by purification and concentration by chloroform-phenol extraction and ethanol precipitation. 30-50  $\mu$ g DNA was resuspended in 20 $\mu$ l sterile water for each transfection at a concentration of approximately 1.5  $\mu$ g/ $\mu$ l. 20 x 10<sup>6</sup> Tie2-DT40 cells were collected by centrifugation at 250g for 5 minutes followed by a cold PBS wash. Cells were then resuspended in 700 $\mu$ l cold PBS. The DNA was placed into a 4mm electroporation cuvette (Cell projects; Harrietsham, UK) followed by the cell suspension. The cuvette was briefly vortexed and incubated on ice for 10 minutes prior to electroporation at 950 $\mu$ F, 250V (BioRad GenePulser). After 20 minutes of incubation, the cells were transferred to a pre-warmed 80cm<sup>2</sup> cell culture flask containing 29.3ml complete medium containing 2X puromycin (1 $\mu$ g/ml) and 2X blasticidin (40 $\mu$ g/ml) was added to give final concentrations of 0.5 $\mu$ g/ml puromycin and blasticidin. Cells were plated into 96-well plates and adjust the final volume at 200 $\mu$ l per well and incubated at 37°C in 5% CO until colonies appeared. Colonies were picked between days 7-14 and grown up in culture flasks.

#### ***2.4.3 Freezing and storage of DT40 cells***

Cells were grown to reach a density of approximately 1X10<sup>6</sup> cells/ml and collected by centrifugation at 250g for 5 minutes. Pellets were resuspended in freezing-

medium (50%FCS, 10%DMSO, 40% complete DT40 medium) to a final density of  $10 \times 10^6$  cells/ml.

#### **2.4.4 Chinese Hamster Ovary cells (CHO)**

CHO cells maintained in RPMI with L-glutamine supplemented with 10% FCS, and 0.1 mM MEM were grown in a 6 well plates to 60% confluence at  $37^\circ\text{C}/5\%\text{CO}_2$  v/v in air. For passaging, the CHO cells monolayer was washed once with PBS and incubated with 2 ml of 0.1% (v/v) Trypsin, 0.02% (v/v) EDTA for 5 min at  $37^\circ\text{C}$  and the flask was tapped gently to facilitated detachment of the cells from the surface. The action of Trypsin/EDTA was arrested by addition of complete media to a final volume of 10 ml. The suspension was centrifuged at 200g for 7 min and the sedimented cells were resuspended in 1 ml of complete media. Cells were seeded with cells dilution required to achieve a cell density of 50,000 cells/cm<sup>2</sup>.

#### **2.4.5 Transfection for CHO cell line by Lipofectamine**

The cells were plated to obtain a confluence of 60-70% on the day of transfection. 10 µg of DNA and 5 µl of Lipofectamine 2000 in 100 µl of OptiMEM I was used in making the transfection complex which was incubated at room temperature for 30 min. This complex was then added to 2 ml of complete media and the cells were incubated overnight at  $37^\circ\text{C}/5\%\text{CO}_2$ . Following transfection, medium was replaced with complete medium and cells lysed after to 24 hrs.

#### **2.4.6 Culture of HUVEC**

HUVECs were cultured in Medium 200 containing LSGS and incubated at  $37^\circ\text{C}$  and 5% CO<sub>2</sub>. Cells were maintained by replacement of the fresh culture medium every 48 hours after the establishment of the subculture. For subculture of HUVECs, the medium was removed from the flask prior to addition of 4ml of Trypsin/EDTA solution to the flask. The flask was rocked to ensure that the entire

surface was covered. The flask was incubated for 3 minute at room temperature followed by viewing the culture under a microscope to assure cell dislodgement from the surface. After that, complete medium was added to neutralise the action of Trypsin/EDTA. The cells were collected by centrifugation at 180 X g for 7 minutes. Supernatant was carefully discarded leaving the pellet at the bottom of the tube. The pellet was then resuspended with complete medium. HUVEC cultures seeded at  $2 \times 10^3$  cells per  $\text{cm}^2$  of growing area. The cells should reach 80% confluence in 5-6 day before subculturing. Six-well plates were seeded at  $2 \times 10^5$  each well and grown to 60% confluency prior to use.

#### **2.4.7 Culture of EA.hy926 cells**

EA.hy926 cells were cultured in DMEM supplemented with 10% (v/v) FCS at 5% (v/v)  $\text{CO}_2$  in air, 37 °C. For experiments cells were detached with Trypsin/EDTA solution (0.1%) diluted in PBS and the effect of Trypsin neutralised with complete medium. Cells were then centrifuged at 250 X g for 5 minutes and resuspended in fresh medium prior to culture cells at  $2 \times 10^5$  per well into each well of six-well plates and grown to 60% confluency depending on future application.

#### **2.4.8 Culture of HEK293 cells**

HEK293 cells were kind gift from Dr Louise Fairall (Biochemistry Department, University of Leicester, UK). Cells were grown in Freestyle media on a platform shaker incubator at 37°C in 5%  $\text{CO}_2$  with rotation at 150 rpm. Cells were maintained between  $0.35 \times 10^6$  and  $2.4 \times 10^6$  cells/ml (the culture volume should not exceed 20% of the total volume of the culture bottle). For transient transfection cells were maintained at  $1 \times 10^6$  cells/ml prior to performing transfection.

## **2.5 Protein Production**

### ***2.5.1 Expression of Soluble Ectodomains***

cDNA encoding wild-type Tie2 ectodomain (1–442) was subcloned into pcDNA 3.1 upstream of a human Fc tag and C-terminal His6 sequence (kindly supplied by Dr Richard Kammerer, Paul Scherrer Institute, Switzerland) for expression of soluble ectodomain in HEK293 cells. Site-directed mutagenesis was performed to modify this wild-type sequence to correspond to the evolved mutant using the QuikChange protocol (Agilent Technologies) and confirmed by sequencing.

### ***2.5.2 Large-scale transient transfection of HEK 293 cells for protein production***

Soluble ectodomain-Fc fusion proteins were achieved by transfection of HEK293 cells in suspension using polyethylenimine (PEI). HEK 293 cells were cultured in 300 ml of medium to a density of  $1 \times 10^6$  cells/ml in 1000ml shaken flask prior to transfection. For a standard protocol of transfection; DNA: PEI ratios (1:2) or 300µg of DNA and 600 µg of the linear isoform of PEI (1mg/ml) were incubated in 30mls of PBS for 20 minutes at room temperature resulting in DNA-PEI complex that are suitable for efficient transfection before addition to the cells. Cells were grown for 3–4 days to allow the fusion proteins to accumulate in the medium.

### ***2.5.3 Protein Purification***

Cells were harvested 4-5 days post-transfection by centrifugation at 6000g at room temperature for 10 minutes. Recombinant His-tagged protein expressed in HEK293 cells was purified from conditioned medium by gravity-flow chromatography using Ni-NTA Agarose beads (Qiagen). Fractions of 0.5ml volume of eluted protein were collected and combined following SDS-PAGE and Coomassie blue staining. Purified protein was stored at 4°C.

#### **2.5.4 Exchanging the elution buffer**

Since the high concentration of salt and imidazole in the elution buffer is not suitable for downstream applications. The eluate required buffer exchange. This can be done by:

##### a) Dialysis

The removal of buffer salt and LMW contaminants from purified protein was conducted using Slide-A-Lyzer Dialysis Cassettes with a 3.5K MW cut off suspended in 5L of appropriate buffer for 18-24 hours at 4°C.

##### b) Desalting

Protein purification was conducted using a Zeba desalting column (10 ml) and buffer exchange into Tris-buffered saline containing 10% glycerol. This device can remove greater than 95% of salt and provided high protein recovery.

#### **2.5.5 Bradford assay for Protein quantification**

Following buffer exchange a Bradford assay was performed to determine the protein concentration. Briefly, the Bradford reagent was diluted in dH<sub>2</sub>O (1 part Bradford: 4 parts d H<sub>2</sub>O), then filtered through a 0.5 micron filter. 10 µl of purified protein was added and mixed in 200 µl of the diluted reagent into 96 well plates allowing the formation of blue colour. The incubation time was at least 5 minutes at room temperature prior to measurement. Additionally, a standard curve was prepared using a serial dilution series (0.05-1.0 mg/ml) of a known BSA sample concentration. The samples and standards were measured the absorbance at 595 nm using the Infinite®200 NanoQuant (Tecan) machine. Finally, the concentration of protein samples was analysed by a standard curve.

#### **2.6 Analysis of Ang1 Ang2 and Ang4 binding to wild-type or evolved ectodomain-Fc by biolayer interferometry.**

Evolved protein was tested by measuring the affinity of the evolved ectodomain-Fc for Ang1, Ang2 and Ang4 at least 3 different concentrations (for Ang1 at 10,

20 and 40nM, for Ang2 and Ang4 at 20, 40 and 60nM) using biolayer interferometry (BLI). Evolved ectodomain-Fc or Wt ectodomain immobilized on sensors for Anti-IgG Fc Capture (AHC) biolayer interferometry. Dip and Read™ Biosensors (ForteBio) were used as per manufacturer's instructions. The apparent observed  $K_{on}$  values for the reaction between the dimeric molecule and multimeric ligand was used to analyse the binding of evolved ectodomain-Fc or Wt ectodomain to Ang2, Ang1 and Ang4.

## **2.7 Binding Assays**

ELISA assays were performed to determine ligand-receptor binding. Briefly, 5 µg/ml Ang1 or Ang2 was coated in 96-well plates by incubating overnight at 4°C. The plate was blocked with washing buffer (TBS containing 1 mg/ml BSA and 0.1% Triton-X 100). Following blocking, different concentrations of fusion protein were allowed to bind for 2 h and, after that, bound fusion proteins were incubated with anti-Tie2 ectodomain antibodies (dilution 1:100). Peroxidase-conjugated secondary antibody (1:5000) was incubated after washing followed by colorimetric quantification. For quantitative comparison, curve fitting to saturation binding data were analysed by nonlinear regression using the Prism 6 software (GraphPad Software Inc). Concentrations of ectodomains at half-maximal binding were calculated from the binding curves. In each ELISA experiment, binding of each mutant is compared to binding of wild-type in binding maximum.

## **2.8 Protein**

### ***2.8.1 Preparation of whole cell lysates for SDS-PAGE***

In HUVEC or EA.hy926 cells, medium was removed from 6 well plates after washing with cold PBS. Cells were harvested with 70µl of 2X sample buffer-DTT per well on ice followed by collection of each cell lysate per well into Eppendorf tubes, 1.5 ml. For DT40 cells,  $1 \times 10^6$  cells were collected by centrifugation at 250g for 5 minutes on ice. Cells lysates either HUVECs or EAhy.926 were then sonicated and boiled at 95°C for 6 minutes prior to centrifugation at 250g for 1

minute to pellet debris. Samples were stored at -20°C if not used directly for SDS-PAGE.

### **2.8.2 SDS-polyacrylamide gel electrophoresis (PAGE)**

The appropriate percentage polyacrylamide solution for the resolving gel was prepared based upon size of protein. The stacking gel was layered over the top of the resolving gel containing a lower concentration of acrylamide and of a lower pH. The gel was immersed in a tank of running buffer. 30 µl of each sample and 10 µl of the protein marker (Precision Plus Kaleidoscope Standards; BioRad; Hemel Hempstead, UK) were loaded on the gel. Gel was resolved at 120V until the molecular weight of the target protein was at the desired location. SDS-PAGE was performed (Table 2.3).

**Table 2.3 SDS-PAGE composition**

	Resolving			Stacking
	7.5%	10%	12%	5%
30%Acryl/Bis (ml)	5.0	6.7	8.0	3.3
ddH2O (ml)	10.9	9.6	7.9	13.7
Tris(ml)	3.7 (2M pH8.8)			2.5 (1M pH6.8)
20% SDS (µl)	100			100
10% APS (µl)	134			200
TEMED (µl)	14			20

### **2.8.3 Western blotting**

The separated proteins were transferred from SDS/PAGE gel onto a Hybond™ECL™nitrocellulose membrane (Amersham; GE Healthcare; Little Chalfont, UK), between filter paper and foam pre-soaked in transfer buffer, within a cassette by electrotransferring as described by Towbin et al. (Towbin, Staehelin & Gordon 1979). Proteins were transferred at 150mA RT overnight or 230-250mA 4°C for 3 hours. The nitrocellulose membrane was then probed as further described.

#### **2.8.4 Immunoblotting**

Nitrocellulose membranes were incubated in blocking buffer (5% non-fat milk/TBS-TX-100) for 1 hour prior to immunoblotting. After washing three times with TBS-TX-100, the membrane was typically incubated with primary antibody diluted in 5% non-fat milk/TBS-TX-100 at 4°C overnight. The membrane was then washed three times in TBS-TX-100 for a total of 30 minutes prior to incubation with secondary antibody and washing three more times. Finally, the membrane was exposed to developer solution for 1 minute. The membrane was then wrapped in cling film and exposed to chemiluminescence (ECL) system (Amersham Pharmacia Biotech; UK) detection Kodak imaging film for 1-5 minutes depending on the intensity of the bands. The films were developed and the protein markers were aligned to the membrane and marked.

For re-probing a membrane, the membrane was stripped of antibody in 1X Re-blot solution (Chemicon International) for 15 minutes. The membrane was then washed in 1XTBS 0.1%TX-100 solution, blocked and probed with appropriate primary and secondary antibodies as detailed in Table 2.4.

#### **2.8.5 Cellular Assays**

The endothelial cell line EA.hy926 and HUVECs were cultured in DMEM containing 10% fetal bovine serum and Medium 200 containing LSGS at 37 °C and 5% CO<sub>2</sub>. Cells were made quiescent by incubation for 4 hour and 1 hour in serum-free medium, respectively. Following incubation in serum free medium, cells were stimulated with Ang1, in the absence or presence of Ang2, with or without 25µg/ml wild-type or evolved ectodomain-Fc for 30 min. After washing, cells were harvested on ice. The detection of phosphoSer-473-Akt and total Akt were resolved by SDS-PAGE and analysed by immunoblotting.

**Table 2.4 Details of conditions used for specific antibodies in Western blotting**

<b>Primary Antibody</b>	<b>Application</b>	<b>Secondary antibody</b>	<b>Application</b>
Phospho-Ser-473-Akt (Cell Signalling Technologies Inc.)	dilution 1:1000 overnight at 4°C	Anti-rabbit IgG HRP (GE Healthcare)	dilution 1:2000 1 hr RT
Akt Antibody (Cell Signalling Technologies Inc.)	dilution 1:1000 overnight at 4°C	Anti-rabbit IgG HRP (GE Healthcare)	dilution 1:2000 1 hr RT
Human Integrin $\alpha_v\beta_3$ , MAb (R&D systems)	dilution 1:1000 overnight at 4°C	Anti-mouse IgG HRP (Sigma Aldrich)	dilution 1:2000 1 hr RT
Anti-Integrin beta 3 MAb (Abcam)	dilution 1:1000 overnight at 4°C	Anti-rabbit IgG HRP (GE Healthcare)	dilution 1:2000 1 hr RT
polyclonal rabbit anti-integrin $\beta_3$ subunit AB1932; Chemicon, (Chemicon International)	dilution 1:1000 overnight at 4°C	Anti-rabbit IgG HRP (GE Healthcare)	dilution 1:2000 1 hr RT
Anti-FLAG M2 (GE Healthcare)	1:1000 45 min RT	Anti-mouse IgG HRP (Sigma Aldrich)	dilution 1:2000 1 hr RT
Anti-human Tie2 Ab (R&D systems)	dilution 1:1000 overnight at 4°C	Polyclonal anti-goat Ig HRP (Dako)	dilution 1:2000 1 hr RT
Goat anti Factor B	dilution 1:1000 overnight at 4°C	donkey anti-goat IgG- HRP	dilution 1:2000 1 hr RT
Anti-ADA polyclonal Ab (Abcam)	dilution 1:1000 overnight at 4°C	Anti-rabbit IgG HRP (GE Healthcare)	dilution 1:2000 1 hr RT
Anti- $\alpha$ -tubulin monoclonal Ab (Sigma)	dilution 1:1000 RT 20 minutes	Anti-mouse IgG HRP (GE Healthcare)  1:5000	dilution 1:2000 20 minutes RT
Anti-His6 Ab (Sigma)	dilution 1:1000 RT 1 hr	Anti-rabbit IgG HRP (GE Healthcare)	dilution 1:2000 30 minutes RT

### **2.8.6 ImageJ analysis**

Immunoblotting films were scanned as black and white 8-bit electronic files of 300 dpi or higher. Calibration was performed for uncalibrated optical density, protein bands were selected and the area under the intensity curve was digitally calculated. Relative optical density was calculated by comparison of sample values with a ubiquitous loading control. Tubulin was used as protein loading for AID expression, while Akt was used as control loading for pAkt.

### **2.8.7 Immunoprecipitation: Ang2 integrin binding Western blot analysis in a cell-free system**

Three 50µl aliquots of Sepharose G beads were centrifuged at 1000g and washed 3 times with 500µl NP40 buffer (100mM Tris-HCl, 300mM NaCl, 10% (v/v) NP40 solution, 10% (v/v) glycerine). In the meantime, Ang2 (300ng), anti-His (dilution 1:500) and 5 µl purified undiluted αVβ3 integrin (R&D system™) with or without 25 µg/ml evolved ectodomain-Fc were incubated on ice for 30 min. Following incubation, samples were incubated with Sepharose G beads in 1.0 ml NP40 buffer overnight at 4°C. Anti-His incubated with integrin was used as control. The immunoprecipitate samples were centrifuged at 1000g for 2minute. The beads were washed 3 times with PBS and boiled with 2X sample buffer, and analysed by SDS-PAGE and immunoblotting for Anti-integrin antibody.

### **2.9 Migration assay**

Transwell migration assays were performed to study the migratory response of endothelial cells to angiogenic inducers or inhibitors using Transwell tissue culture wells containing 8-µm pore size inserts (BD Biosciences, Oxford, UK). Serum-free medium containing 250µg/ ml BSA together with Ang1 or Ang2, in the absence or presence of soluble ectodomain-Fc fusion protein, was placed in the lower chamber of the wells. 10<sup>5</sup> endothelial cells, in serum-free medium containing 250µg /ml BSA, were placed in the upper chambers. Following an incubation period for 4 hours at 37°C, to allow cells to migrate through the membrane depend on the test agents, cells that did not migrate through the pores

were gently removed with a cotton bud. Cells on the lower side of the insert filter were fixed in 4% formaldehyde. After washing, nuclei were stained with 4', 6-diamidino-2-phenylindole (0.1 µg/ml). Membranes were then mounted in glycerol and the numbers of cells migrating to the lower side of the membrane were counted in five random fields a light microscope at x20 magnification.

## **2.10 Flow cytometry & Florescence Activated Cell Sorting (FACS)**

### ***2.10.1 Binding and fluorescent cell labelling reagents***

Biotinylated Recombinant Human Angiopoietin-2, Recombinant Human Angiopoietin-2 and Recombinant Human Angiopoietin-1 were all obtained from R&D Systems™ (UK) and diluted in PBS to the required experimental concentration. Dilution of staining reagents, washes and incubations of cells were performed in 10% FCS/90%PBS throughout the experiments.

### ***2.10.2 On-cell binding and labelling procedure***

DT40 stably expressing Tie2 ectodomain were collected by centrifugation at 250g and washed. After that, cells were allowed to bind 3.4nM Ang1 and 0.5nM biotinylated Ang2 at room temperature for 30 minutes. All incubations were then washed followed by staining with angiopoietin; anti-FLAG-FITC antibody and fluorescent secondary antibody (streptavidin-PE/Cy5) at 4°C for 30 minutes. Finally, each group of cells were transferred into 5 ml Falcon FACS tubes and kept in ice box until flow cytometry analysis. All subsequent steps were performed keeping the sample in the dark as much as possible by covering the samples with foil to avoid photobleaching.

### ***2.10.3 Flow cytometry***

Cells were labelled, washed and resuspended in approximately 500µl volume PBS/FCS in a 5ml Falcon polystyrene tube. Unstained cells were used in each

assay to quantify autofluorescence and compare with the stained cells. A BD FACSAria™II cell sorter was utilised with an 85µm nozzle. Excitation lasers and emission bandpass filters were employed for the various fluorophores as stated in Table 2.5. Live cells were gated based on forward and side scatter characteristics. Ten thousand events were recorded for each analysis with BD FACSDiva™ software. The FCS files which contain raw flow cytometry data were analysed in WinMDI (Windows Multiple Document Interface for Flow Cytometry).

**Table 2.5 Fluorescence spectra**

	Excitation laser (nm)	Bandpass filter (nm)
FITC	488	530/30
Streptavidin-PE		582/15
Streptavidin-PE/Cy5		660/20

#### ***2.10.4 Competitive equilibrium Ang1 and Ang2***

5 x 10<sup>5</sup> cells per data point were collected by centrifugation at 250g for 5 minutes. Aliquots of cells of serially diluted recombinant Ang1 together with 0.5nM biotinylated recombinant Ang2 were incubated at RT for 1hour to produce the desired concentrations. Cells were then collected by centrifugation at 700g 4°C for 1 minute and washed once. Each aliquot was resuspended in 50µl cold streptavidin-RPE and incubated at 4°C for 30 minutes. Cells were again washed and collected as previously.

#### ***2.10.5 Fluorescence Activated Cell Sorting (FACS)***

Before flow cytometry and FACS analysis, controls were used for setting gates and discriminating positive population. For meaningful data analysis, the cell population was gated to exclude the dead cells from the viable cells. The dead cells can be distinguished from viable cells by analysing the sample through the flow cytometer based on the forward and side scatter setting which distinguish the size and complexity of the cells in the sample. Dead cells have lower forward

scatter and higher side scatter than live cells. Once the viable cells were gated, the negative and positive control samples were placed into the flow cytometer and acquisition was com in set up mode. The unstained cells served as controls to account for autofluorescence from cells due to normal cell components which fluorescence, such as riboflavin and flavoprotein (Aubin 1979). Single stained controls were used to set fluorescence compensation to account for spillover of the emission of one flurochrome into the emission from as other. The single stained controls were stained for FLAG epitope tag with anti-FLAG-FITC and for Ang2 with streptavidin-PE/Cy5 (Table 2.6).

**Table 2.6 Antibodies used for FACS**

Detection	Reagent	Dilution
FLAG	Anti-FLAG M2-FITC monoclonal AB (Sigma Aldrich)	1:100
Biotinylated Ang2	streptavidin-R-phycoerythrin conjugate (Sigma) or streptavidin-PE/Cy5 (BD Pharmingen™)	1:25 1:25

DT40 stable cells were stained as previously described. Under sterile condition, the cells were resuspended in PBS at a density of  $10 \times 10^6$  cells /ml. They were then subjected to FACS analysis. The samples lines of machine were rinsed thoroughly with FACS clean solution and sterile 1 x PBS was used as sheath fluid. The stream was adjusted and the machine calibrated by drop delay. An 85µm nozzle was used and the 488 nm Argon laser was used for excitation of the chromophore the FLAG-FITC and the PE-Cy5 Streptavidin chromophore. Compensation can be used to correct for spillover and cells were also gated and sorted on live cells by FSC versus SSC. The sorted cells were run at 1000 events/sec. They were collected directly into 4°C sterile complete medium and cultured in flasks as soon as possible.

### **2.11 Method for in vivo experiments**

Littermate C57Bl/6 (age and sex matched) were taken from colonies bred in a specific pathogen barrier unit at University of Leicester (PPL 60/4327). Mice were humanely restrained, and received 5µg LPS (*E. coli* 0111:B4, TLR grade; Enzo Life Sciences, Inc) with or without 15µg purified evolved ectodomain or control ectodomain protein in 10µl volumes diluted in PBS. The injection site was the mouse hock, a refinement over models eliciting oedema in the foot-pad. The procedure was compliant with Home Office regulations and institutional guidelines. After two hours, mice were culled by cervical dislocation and hock was prepared for histological analysis. These procedures were performed by Dr. Cordula Stover (University of Leicester). The tissues were fixed and decalcified using 6% (v/v) trichloroacetic acid in neutral buffer saline, and paraffin embedding. 5µm sections were stained with Wright's stain and those selected in which the distance of the tibia periost to epidermis could be comparatively measured using Delta Pix Insight (v.3.3.1) imaging software, providing a value of subcutis thickness (local oedema). Nine to thirteen points were obtained from each section, blinded for treatment.

## Chapter 3: Evolution of Tie2 ectodomain

This chapter describes the use of SHM-driven directed evolution to generate novel variants of Tie2 ectodomain which exhibit preferential binding to Ang2. However, before the experiment could be performed it was necessary to establish and optimize the methodology. This chapter describes establishment of FACS protocol, cell staining, plasmid recovery and sequencing. In addition, the cloning and expression of AID is described. After establishing all methodology, the evolution of Tie2 ectodomain was attempted.

### 3.1 Establishing FACS

Optimizing FACS was performed before starting the experiment. Briefly, 10 million Tie2-DT40 cells were collected by centrifugation. These cells were then washed with cold 10% FCS-PBS solution and incubated with biotinylated-Ang2 at a concentration of 0.5 nM for 30 min. This concentration was based on previous experiments performed by Dr. K. Steele (Table 3.1). Briefly, Tie2-DT40 cells were incubated to equilibrium with varying concentration of biotinylated Ang2 followed by labelling with anti-FLAG-FITC and streptavidin-R-PE. Cells were then subjected to flow cytometry for examination. An Ang2 concentration, 0.5 nM was suitable for the early round of equilibrium sorting, should capture the majority of desired mutants. Following the third rounds the Ang2 concentration was adjusted to 0.25nM.

**Table 3.1 Fluorescence intensity by Ang2 concentration**

Ang2 (nM)	Geometric MFI
0	40
0.125	55
0.25	75
0.5	155

Following the incubation, cells were then labelled with anti-FLAG-FITC and streptavidin R-PE. The primary anti-FLAG-FITC was used to detect cell surface

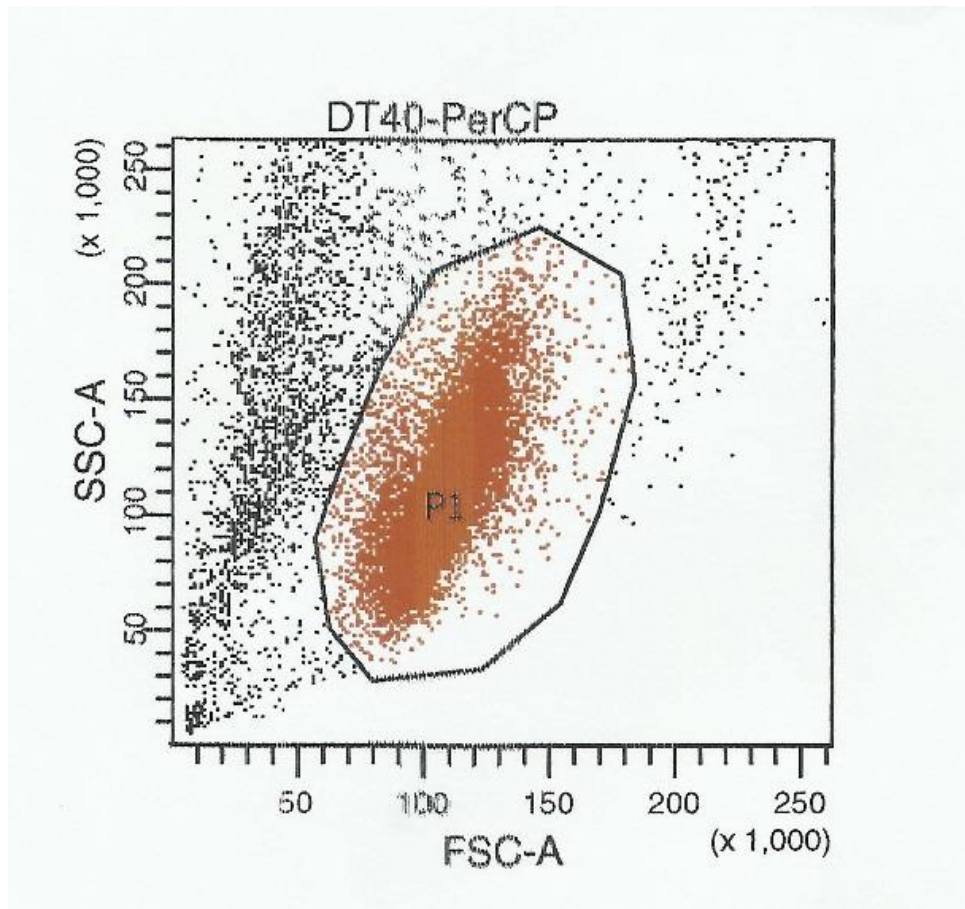
Tie2 which has a FLAG-epitope tag and cells were subsequently labelled with streptavidin R-PE to detect the levels of Ang2 bound Tie2 receptors. The cells were analysed and selected for high affinity binding to Ang2 by FACS.

The forward and side scatter dot plot for a typical fluorescent labelled cell population is shown in Figure 3.1. The cells contained in the region P1 are live cells, whereas other cells are dead cells. There are differences in complexity, granularity and size between live cells and dead cells. Thus, only the live cells in the region P1 were further analysed.

Three controls were analysed; these were (i) un-labelled cells (ii) anti-FLAG-FITC antibody only (iii) Ang2 and streptavidin R-PE only. Unlabelled cells were initially used to account for auto-fluorescence of the cells to adjust the cut-off for the flow cytometric parameters. An example of dot plot showing the low signal of the unstained population is shown in Figure 3.2. In addition, single antibody labelled controls were used for fluorescence compensation to correct the detected spillover of the emission of one fluorophore into the emission of another fluorophore. The single labelled controls which were labelled with the FLAG epitope tag by FITC and for Ang2 by streptavidin R-PE. For FITC labelling, a FITC channel can be set for maximal FITC and minimal FITC signal in the streptavidin-R-PE channel. Similarly, PE channel was set to record streptavidin-R-PE signal in FITC channel. The amount of the spillover from each fluorophore channel into each of other fluorophore was then determined and compensated. Figure 3.3A shows clear staining for FLAG-FITC and no staining streptavidin-R-PE channel. Likewise, streptavidin-R-PE staining and no FLAG-FITC were seen in streptavidin-R-PE channel as shown Figure 3.3B.

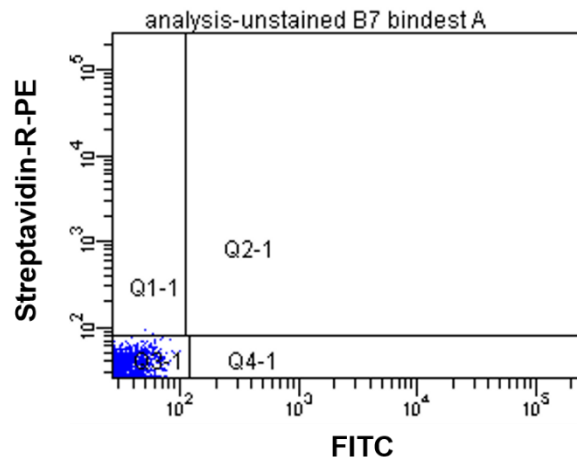
In order to sort cells for highest binding to Ang2 it is necessary to normalize the Ang2 binding for the level of Tie2 expression by each cell. To do this, cells were dual stained for Ang2-binding via streptavidin R-PE and Tie2 expression via the FLAG Tag on Tie2. Dual stained cells are shown in

Figure **3.4A**.



**Figure 3.1 Representative dot plot showing the population of live cells in the square P1.**

The X axis is forward scatter which indicates the size of cells, whereas the Y axis representing side scatter showed the complexity of cells. The dead cells and debris which were black dot that can be separated and excluded from analysing by forward and side scatter dot plot. Therefore, only live cells in the region P1 were analysed in the next step.



**Figure 3.2** Representative dot plot showing the signal for FLAG and Ang2 in unstained cells.

An example of dot plot showing the unstained Tie2-DT40. The cells are only in left lower quadrant (Q3) indicating the low signal for FLAG and Ang2.

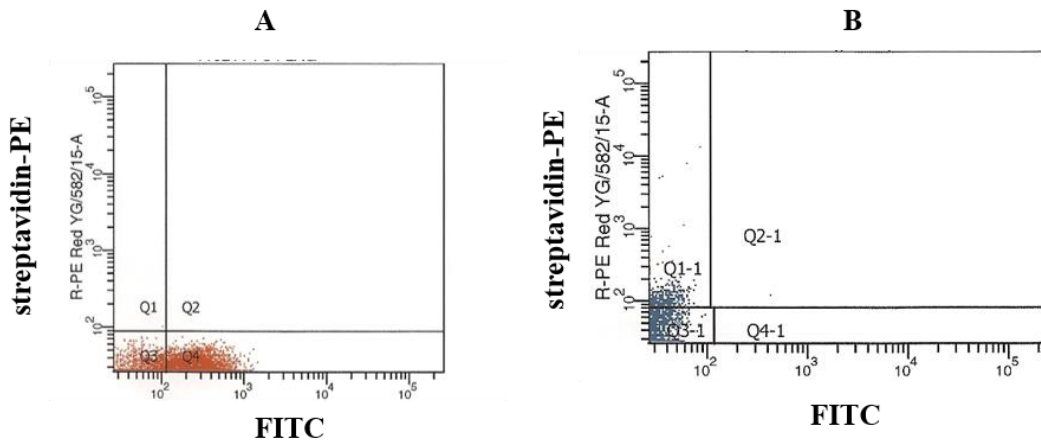


**Figure 3.3** Representative dot plot showing the single stained control.

- (A) The DT40 expressing Tie2 cells were labelled with anti-FLAG staining only.
- (B) Cells were stained with biotinylated-Ang2 and streptavidin-R-PE staining only

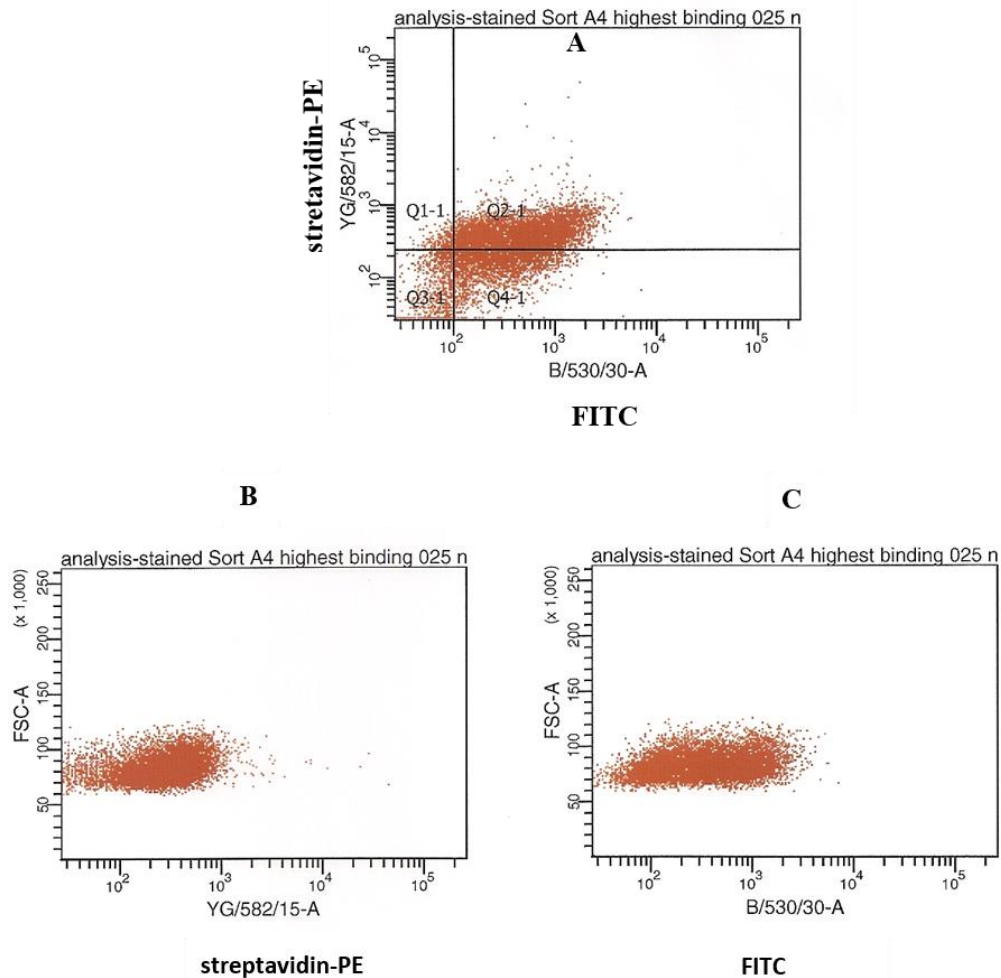


**Figure 3.4 Dual staining dot plots showing the signal of Ang 2 binding cell surface expressed Tie2 ectodomain.**

(A) The levels of Ang2 bound to the Tie2 expression on DT40 cell surface. Y axis and X axis are Ang2 binding and Tie2 expression signal, respectively.

(B) Forward scatter dot plot detected Ang2 binding to Tie2 on DT40 cell surface by streptavidin-PE.

(C) Forward scatter dot plot detected FLAG-tagged Tie2 expression on DT40 cell surface by the FITC dye.

The primary anti-FLAG-FITC and streptavidin R-PE were used to detect cell surface FLAG-taggedTie2 and Tie2 bound Ang2 respectively. Cells labelled streptavidin R-PE reflected the Ang2 bound to the Tie2 receptor as shown in

Figure 3.4B while cells labelled the FITC-FLAG tag on Tie2 represented the levels of Tie2 expression as shown in Figure 3.4C. Figure 3.4A is a dot plot representing the Ang2 bound (Y axis) against the level of Tie2 expression (X axis) on each cell. The cells in the Q3 show the Ang2 bound to Tie2 with lower affinity. The cells in the Q2 quadrant were cells that bound Tie2 with higher affinity.

For maximal sensitivity, a large signal for Ang2 binding and low carry over into FLAG binding is required. At first, Streptavidin PE and FITC were used for double labelling FACS analysis. Alternative fluorophore sets would be FITC and streptavidin-PE/Cy5, as streptavidin-PE/Cy5 has a stronger fluorescent signal. Streptavidin-PE/Cy5 is a tandem conjugate between streptavidin-R-PE and Cy5. In order to compare a streptavidin-PE/Cy5 with streptavidin R-PE, an experiment was set up. In this experiment groups of cells were compared: unstained Tie2-DT40, Tie2-DT40 cells which were incubated and labelled with biotinylated-Ang2 and streptavidin-PE/Cy5 respectively, Tie2-DT40 cells labelled with streptavidin-PE/Cy5 alone, and Tie2-DT40 cells that incubated and labelled with biotinylated-Ang2 and streptavidin R-PE respectively.

The results show that the streptavidin-PE/Cy5 using yellow green laser gave a stronger fluorescence signal than streptavidin R-PE as shown in Figure 3.5. Figure 3.5B and Figure 3.D show the background staining of streptavidin-PE/Cy5 indicating low background level of signal in cells stained with streptavidin-PE/Cy5 only. Therefore, streptavidin-PE/Cy5 was used instead of Streptavidin PE since streptavidin-PE/Cy5 could detect Ang2 binding without contributing to the FLAG-FITC signal.

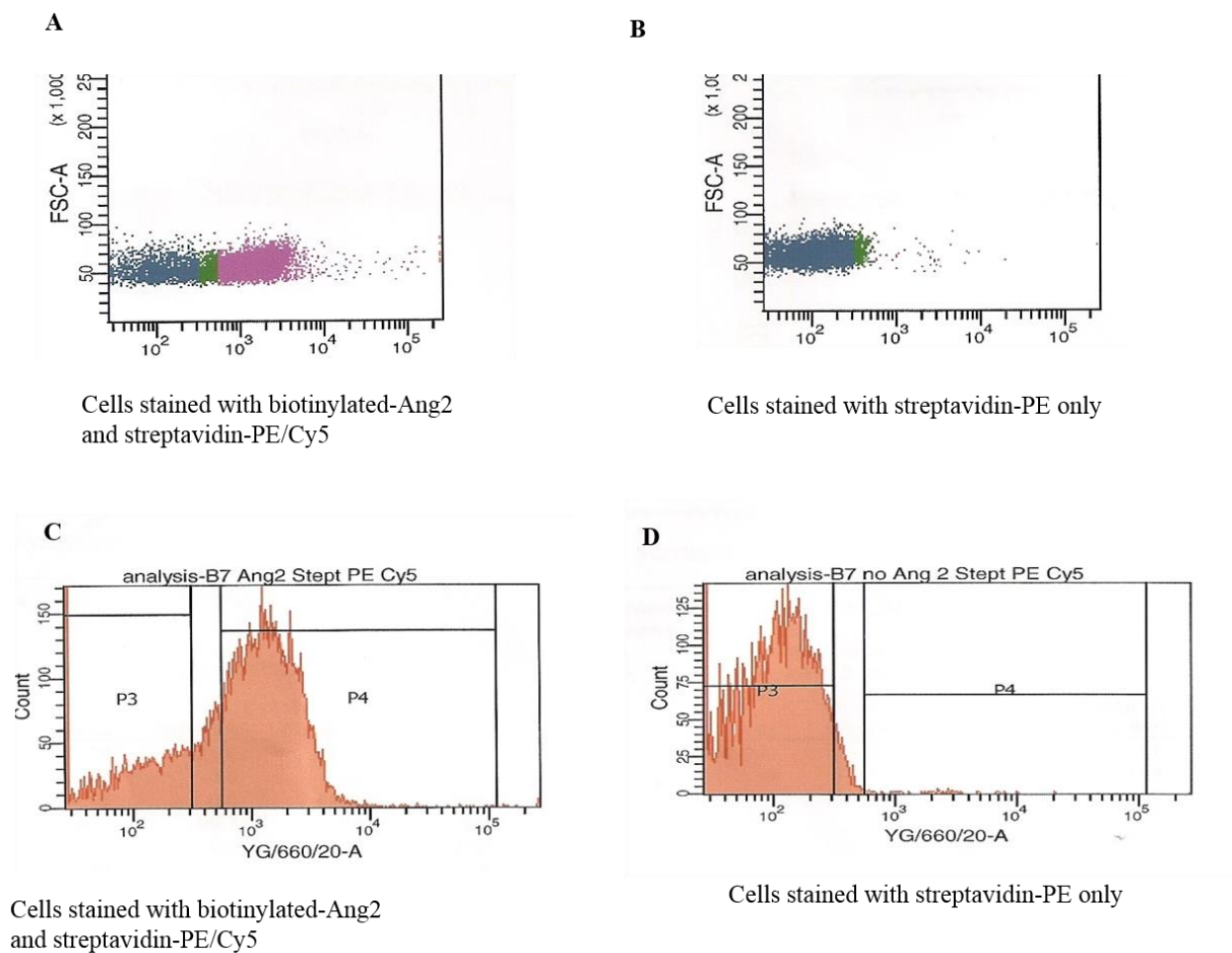


**Figure 3.5 Dot plot and histogram comparing the fluorescence signal of streptavidin-PE/Cy5 between cells incubated biotinylated-Ang2 and cells without Ang2.**

(A) The dot plot indicates the signal of Ang2 incubated with biotinylated-Ang2 and streptavidin-PE/Cy5. (B) The dot plot indicates the signal of cells stained with streptavidin-PE/Cy5 only. (C) The histogram shows the strong signal of Ang2 in the cells incubated and stained with biotinylated-Ang2 and streptavidin-PE/Cy5. (D) The histogram represented low background levels of signal in cells stained with streptavidin-PE/Cy5 only.

### 3.2 DNA recovery and sequencing from sorted cells

Once, the cells had been sorted. It would be necessary to be able to recover the DNA encoding Tie2 and determine their sequences. To establish the methodology for this, sequencing of sorted cells were performed. For FACS sorting, cells were screened and the desired mutant phenotypes selected under sterile conditions. Cells were resuspended at a density of approximately  $2.5 \times 10^6$  per ml in 5ml Falcon polystyrene tubes and stored on ice. An example of dot plot representing cells was selected from the sorted gates that specified live cell population. Sorting was performed in 2-way purity mode at maximum speed of 2000 events per second. Sorted cells were directly collected into sterile complete medium for further growth. This sorted population was labelled (Figure 3.6).

Cells enriched for Ang2 binding (Population A) shown in the triangle P2 ( Figure 3.6) were sorted and collected. These sorted cells were used to prepare mRNA before proceeding to RT-PCR and PCR. The PCR product was then checked by agarose gel electrophoresis before gel purification. Subsequently, addition of the A overhang in PCR product was performed. PCR product was cloned into a TA cloning vector (pCR4-TOPO, Invitrogen) and then transformed into *E. coli*. Once clones were obtained they were sequenced. There were five colonies on the ampicillin agar plate at first and second time. The low number of colonies may reflect an inefficient ligation. To attempt to improve on this, the incubation of cloning reaction was extended for 1 hour instead of only 20 minutes before proceeding to transformation. The transformant cells were further plated on agar plate with ampicillin and incubated for 18 hours at 37°C. Increased number of colonies were found after the increased incubation time of the cloning reaction. There were 70 colonies on Agar plate. Therefore the methodology for recovery of plasmid for sorted DT40 cells was established.

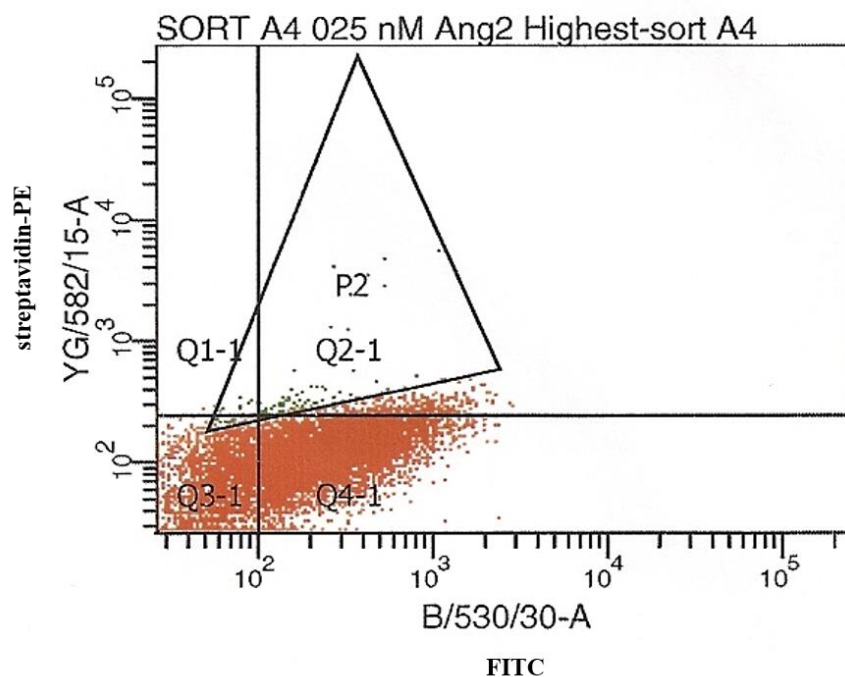


**Figure 3.6 Dual staining dot plots showing the sorted cells.**

10 million Tie2-DT40 cells were incubated with 0.25nM biotinylated-Ang2 prior to labelling with streptavidin-PE/Cy5 and anti-FLAG-FITC. Ang2 binding cells were sorted via 2-way purity. 1% of the gated live cell population in triangle P2 were sorted by FACS.

### 3.3 Cloning and expression of AID in the cells to maximize mutations

In order to test whether Tie2 ectodomain in DT40 cells was undergoing any mutation, DNA was recovered from cells at day 0 and after 12 weeks of growth. Of 20 sequencing analysed, 3 deletions and three point mutations was detected after 12 weeks. Three mutations were not in the binding domain. This suggests the cells were limited in their ability to mutate the Tie2 ectodomain. In order to maximize SHM, therefore, increasing expression levels of AID were attempted by overexpressing cDNA encoding the enzyme. AID was cloned into pEF6/V5-His-TOPO<sup>®</sup>. Briefly, the cDNA encoding AID (which was a kind gift of Dr. K. Steele) was amplified using AID primers (Appendix 1) and cloned in frame with V5 and Histags in the expression vector pEF6/V5-His-TOPO<sup>®</sup> (Appendix 7.4). This vector contains the human elongation factor 1 $\alpha$  promoter for high-level expression in mammalian cells. In addition, this vector contains the blasticidin resistant gene for selection of stable mammalian cell lines. The strategy for cloning AID is outlined in Figure 3.7. The AID was amplified by PCR using AID primers at an annealing temperature of 60°C. The PCR product size was confirmed by running 10  $\mu$ l of the PCR product on the agarose gel and was found to be of the expected size of approximately 600 bp seen in agarose gel (data not shown). The amplified product was ligated to the pEF6/V5-His TOPO<sup>®</sup> expression vector by TA cloning. Competent cells were transformed with ligation reaction and plated onto selective agar plates. Four colonies labelled 1-4 were picked from the transformation plate and inoculated in selective medium. Plasmid preparations were analysed by restriction enzyme. The entire molecular length of the pEF6/V5-His-TOPO<sup>®</sup> is 5840 bp. The 600 bp of PCR product was inserted in bases 1760 to 1761. The EcorRV and SnaB1 were chosen to cut the two regions of inserted DNA. So, the expected size of the positive clones should be 510 bp. A band of the expected size was seen in clone 3 indicating this AID plasmid was positive cloned as shown in Figure 3.8. This plasmid was then sequenced at the Protein and Nucleic Acid Chemistry Laboratory (PNCL), University of Leicester. The plasmid was obtained with the correct sequence (Appendix 6).

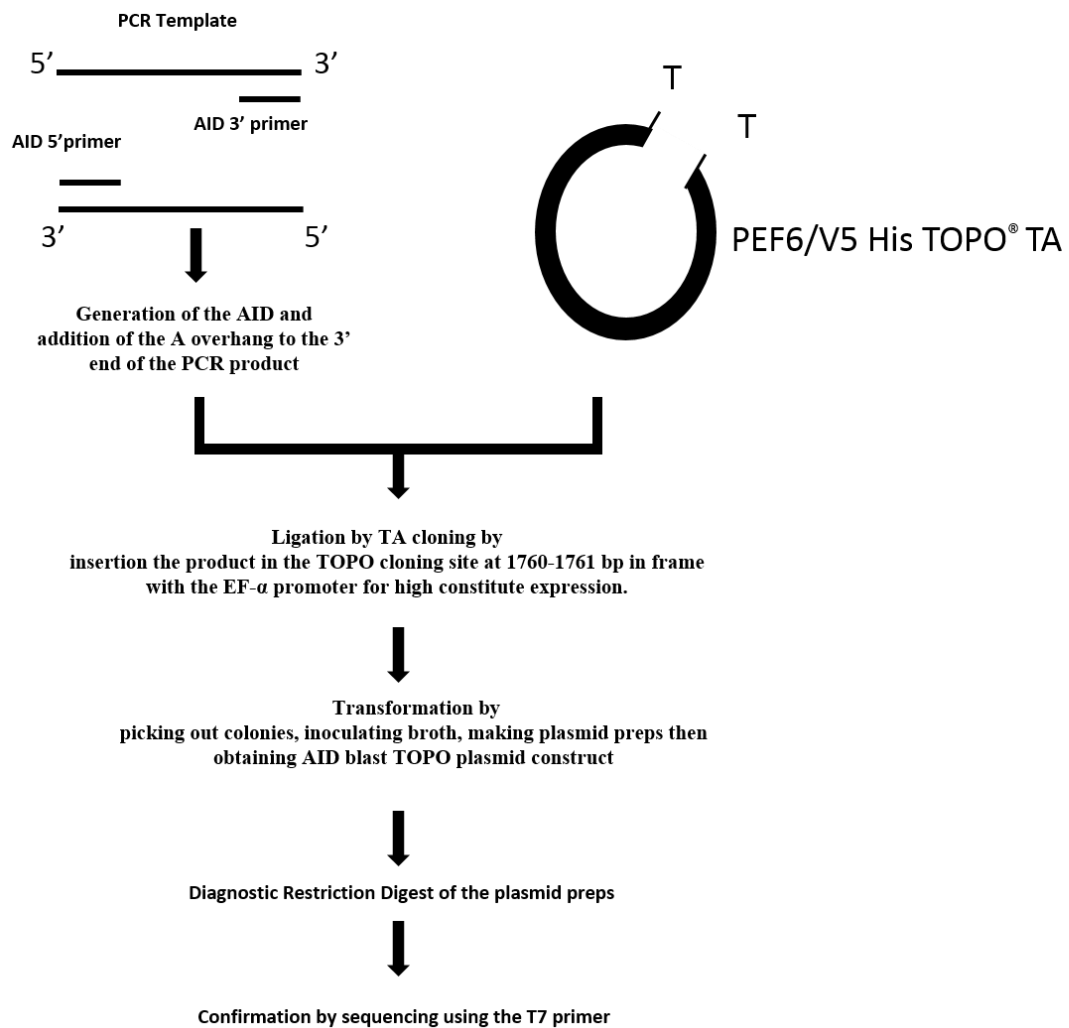


**Figure 3.7 Schematic depicting cloning strategy of human AID into pEF6/V5-His-TOPO®.**

The template of AID was amplified by proof-reading polymerase. The PCR product was cloned using the TA cloning method to produce pAID-TOPOblast<sup>r</sup> before proceeding to transformation and inoculation. The plasmid preparation was confirmed by sequencing.

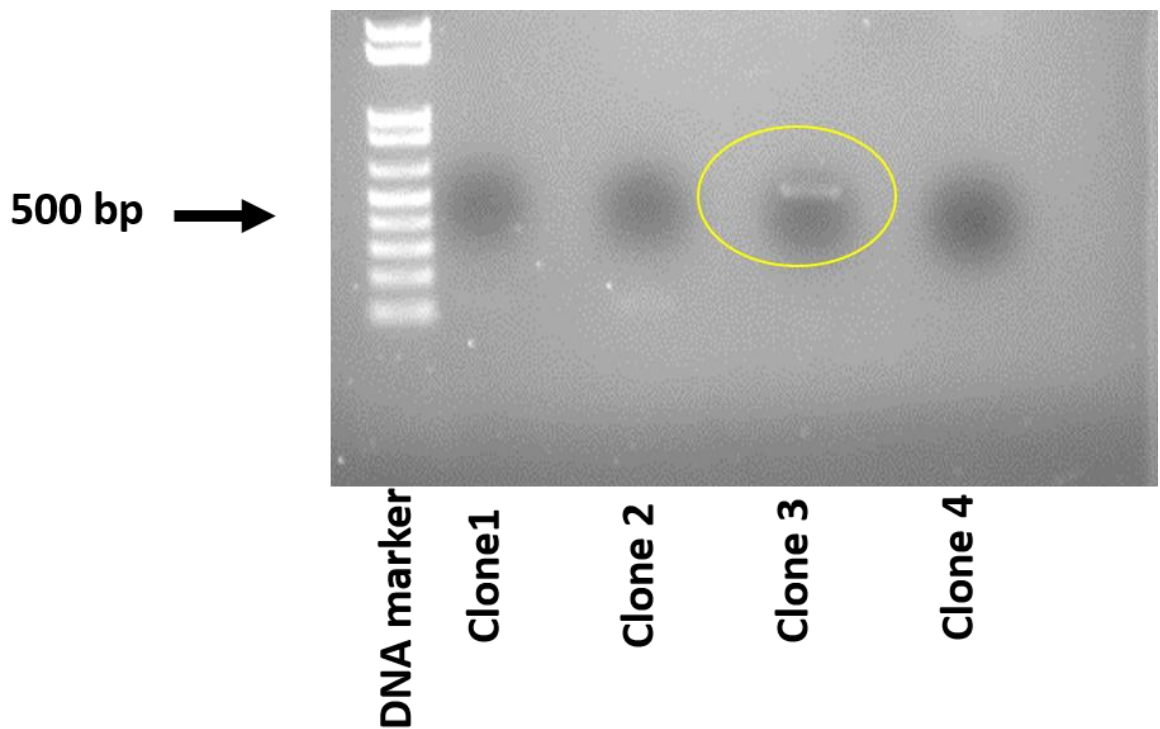


**Figure 3.8 Restriction digest for AID positive clone.**

Cloning was performed as described in Section 3.5. The four clones were picked out from agar plate and inoculated for Miniprep DNA. The four plasmids were digested with restriction enzymes which were the EcorRV and SnaB1. AID excised from the vector in positive clone. The product was resolved by electrophoresis on 1% agarose gel. The positions of molecular size markers are indicated. The expected size should be 510 bp. Band obtained for plasmid 3 indicating positive clone.

This plasmid was subsequently used for expression of AID in mammalian cells. The AID construct was analysed to confirm expression of the AID in mammalian cells. CHO cells were transfected when 60% confluent in 6-well plate using 10µg AID construct and Lipofectamine 2000 as described in Section 2.4.5.

CHO cells were harvested by lysis buffer after 24 hours post-transfection. SDS/PAGE and Western blot were run to analyse the cell lysate from transfection. The expected size of the AID protein is approximately 25 kDa. A band between 20 and 25 kDa was obtained in lane 4. Lane 2 served as a control and Lane 3, 5 were cells transfected with negative clones. As can be seen in Figure 3.9, a clear AID-immunoreactive protein of the expected size was expressed in the cells transfected with the AID plasmid. It was concluded that AID construct was expressed in mammalian cells.

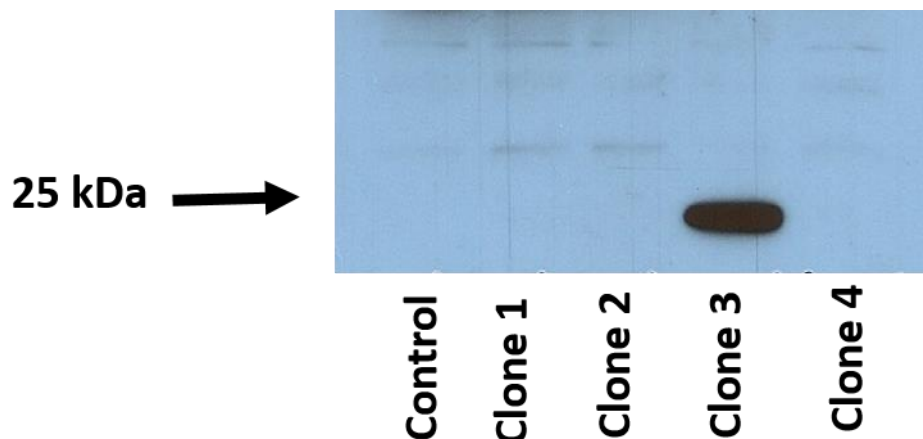


**Figure 3.9 Expression of AID in CHO cells.**

CHO cells were transfected with each plasmid from four clones. Post transfected cell lysate samples were subjected to SDS/PAGE and Western blotting. Immunoblotting analysis was performed with anti-AID polyclonal antibody. The positions of molecular size markers are indicated. The expected size of is approximately 25kDa. The expected band was seen in clone 3.

### 3.4 AID Transfection into Tie2-DT40 cells

AID was cloned into pEF6/V5-His-TOPO as described in Section 3.3. To establish Tie2-DT40 stable cell lines overexpressing AID, Maxiprep of AID-blast<sup>r</sup>-TOPO was performed as described in Section 2.2.4. For transfection both circular and linearized plasmid were used in separate transfections. Ethanol precipitation of AID-blast<sup>r</sup>-TOPO was performed prior to transfection of circular DNA

For linearisation of AID-blast<sup>r</sup>-TOPO, 50µg DNA was digested by using 1 unit of SspI enzyme per 1µg DNA overnight at 37°C. Small sample of the cut DNA was then run on agarose gel to check linearisation. One discrete band was obtained as shown in Figure 3.10 indicating linearisation. The digested DNA was then subjected to chloroform-phenol extraction and ethanol precipitation. Blasticidin selection was performed with 20µg/ml.

For transfection of circular DNA, DT40 Tie2 expressing cell lines was transfected with plasmid AID by electroporation (Section 2.4.2) and stable cell lines generated using the blasticidin selection. The cells were electroporated at 250V 950 µF (level 3). The electroporated cells were transferred in 30 ml complete medium incubated at 41°C. Blasticidin was added to the medium to select the AID positive cells. The cells were plated out 200µl per well in 96 well plates. And cultured for 7 to 10 days. Similar to circular DNA transfection, linearized DNA were performed using the same techniques but with different electroporation condition; electroporation at 700V 25µF was used. After 10 days, several AID-DT40 clones were seen in the 96 well plates. Seven separate AID-DT40 clones were picked and transferred into the flasks under the blasticidin selective pressure until becoming more confluent. Each clone of cells were harvested and further examined by SDS/PAGE and Western blotting to verify the presence and amount of AID in each clone. Clone Tie2-DT40 cells and AID negative clone-Tie2-DT40 cells were included as control. The membranes were first probed with anti-AID antibody following re-probing with tubulin anti-mouse HRP to check protein loading.

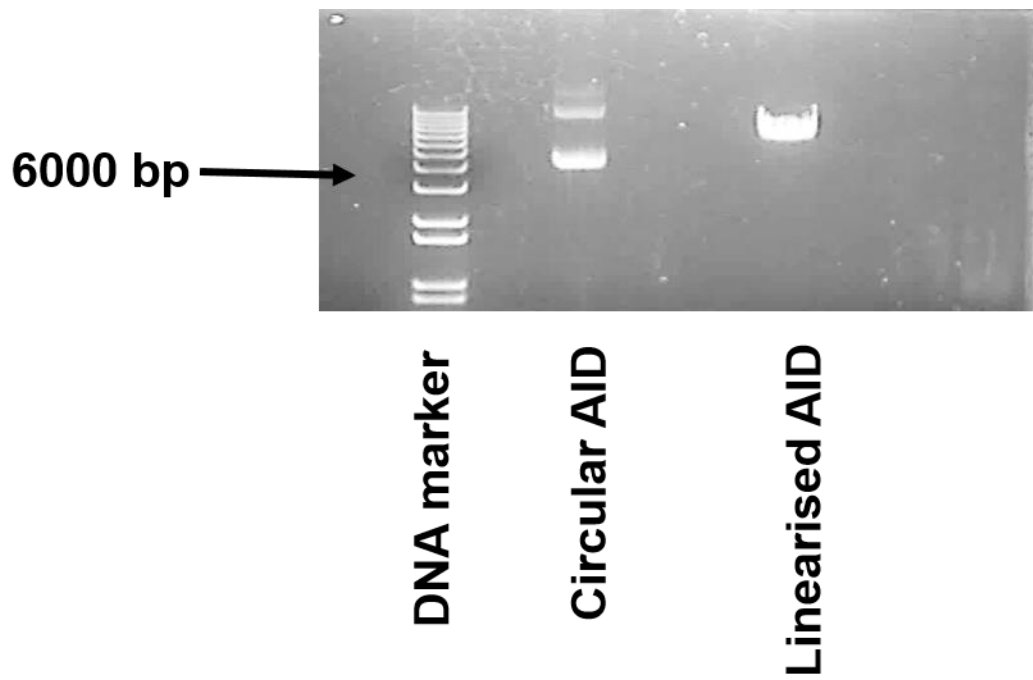


**Figure 3.10 Linearisation of AID-blast<sup>r</sup>-TOPO.**

Plasmid DNA of AID was digested by SspI restriction enzyme before checking linearisation on agarose gel. Lane 1 is DNA size marker, lane 2 circular AID plasmid, lane 3 linearised AID plasmid. The third lane confirmed linearisation of AID. The positions of molecular size markers are indicated.

Expression of the AID was detectable by Western blot of DT40 cells in both transfected circular and linearized AID as shown in Figure 3.11. The expected size of AID is approximately 25kDa. For transfection of circular AID, AID expression was observed in all clones, including the positive control. The highest of AID expression was obtained from clone 5 (Figure 3.11A). Membranes were stripped and reprobed with anti-FLAG antibody for detecting the expression of Tie2 in the AID clone-Tie2-DT40 cell line. The expression of Tie2 receptors was very low compared to original Tie2-DT40 cells.

For transfection of linearised AID, the AID-immunoreactive proteins of the expected size were expressed in AID-clone Tie2-DT40 cells which were clone 1, 3, and 7. However, Tie2 expression was seen only wild-type Tie2-DT40 and AID clone 1. (Figure 3.11B). It was concluded that AID constructs were expressed in Tie2-DT40 cells in both circular and linearised AID clones but it is likely that circular AID clones was more highly expressed than the linearised AID clone. However, the expression of Tie2 was low in both stably transfected cells.

Additional sets of circular AID transfection experiments were performed (Figure 3.12). Initially, Tie2-DT40 cells were confirmed for Tie2 expression by FACS. Then, Tie2-DT40 cells were stably transfected with circular AID. An AID clone Tie2-DT40 was obtained and it was likely that AID expression was equal to levels in Tie2-DT40 clone. Therefore, it was not possible to test the effect of AID expression on mutation rate in Tie2-DT40 clone cells compared to Tie2-DT40 cells.

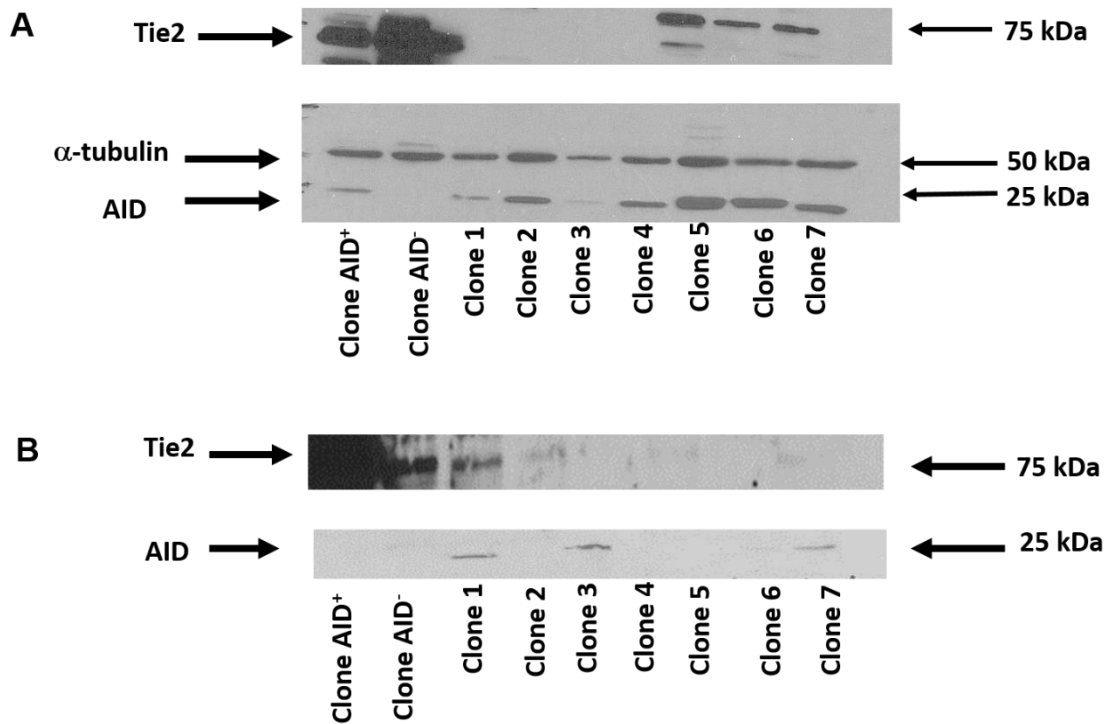


**Figure 3.11 Electroporated circular and linearised transfection of the AID in DT40 expressing Tie2 cell line.**

Tie2-DT40 cells were transfected with circular and linearised pAID-TOPOblast<sup>r</sup> by electroporation. Post transfected cell lysate samples were subjected to SDS/PAGE and Western blotting. Immunoblotting analysis was performed with anti-AID monoclonal antibody and anti- $\alpha$ -tubulin monoclonal antibody. The positions of molecular size markers are indicated. The expected size of AID is approximately 25kDa. Membrane was stripped and reprobed with Anti-FLAG for detecting the expression of Tie2 on DT40 cell line. Circular and linearised transfection of the AID are shown in panel A and B, respectively.

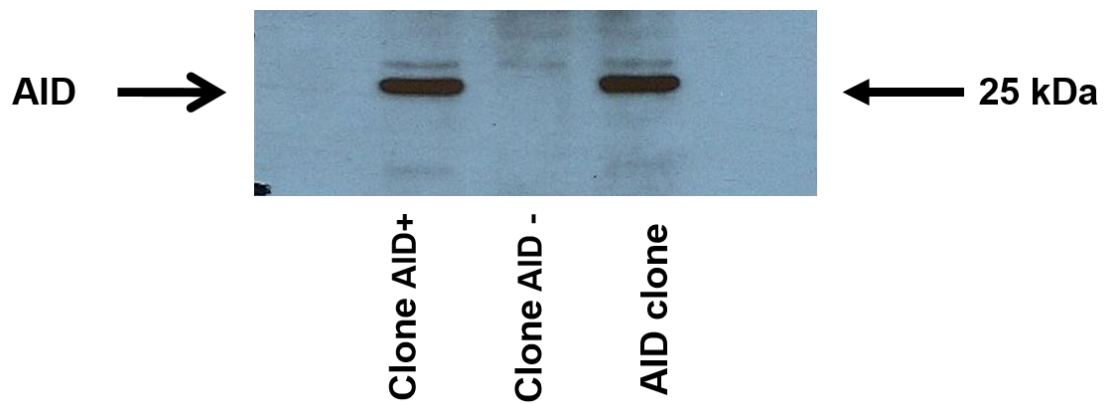


**Figure 3.12 Electroporated circular transfection of the AID in DT40 expressing Tie2 cell line.**

Tie2-DT40 cells were stably transfected with circular pAID-TOPOblastr by electroporation. The positions of molecular size markers are indicated. The expected size of AID is approximately 25kDa.

### **3.5 Selection of Tie2-DT40 for preferential Ang2 binding**

FACS experiments were performed to select cells expressing Tie2 variants with increased Ang2 binding relative to Ang1 binding. As it might not be possible to increase absolute Ang2 binding a strategy was decided in which Ang2 binding would be performed in the presence of the competitor Ang1. This would allow selection of any variants whose Ang2 binding activity was increased relative to Ang1 binding. This could occur by increased Ang2 binding or decreased Ang1 binding while maintaining Ang2 binding.

An initial experiment was performed to confirm Ang1 competition with Ang2 for binding to Tie2-DT40. In this experiment cells were incubated with 0.25nM biotinylated Ang2 in the presence of different concentrations of Ang1 for 30min. Binding of Ang2 to cells was then detected using streptavidin-PE-Cy5 and cells subjected to flow cytometry. The mean fluorescence intensity of the Ang2 bound population was normalised with that for Ang2 alone (100%) and plotted as a percentage of Ang2 alone for each Ang1 concentration (Figure 3.13). the maximum concentration of Ang1 used in these experiments was 5nM due to the commercial cost of the ligand. As shown in Figure 3.13 increasing Ang1 decreasing Ang2 binding as expected. However, even at 5nM Ang1 (20 fold the concentration of Ang2) there was still a residual 40% Ang2 binding. Therefore, it was decided to use an Ang1 concentration that produced a 50% decreased Ang2 binding for selection experiments. From figure 3.13 this was approximately 3.4nM.

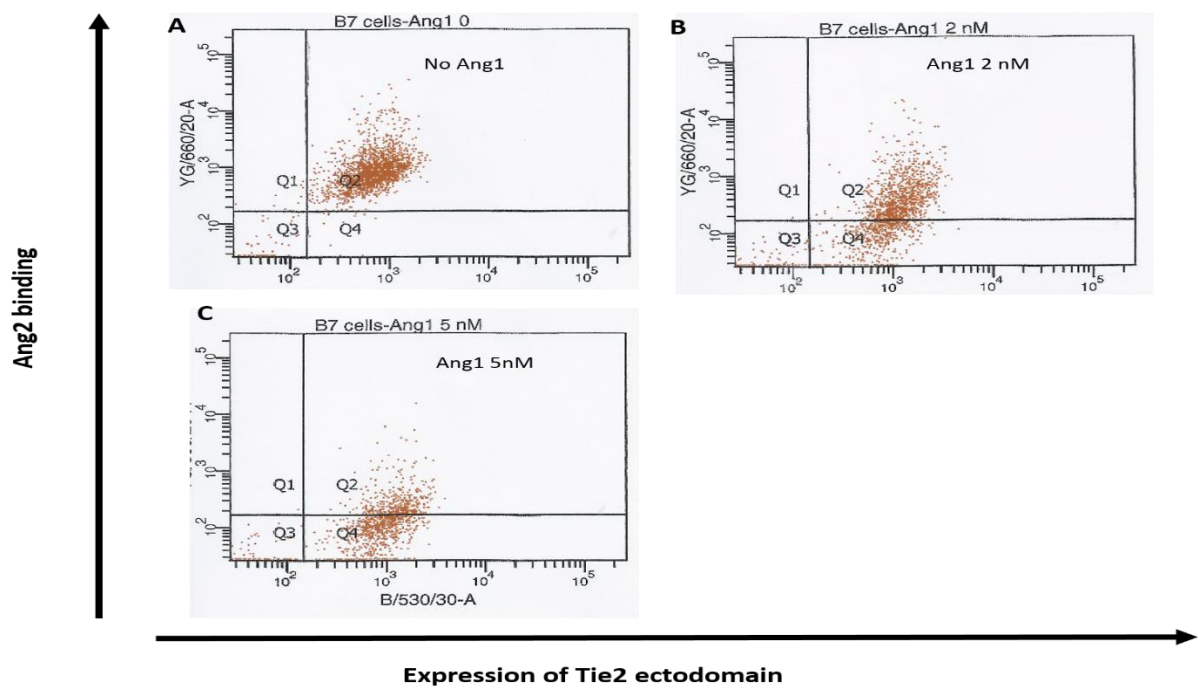


**Figure 3.13 Competitive equilibrium of Ang1 versus Ang2.**

Tie2-DT40 cells were incubated with 0.25nM biotinylated-Ang2 and varying concentrations of Ang1 prior to labelling with streptavidin PE-Cy5. Geometric mean FI was determined by flow cytometry. Mean and standard error bars are shown. A single experiment is shown in Panels A-C. Panel D shows results of three experiments as mean and SEM

### **3.6 Iterative sorts to select for preferential Ang2 binding**

In order to enrich for cells with enhanced Ang2 binding over Ang1  $10 \times 10^6$  Tie2-DT40 cells were incubated with 0.5nM biotinylated-Ang2 in the presence of 3.4nM Ang1 for 30 min. Cells were then labelled for bound Ang2 using streptavidin-PE/Cy5 and also for Tie2 expression with anti-FLAG-FITC and subjected to FACS. As shown in Figure 3.14, 2% of the cells from quadrants 1 and 2 were selected.

This represented approximately  $10^5$  cells after accounting for cell losses during labelling. Selected cells were then grown to  $10 \times 10^6$  and subjected to another selection under the same conditions for two more iteration but selecting the top 0.2% of Ang2 binding cells each time (Figure 3.14B). Each round of selection and growth required an approximately 2 weeks. There was an initial suggestion of some population diversity with improved Ang2 binding, indicated by increased number of outlying cells in the diagonal above the main cell population. However, attempts to enrich this by performing further selections in this region failed to produce a clear emergent population of cells with improved Ang2 binding after six sort and re-growth iterations (Figure 3.14C). An additional set of mutation and selection experiments was performed but this also did not produce any clear improved population.

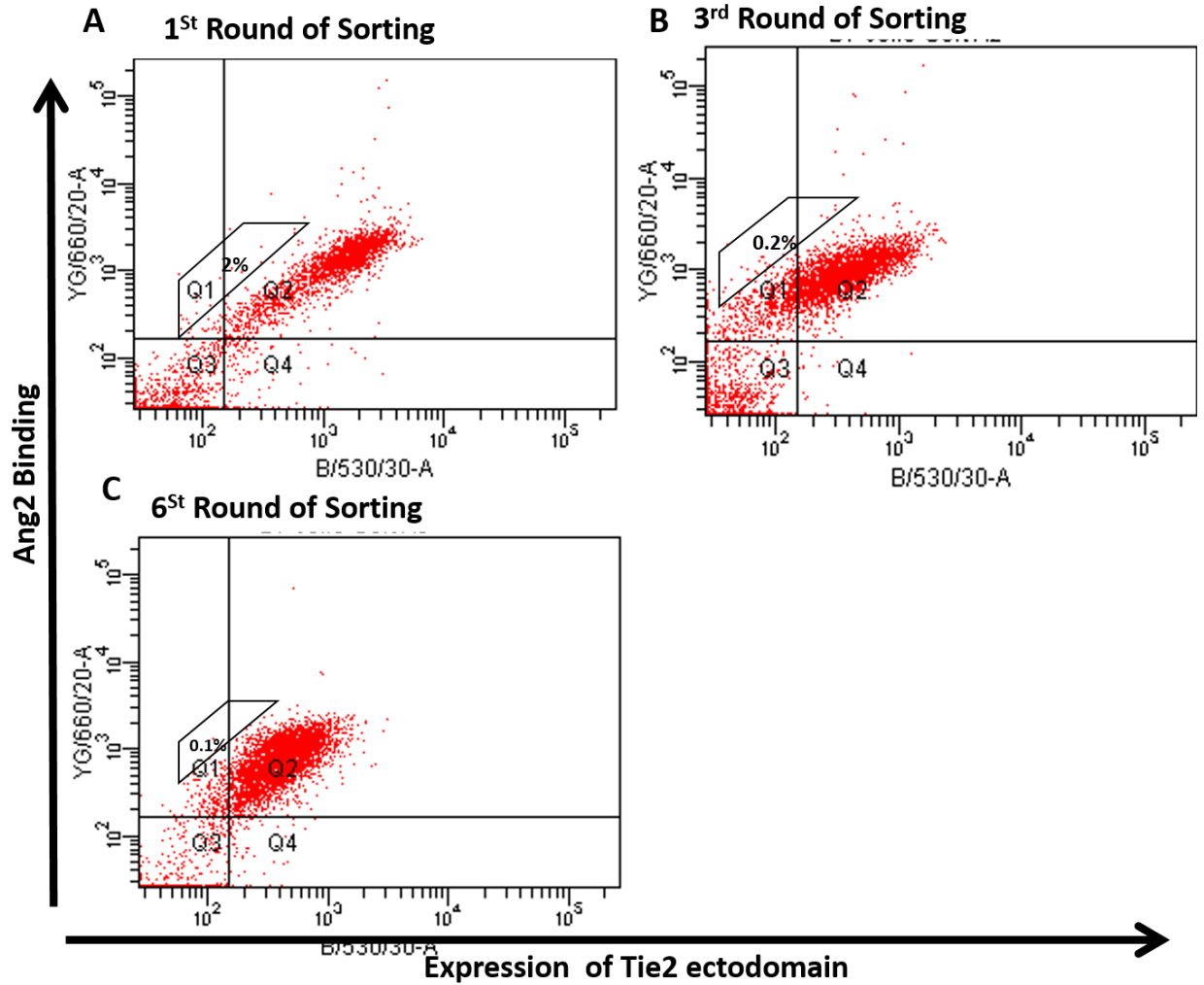


**Figure 3.14 Sorting for high Affinity Ang2 binders.**

These are examples of FACS from the first to sixth rounds of sorting. 10 million Tie2- DT40 cells were incubated with 0.5nM biotinylated-Ang2 and 3.4 nM Ang1 for 30 min prior to labelling with streptavidin-PE-Cy5 and anti-FLAG-FITC. Ang2 binding cells were sorted by one-way purity as per sorted window in dual staining dot plot.

### 3.7 Discussion

The angiopoietin-Tie system plays a principal role in endothelial cell survival, vascular maturation and stability (Loughna and Sato, 2001). Ang1 and Ang2 are agonist and antagonist Tie2 ligands respectively which activate a range of Tie2 signalling pathways. Ang2 may contribute to the pathophysiology of vascular and inflammatory diseases (Rasul et al., 2011). Therefore, inhibition of Ang2 is a desirable therapeutic option. This could be accomplished by engineering Tie2-ectodomain to bind specifically to Ang2. One option for creating Ang2 binding preferentially to Tie2 is to use directed protein evolution. This study attempted to use SHM of the ligand binding domain of Tie2 together with fluorescent labelled angiopoietin ligands and FACS to evolve variant of Tie2 ectodomain with preferential binding to Ang2.

To fulfil the project aims it was first necessary to establish the methodology required for performing SHM-driven directed evolution. Firstly, FACS was set up and optimised. DT40-expressing Tie2 ectodomain has been used for SHM-driven directed evolution in this project. Cells double-labelled with FITC-conjugated anti-FLAG and fluorescently-labelled streptavidin reflected the cell surface-expressed Tie2 and Ang2 binding, respectively in dual-colour flow cytometry. An important part of flow cytometry data analysis is to distinguish live cells from unwanted particles such as dead cells and debris by gating.

Generally, a dot plot of forward scatter data against side scatter data is used to detect the size of cells and cell granularity respectively. Dead cells have lower forward scatter signal and higher side scatter signal than live cells. The live cells were gated based on forward and side scatter profile before this cell population gate was subsequently analysed by flow cytometry.

In order to correctly analyse flow cytometry data, unstained cells of the same type and condition need to be included in every experiments. Unstained samples are also used to detect auto-fluorescence or background. A dot plot of unstained cells represented the low signal for FLAG and Ang2 binding as expected. The auto-fluorescence occurs from the cell components of normal cells which give

fluorescence. If fluorescence of unstained control is present, it is likely auto-fluorescence. Fluorescent labelled antibody was therefore selected that is different from the colour of auto-fluorescence. However, significant auto-fluorescence was not seen in this study.

Initially, FITC and streptavidin-R-PE were the fluorophores used in this study. However, the emission wavelength of FITC and streptavidin R-PE is close. The signal of Ang2 binding could be carried over into FLAG binding. A large signal from Ang2 binding and low carry over into FLAG binding were needed for selecting Ang2 binding in this study. Alternative fluorophore set would be FITC and streptavidin-PE/Cy5, as streptavidin-PE/Cy5 has a stronger fluorescent signal. Streptavidin- PE/Cy5 can be excited at 488nm, and wavelength of maximal emission is 670nm. The cells labelled with streptavidin R-PE were compared to the cells labelled with streptavidin-PE/Cy5. The results indicate that streptavidin-PE/Cy5 gave a stronger fluorescent signal than streptavidin-R-PE. Moreover, streptavidin-PE/Cy5 has minimal spectral overlap into FITC channel. It is presented that streptavidin-PE/Cy5 is mainly better signal without contributing to the FLAG-FITC signal.

Flow cytometry analysis was used to detect the levels of Ang2 bound Tie2 receptors on DT40 cell surface, whereas sorting cells by FACS used to screen and select the highest Ang2 binding. As shown in the results the methodology established in the present study allows dual labelling of Tie2-DT40 cells and permits selection of cell populations. It was intended that cells with improved Ang2 binding would be sorted and collected iteratively over many rounds till the Ang2 binding properties are optimal. The sorted cells would then be used to recover the mutated DNA sequences and the DNA sequences of mutant Tie2 ectodomain determined.

To confirm the method for recovery of DNA for sorted Ang2 binding population, mRNA was extracted from the sorted cells before processing to RT-PCR, PCR, addition of A overhangs, cloning the Tie2 ectodomain into TA sequencing vector and transformation. Transformanted cells were plated on agar plates containing ampicillin. The transformants were incubated at 37°C overnight. There were five

colonies on agar plate. This problem was thought to be caused by the short incubation of cloning reaction. Thus, the experiment was optimised and repeated. When the cloning reaction was left for one hour, the number of colonies increased to 70. This would provide sufficient material for DNA sequencing in future experiments.

SHM-driven evolution requires AID to mutate the Tie2 ectodomain. Mutation rates were compared in low and high AID expressing DT40 clones to determine the cells with maximal capacity for diversifying the target gene (Tie2). These cells were grown and screened for mutants with preferential Ang2-binding by FACS using biotinylated-Ang2 as described earlier. To increase the mutation rate, AID was cloned into the pEF6/V5-His-TOPO<sup>®</sup> TA and stably expressed in Tie2 -DT40 cells. The positive clone was confirmed by restriction enzyme digestion and the DNA sequences of the AID plasmid were analysed. There was one point mutation which did not change the amino acid, therefore the protein remains unchanged. The AID plasmid was further transfected for determining of expression in CHO cells. The results showed that AID constructs can be expressed in mammalian cells. This successful AID construct can be further used to establish stably AID in DT40 expressing Tie2 ectodomain.

The stable AID expressing cell line needed to be established. There were two choices of stable cell lines that consist of circular and linearised DNA stable cell line. The AID blast<sup>r</sup> TOPO was transfected using an electroporation method. Circular and linearised DNA constructs were generated and used to transfect AID expression in Tie2-DT40 cells. Both circular and linearised DNA produced successful transfections and AID overexpression in DT40 cells. Despite AID was expressed in several clones, Tie2 expression levels were very low. The possibility of low expression of the Tie2 ectodomain might come from mutation or loss of Flag-tagged Tie2 over time. Thus early passage of DT40 expressing Tie2 was required for transfection. Additionally, DT40 cells needed to be sorted for Tie2 expression by FACS prior to transfection. The number of transfections was repeated but only single colonies were produced. These were expanded followed by preparation of whole cell lysate and Western immunoblotting for AID expression. AID was likely to be expressed equally to the parent DT40 cell line.

This suggests limitation on how much AID can be expressed in the cells. The endogenous AID expression in the Tie2-DT40 cell line might be optimal for driving the mutation rate of Tie2 ectodomain. It was intended that Tie2-DT40 cells would be further used in the evolution of Tie2 ectodomain. In the meantime, an alternative strategy for improved transfection of AID in Tie2-DT40 should be optimised in the future.

The results of these experiments are that the methodology is now established for performing directed evolution experiments. In addition to screening for increased affinity for Ang2 it established competition screens in which Ang1 and Ang2 are both present. In the present study sorted window of Ang2 binding against Tie2 expression was used to screen and select desired Ang2 binders. A population with highest Ang2 binding relative to Tie2 expression was selected. For each of these selections, cell growth and re-selection was performed iteratively to obtain cells with the highest Ang2 binding characteristics. After 6 rounds iteration of this enrichment process, a distinct population did not resolve. It is possible that this screening of selection was not sensitive enough to resolve population discrimination. The improved Ang2 binding cells could be rarely expressed between rounds of sorting. Therefore, I have stopped evolving for further iterative selection.

## Chapter 4: Characterisation of Evolved ectodomain

Experiments to evolve a specific Ang2-binding of Tie2 ectodomain using SHM are described in Chapter 3. They did not produce an evolved ectodomain. However in parallel experiments performed by others in the group an Ang2-specific binding ectodomain was evolved. They used a different window for selection by using a sort strategy of Ang1 binding versus Tie2 expression for selecting low Ang1 binding population. Expression of Tie2 ectodomain was monitored by staining with FITC-conjugated anti-FLAG while Ang1 binding was monitored by staining with anti-Ang1/fluorescent secondary antibody. After 4 rounds of sorting, the selection strategy was changed to select cells with the highest Ang2 binding whilst maintaining low Ang1 binding. Binding of two ligands was monitored with anti-Ang1 and fluorescent secondary antibody and fluorescently labelled streptavidin. Population diversity of cells with lower Ang1 binding but high Ang2 binding was achieved. After a total 8 rounds of sorting, an evolved ectodomain that preferential bound to Ang2 was successfully evolved. DNA encoding their Ang2-binding Tie2-variants was recovered and sequenced. It was then intended that the mutant proteins would be generated as soluble Tie2 ectodomains. Mutant ectodomains were characterizing for Ang1 and Ang2 binding kinetics in vitro. Furthermore, cell culture experiments will be performed to assess the ability of mutant proteins to block Ang2 inhibition of Ang1 effects in endothelial cells.

In this chapter, experiments were conducted to characterise the binding and cellular activity of this evolved ectodomain. The evolved ectodomain (designated R3) is identical to the wild-type ectodomain (Wt) but has an Ile substitution in place of Phe161 and Arg167 and His168 are deleted as indicated in Figure 4.1. Evolution of this ectodomain is described in (Brindle et al., 2013).

To analyse the binding characteristics of the evolved ectodomain, the Wt with a carboxyl-terminal Fc tag was used and the F/I and RH deletion introduced into this sequence by site directed mutagenesis.

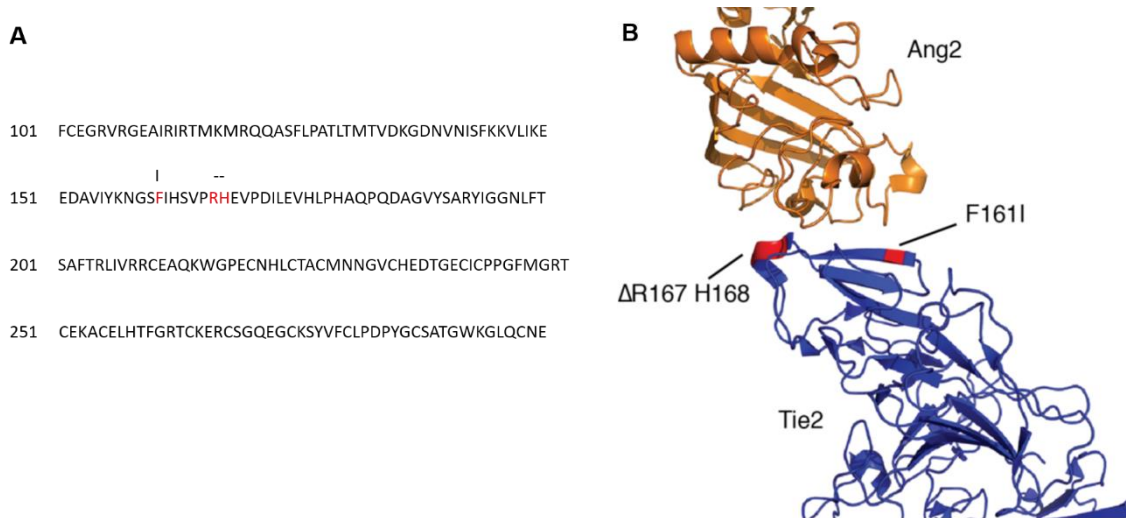


**Figure 4.1 Three amino acid changes switch binding specificity of Tie2.**

A, The amino acid changes of evolved ectodomain (R3), dash indicated deletion.  
 B, The position of the amino acid changes in the evolved are indicated on the structure of Tie2 in complex with Ang2 (PDB accession 2GY7. The F161I substitution is positioned on a beta sheet and the R167, H168 deletion occur on a turn at the receptor-ligand interface (modified from Brindle et al. 2013).

The secreted soluble Wt-Fc and R3-Fc proteins were purified with Ni-NTA chromatography following transfection and expression in human embryonic kidney HEK293 cells. The molecular weight of purified R3 ectodomains that were expressed in HEK293 cells was approximately 80 kDa. Binding of the wild-type ectodomain and the evolved ectodomain to Ang1 and Ang2 was examined using ELISA assays and BLI analysis. In addition, the effect of R3 ectodomain was further tested in cell signalling analysis and cellular functional assay.

#### **4.1 Expression of Soluble wild-type and R3 ectodomain in HEK293 cells**

The ectodomain of wild-type and R3 ectodomains were expressed as soluble proteins by using the HEK293 gene expression platform which has proven successful for expressing a wide range of proteins with post-translational modifications. The primary objective in the expression of the R3 and wild-type ectodomain was to obtain sufficient quantities of the active proteins for biochemical characterisation. HEK293 suspension cells were grown in serum free Freestyle medium at 37°C in 5% CO<sub>2</sub> incubation. Transient transfection was performed as described in Section 2.5.2. For production of secreted proteins, the fusion protein expression and production of soluble recombinant protein was continued for 4-5 days after transfection. The fusion proteins were purified under native condition by Ni-NTA chromatography (Qiagen) as described in Section 2.5.3. After purification, protein concentrations were determined by Bradford assay after buffer exchange into tris buffer saline containing 10% glycerol.

SDS/PAGE was used to judge the molecular mass of the purified protein and assess purity. As shown in Figure 4.2 for R3, a single band of approximately 100 kDa was observed. The calculated mass of Wt-Fc and R3-Fc is 75.6 kDa. It is likely the highest mass observed on gel electrophoresis reflects glycosylation. The purity of the protein following elution was estimated at 95%±1.5 in 3 independent preparations. To confirm the identity of the purified protein, immunoblotting was performed with anti-Tie2 ectodomain antibody. As shown in Figure 4.3 bands for R3-Fc were observed at approximately 100 kDa corresponding to the band seen in Coomassie stained gels.

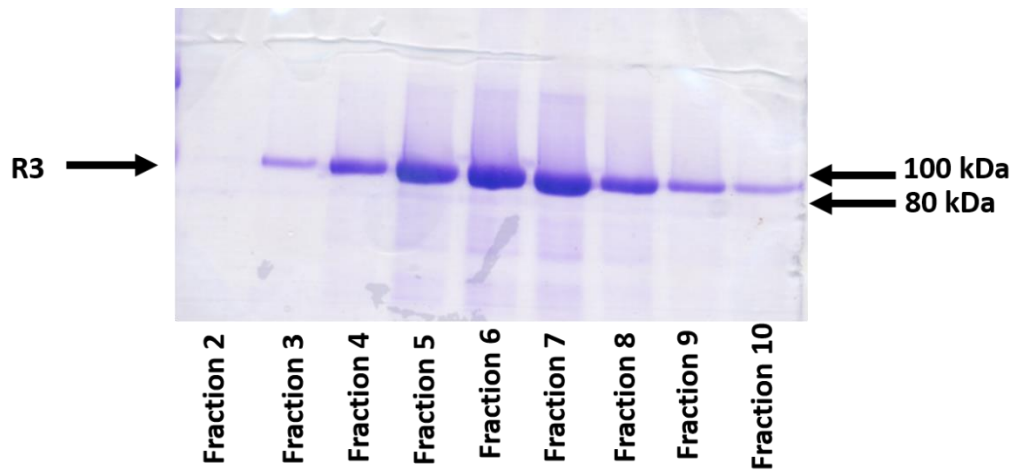


**Figure 4.2 Coomassie stained SDS gel of R3 eluate from nickel column.**

Soluble R3-Fc was purified with Ni-NTA chromatography following expression in HEK293 cells. Elution fractions 2-10 were resolved by SDS/PAGE and gel stained by Coomassie blue. Migration of mass markers is indicated in kDa. Typical yield for 1 L transfection was 1.2mg.

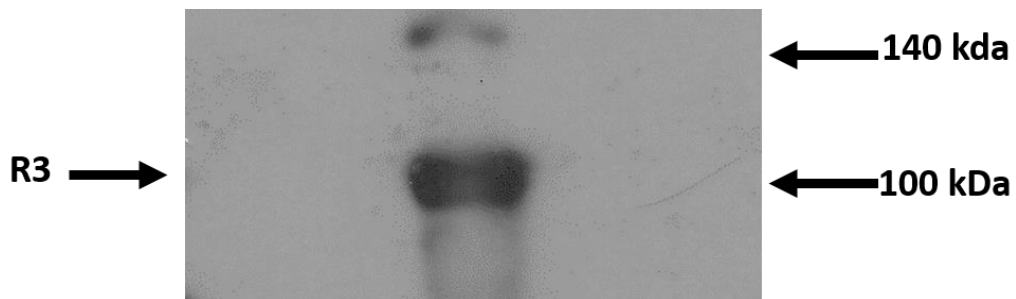


**Figure 4.3 Western Blot of R3-Fc probed for Tie2.**

Soluble R3-Fc was purified following expression in HEK293 cells. R3-Fc was resolved by SDS/PAGE and Western blotting as described in Section 2.5. Immunoblotting analysis was performed with anti-Tie2 antibody. The positions of molecular weight marker are indicated.

## 4.2 Binding kinetics of the R3-Fc and Wt-Fc ectodomain to Ang1 and Ang2

To measure the binding kinetics of the R3 and Wt ectodomain to Ang1 or Ang2, R3-Fc or Wt-Fc ectodomain containing Fc region was captured and immobilized onto the anti-human IgG biosensor surface of an Octet RED bio-layer interferometry machine resulting in the production of a stable surface suitable for kinetic interaction analysis. The Octet RED has biolayer interferometry (BLI) to detect binding interactions in real time. Calculation of affinity or  $K_d$  is not possible with this approach because angiopoietins are multivalent mixtures and ectodomain-Fc are divalent and there are no adequate mathematic model to account for these avidity effect. The BLI data therefore is primarily qualitative in this case. Individual BLI sensorgrams are presented in Figure 4.4, Figure 4.5, Figure 4.6 and Figure 4.7. BLI data showed Wt-Fc bound to human Ang1 as well as Ang2 as expected, while the R3-Fc only bound to Ang2 but not Ang1 in this assay. Ang2-binding ability of Wt-Fc was higher than that of R3-Fc.

In addition, the binding of R3 and wild-type ectodomain to Ang4 was determined. Ang4 is the only other angiopoietin expressed in humans (Valenzuela et al. 1999). Ang4 has not been understood in depth but a previous paper reported that Ang4 acts as an agonist of Tie2, mediating Akt phosphorylation that induces survival and migration in primary cultured HUVECs (Lee et al., 2004). BLI analysis was performed to test the ability of R3 to bind Ang4 compared with the wild-type ectodomain. The sensorgram of BLI in Figure 4.8 demonstrates wild-type Tie2 ectodomain bound to Ang4 whereas the binding of Ang4 to R3-Fc was not detected.

Therefore, the evolved protein is a selective Ang2 trap and has no effect on Ang1 and Ang4 which are vasculoprotective molecules. These properties suggest R3 could be useful in the treatment of diseases associated with upregulation of Ang2.

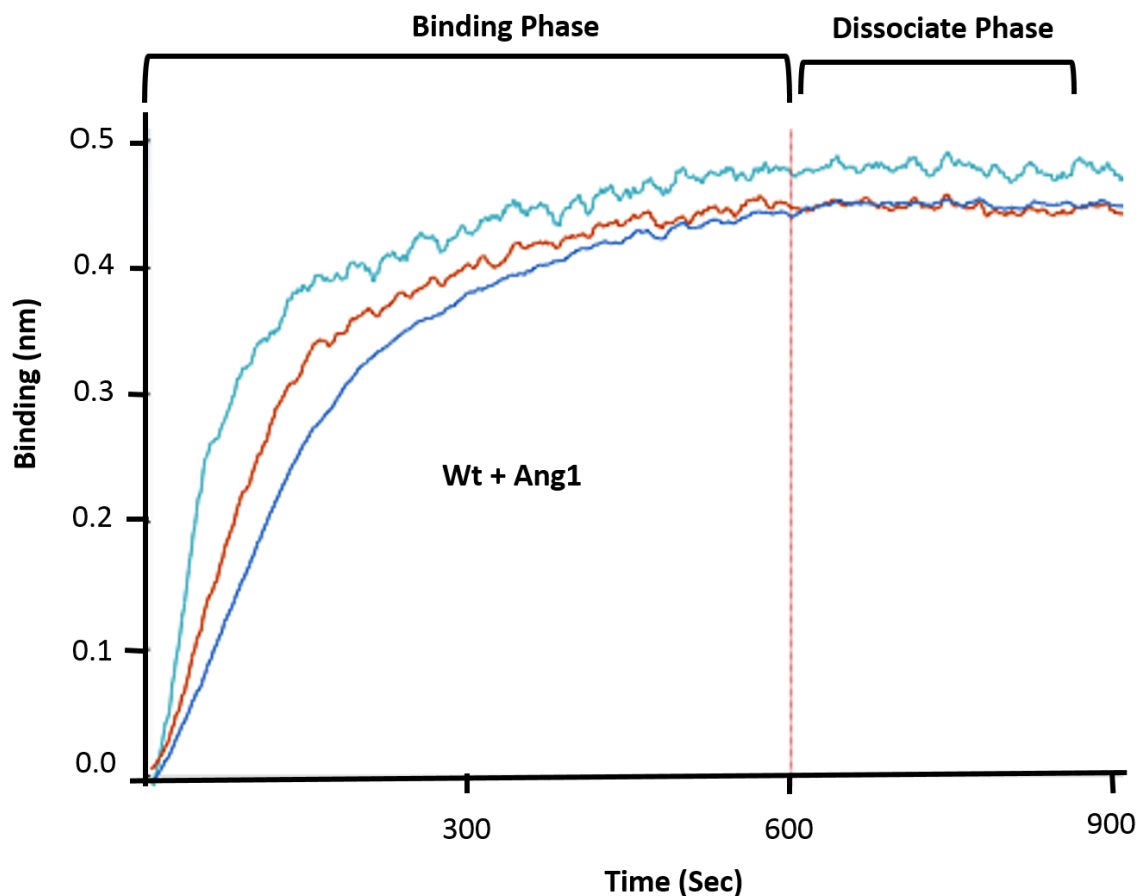


**Figure 4.4 Sensorgram for binding of Ang1 to the Wt-Fc measured by BLI.**

Wt-Fc (5 $\mu$ g/ml) was immobilized on sensors and binding of 10 nM (blue), 20 (red) and 40 nM (turquoise) Ang1 monitored by BLI. Binding and dissociation phase are shown. A single experiment is shown, representative of three independent experiments.

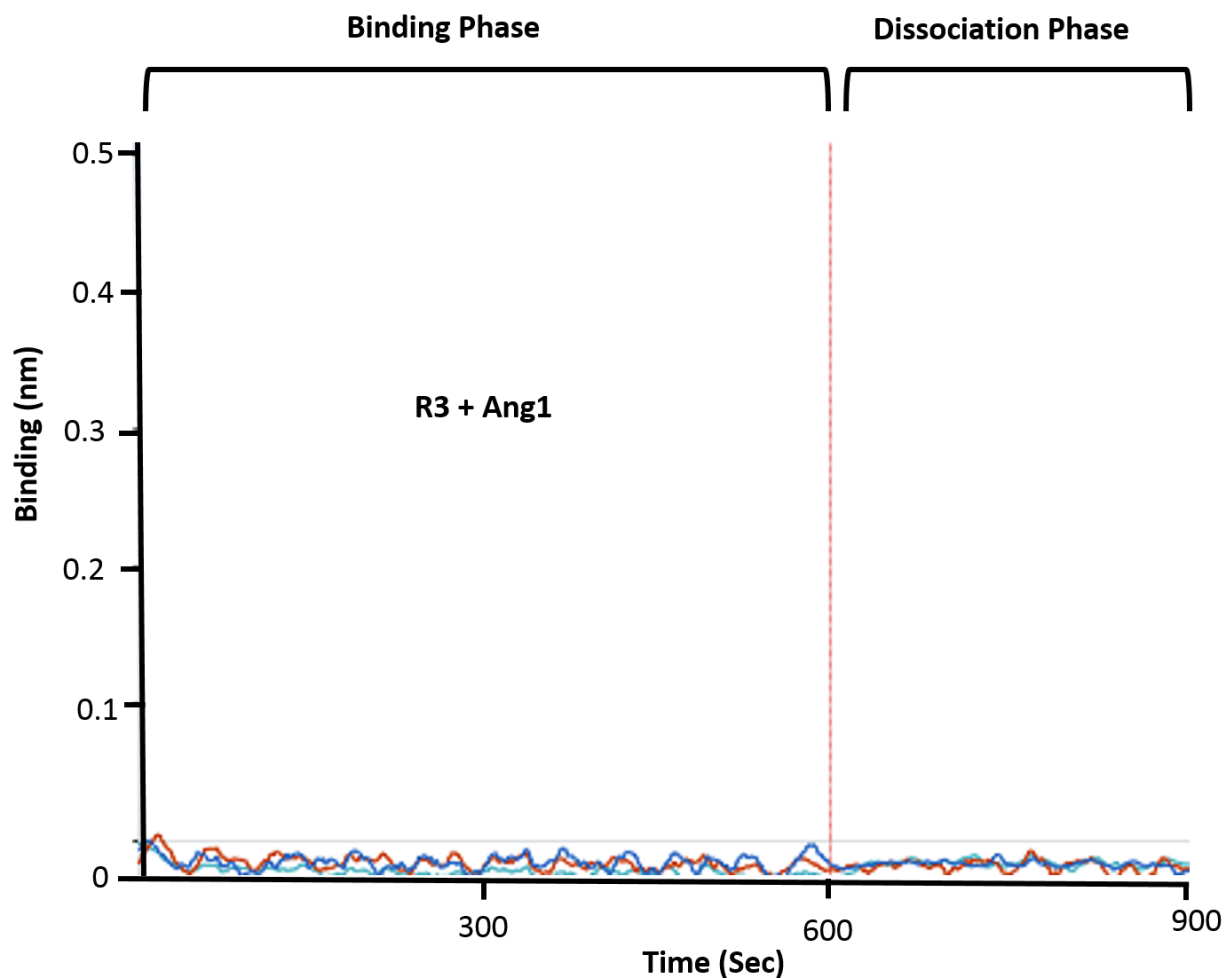


**Figure 4.5 Sensorgram for binding of Ang1 to the R3-Fc measured by BLI.**

R3-Fc (5 $\mu$ g/ml) was immobilized on sensors and binding of 10 nM (blue), 20 (red) and 40 nM (turquoise) Ang1 monitored by BLI. Binding and dissociation phase are shown. A single experiment is shown, representative of three independent experiments.

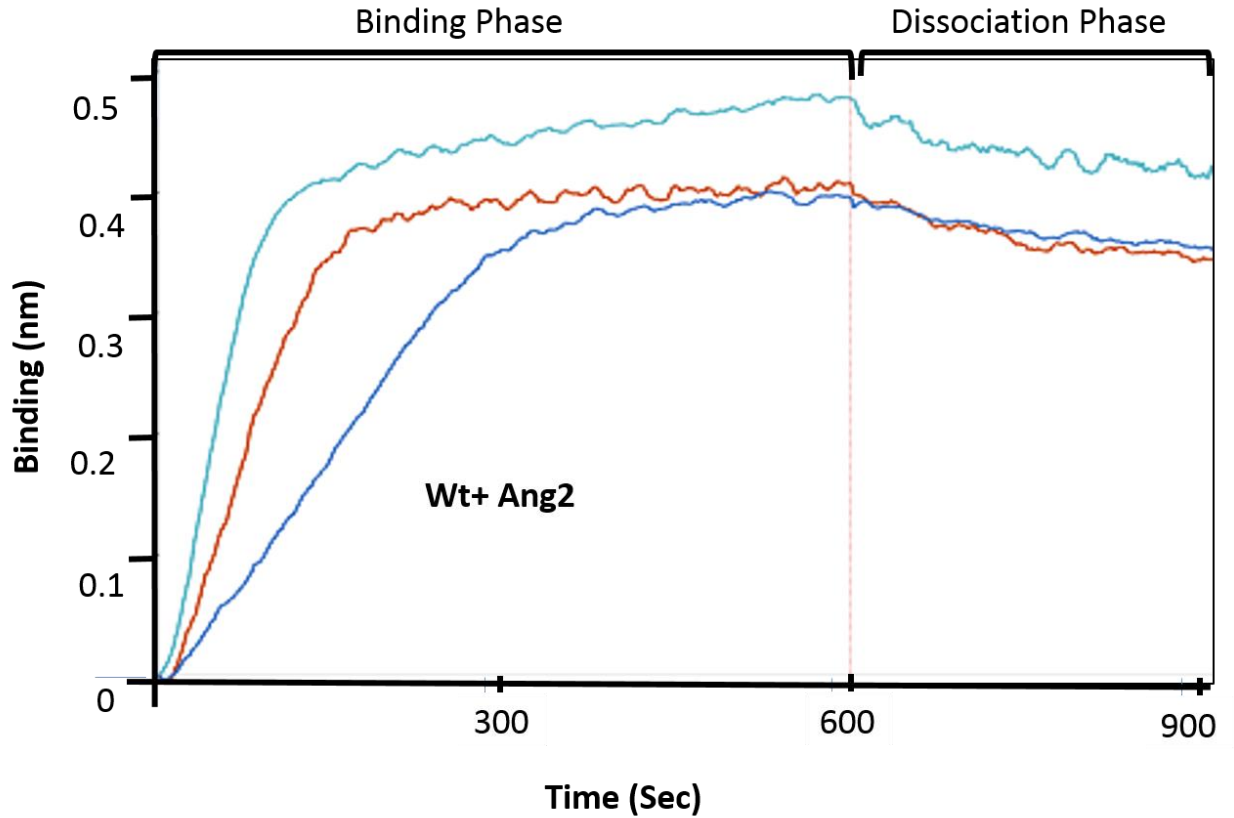


**Figure 4.6 Sensorgram for binding of Ang2 to the Wt-Fc measured by BLI.**

Wt-Fc (5 $\mu$ g/ml) was immobilized on sensors and binding of 20 nM (blue), 40 (red) and 60 nM (turquoise) Ang2 monitored by BLI. Binding and dissociation phase are shown. A single experiment is shown, representative of three independent experiments.

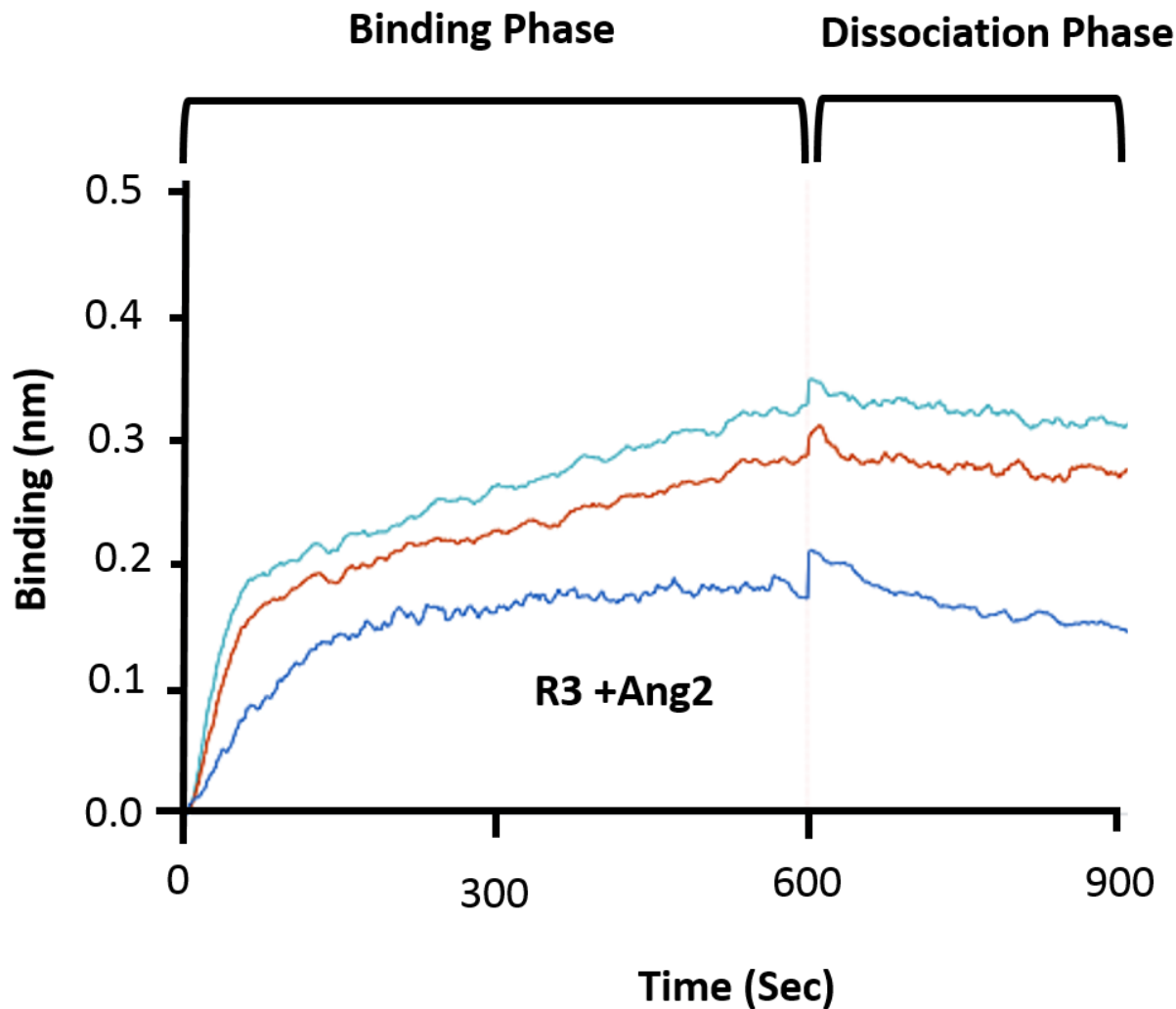


**Figure 4.7 Sensorgram for binding of Ang2 to the R3-Fc measured by BLI.**

R3-Fc (5 $\mu$ g/ml) was immobilized on sensors and binding of 20 nM (blue), 40 (red) and 60 nM (turquoise) Ang2 monitored by BLI. Binding and dissociation phase are shown. A single experiment is shown, representative of three independent experiments.

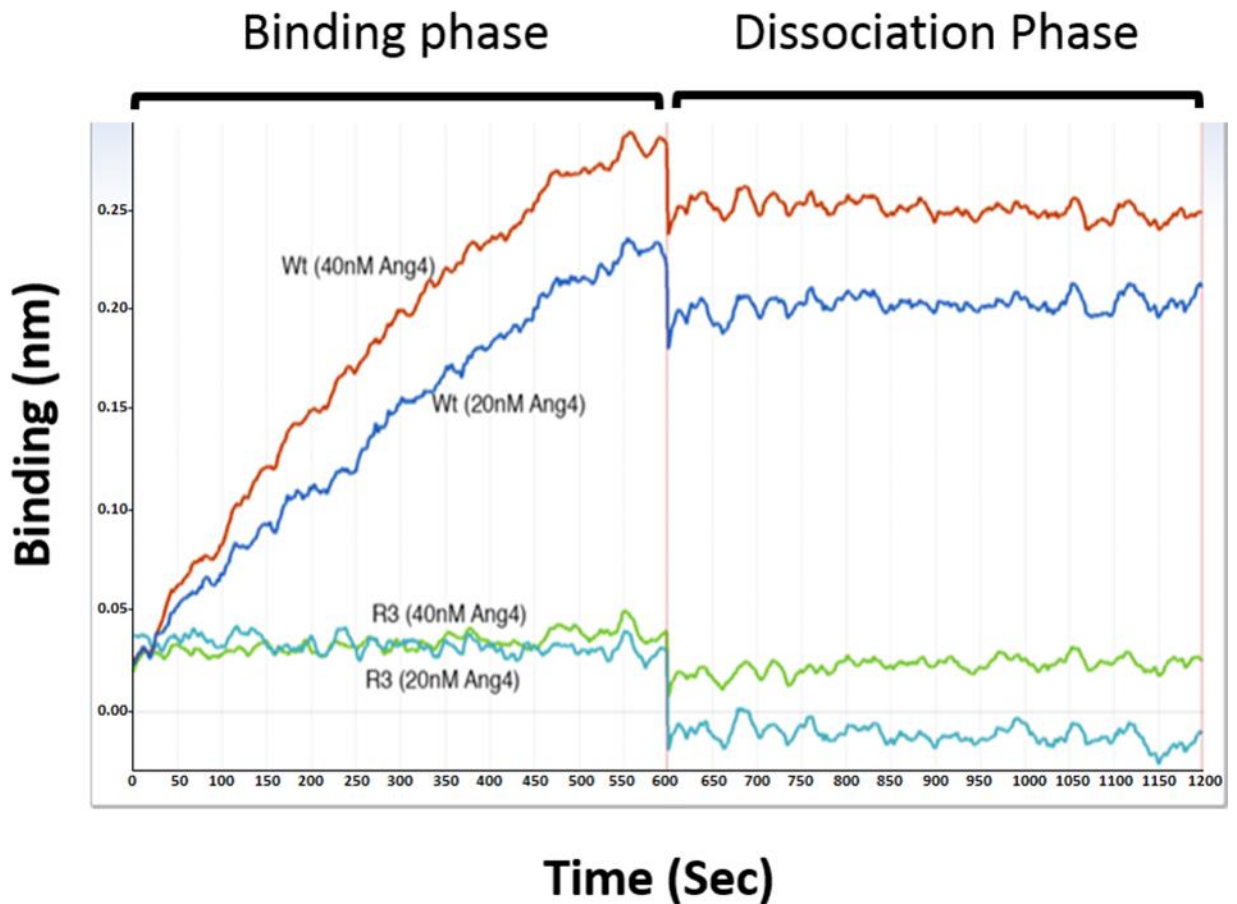


**Figure 4.8 Sensorgram for binding of Ang4 to the R3-Fc and Wt-Fc measured by BLI.**

Wt-Fc or R3-Fc (as indicated) were immobilized on sensors and binding of 20 nM (blue) and 40 nM (red) Ang 4 monitored by BLI. Binding and dissociation phase are shown. A single experiment is shown, representative of three independent experiments.

### **4.3 Quantitative analysis of binding of the evolved and wild-type ectodomain to Ang1 and Ang2 using ELISA**

It is important to determine quantitatively the relative binding abilities of Wt-Fc and R3-Fc to Ang1 and Ang2. As described earlier BLI is not able to provide quantitative affinity constants due to the multivalent nature of the binding. An alternative assay was therefore used, enzyme-linked immunosorbent assay (ELISA). Whilst ELISA cannot easily provide  $K_d$  or  $K_a$  values, it can be used to assess relative binding of different molecules under the same conditions by measuring the concentration of the binder that results in half maximal binding. In this ELISA experiment, Ang1 or Ang2 was immobilized on the plate and binding of the Wt-Fc or R3-Fc at different concentrations was tested. Bound ectodomain was detected with anti-Tie2 ectodomain antibody and colorimetric detection. The data (Figure 4.9, Figure 4.10) demonstrate the Wt-Fc was able to bind Ang1 and Ang2 while the R3-Fc only bound to Ang2, but not Ang1 that correspond to the qualitative data from BLI analysis (Figure 4.4-4.7). However, the ability of R3-Fc to bind Ang2 was lower than that of Wt-Fc since the R3-Fc required a higher concentration for achieving the half maximal binding (Table 4.1). Nevertheless, this evolved ectodomain still showed the preferential binding to Ang2 over Ang1 compared to wild-type ectodomain.

### **4.4 Quantitative analysis of binding of the F161I substitution and double R167, H168 deletion to Ang1 and Ang2 using ELISA**

In order to determine the individual effects of each mutation of the evolved ectodomain on binding, the soluble form of the F161I substitution and double R167/H168 deletion were produced. The construct of the wild-type ectodomain were introduced the corresponding mutation by site directed mutagenesis prior to expression in HEK923 and purification as described in Chapter 2.5. The relative binding abilities of F161I and R167/H168 deletion to Ang1 and Ang2 was determine using ELISA as described earlier.

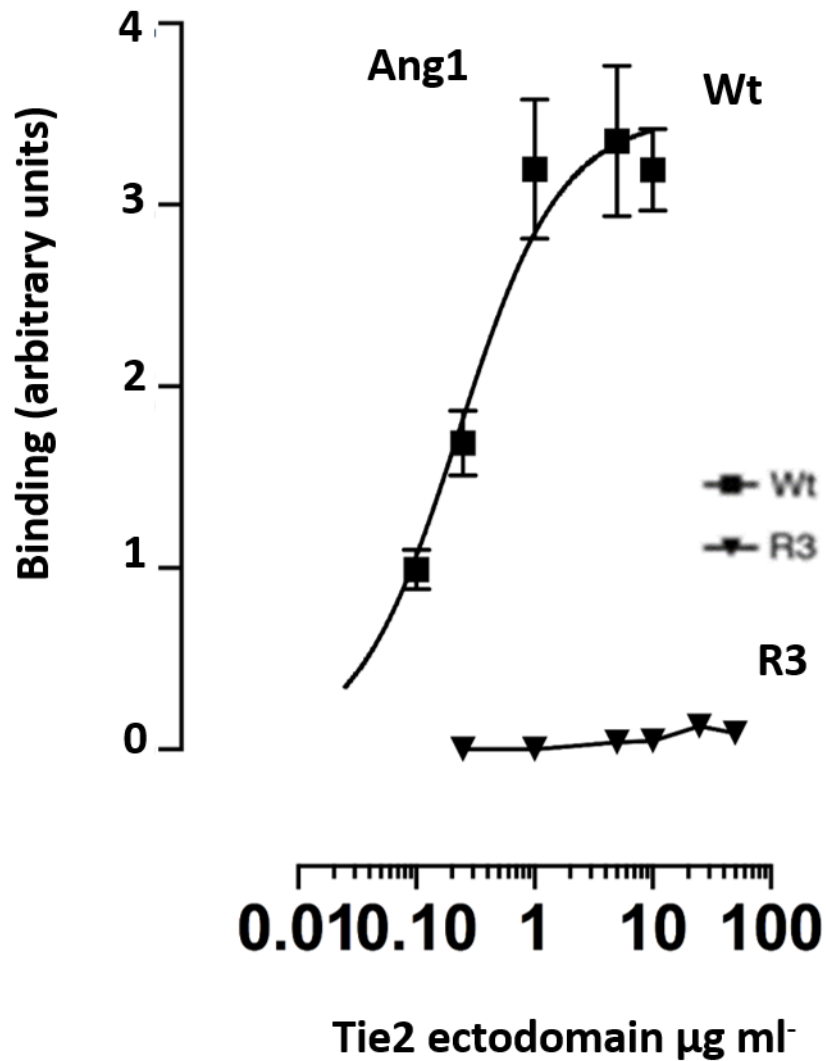


**Figure 4.9 Binding of Wt-Fc and R3-Fc to Ang1.**

Secreted Wt-Fc (squares) and R3-Fc (inverted triangle) were analysed for binding to immobilized Ang1 by ELISA, as indicated. Data are shown as means and standard deviations from triplicate determinations in a single experiment. All binding assays were repeated at least three times and the data are summarized in Table 4.1.

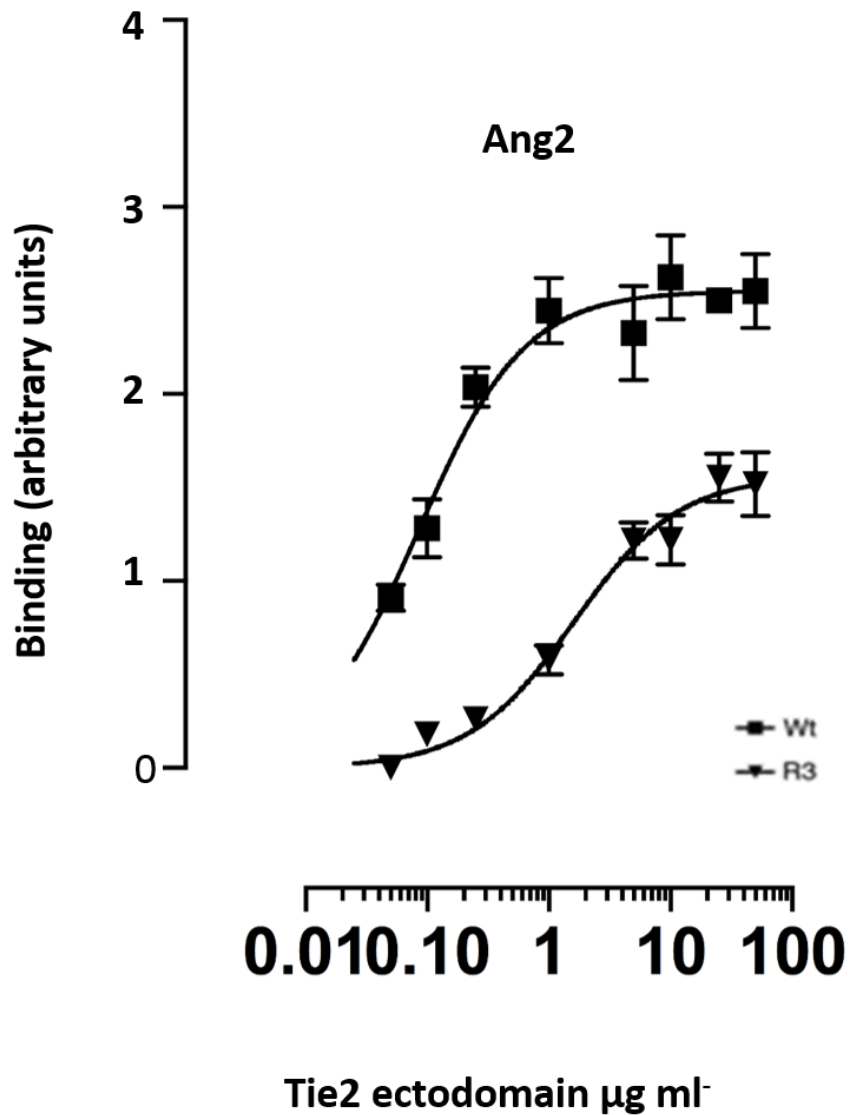


**Figure 4.10 Binding of Wt-Fc and R3-Fc to Ang2.**

Secreted Wt-Fc (squares) and R3-Fc (inverted triangle) were analysed for binding to immobilized Ang2 by ELISA, as indicated. Data are shown as means and standard deviations from triplicate determinations in a single experiment. All binding assays were repeated at least three times, and the data are summarized in Table 4.1.

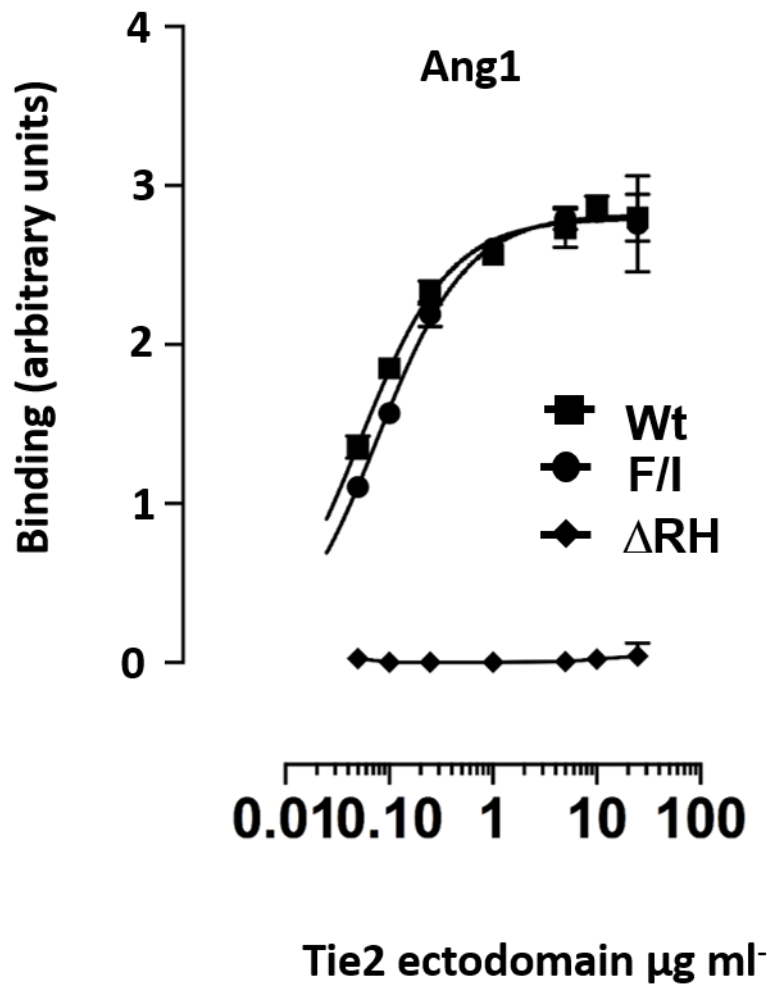


**Figure 4.11 Binding of F/I and  $\Delta$ RH mutants to Ang1**

Secreted Wt-Fc and ectodomains with either F161I substitution (F/I; circles) or the double Arg-167/His-168 deletion ( $\Delta$ RH; diamonds) were analysed for binding to immobilized Ang1 by ELISA, as indicated. Data are shown as means and standard deviations from triplicate determinations in a single experiment. All binding assays were repeated at least three times, and the data are summarized in Table 4.1.

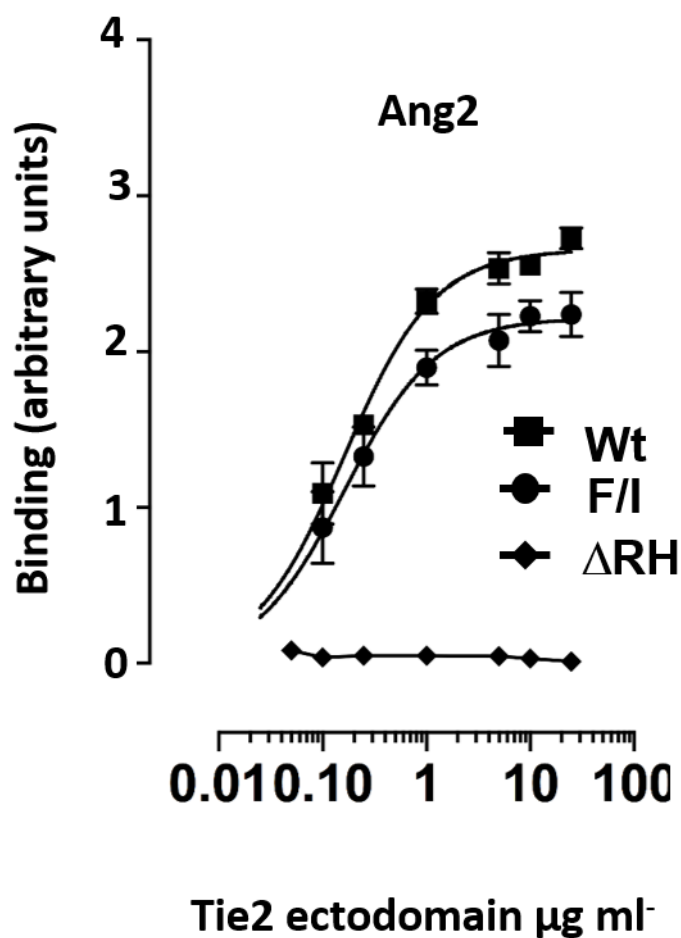


**Figure 4.12 Binding of F/I and  $\Delta\text{RH}$  mutants to Ang2.**

Secreted Wt-Fc and ectodomains with either F161I substitution (F/I; circles) or the double Arg-167/His-168 deletion ( $\Delta\text{RH}$ ; diamonds) were analysed for binding to immobilized Ang2 by ELISA, as indicated. Data are shown as means and standard deviations from triplicate determinations in a single experiment. All binding assays were repeated at least three times, and the data are summarized in Table 4.1.

**Table 4.1 Relative binding of ectodomain mutants**

	Ang1		Ang2	
	Max binding (% of Wt)	Half max binding conc. ( $\mu\text{g/ml}$ )	Max binding (% of Wt)	Half max binding conc. ( $\mu\text{g/ml}$ )
Wt-Fc	100.00	$0.04 \pm 0.01$	100.00	$0.25 \pm 0.09$
R3-Fc	$3.00 \pm 3.29^*$	—	$59.40 \pm 5.28^*$	$6.98 \pm 2.12^*$
F/I	$97.84 \pm 2.63$	$0.06 \pm 0.02$	$90.48 \pm 4.62$	$0.29 \pm 0.17$
$\Delta\text{RH}$	$0.29 \pm 0.16^*$	—	$0.58 \pm 0.58^*$	—

Wild-type (Wt-Fc) and evolved (R3-Fc) ectodomains, as well as ectodomains with F161I (F/I) substitution or Arg-167 and His-168 ( $\Delta\text{RH}$ ) deletion were analysed for binding to immobilized Ang1 or Ang2 by ELISA (Fig. 4.9-4.12). Maximum binding relative to Wt-Fc and concentrations (conc.) of ectodomains at half-maximal binding were calculated from saturation binding curves fitted by nonlinear regression (— indicates the absence of measurable binding precludes determination of half maximal binding concentration). Data are means and S.E. for at least three independent experiments (\* indicates  $p < 0.01$  compared with wild-type, Student's t test).

As shown in Figure 4.11, Figure 4.12 and Table 4.1 there was no significant difference between wild-type and F161I ectodomain in Ang1 binding. In the same way, F161I ectodomain and wild-type equally bound to Ang2. In contrast to F161I, the deletion of R167 and H168 completely abolished both ligand binding. This shows the Ang2 binding specificity of the R3 ectodomain requires the combination of three amino acid changes activity together.

#### **4.5 Effect of evolved ectodomain on angiopoietins signalling in endothelial cells**

In order to test whether R3 affects angiopoietins in a cellular context, experiments were performed to measure angiopoietin signalling. Ang1 is known to stimulate the Akt pathway resulting in increased phosphorylation of Akt on Ser 473 (Kim et al. 2000). Ang2 is known to antagonize this stimulatory effect. To test whether R3 could block the effect of Ang2, the endothelial cell line EA.hy926 was stimulated with Ang1 together with Ang2 and also either Wt-Fc or R3-Fc. As shown in Figure 4.13 Ang1 stimulated phosphorylation of Akt (pAkt) and this was inhibited by Ang2. Adding Wt-Fc as well as Ang2 caused a further decrease in pAkt. This is expected as Wt-Fc will bind Ang2 but also bind and block Ang1. When R3-Fc was added together with Ang2 to Ang1 stimulated cells, the ability of Ang2 to inhibit Ang1 is reversed. This suggests the Ang2 binding activity of R3-Fc can prevent Ang2 from antagonizing Ang1 action on endothelial cells. A similar set of experiments were performed with HUVECs (Figure 4.14). As with EA.hy926, addition of R3-Fc reversed the antagonistic effect of Ang2 on Ang1 stimulation of Akt.

Many studies report that high concentrations of Ang2 can stimulate the Akt pathway (Kim et al. 2000, Yuan et al. 2009). It was important to test whether R3-Fc could block the agonist effects of high Ang2 concentrations. To test this HUVECs were challenged with Ang2 and Akt activation examined. As shown in Figure 4.15, 6nM Ang2 stimulated Akt. Different concentrations of R3-Fc, from 25µg/ml to 100µg/ml, were added to block the agonist activity of Ang2 resulting in a decreased of Akt phosphorylation that was concentration dependent. As shown in Figure 4.15 the inhibition of agonist activity of Ang2 required higher concentration of R3 ectodomain for inhibiting agonist activity of Ang2 compared to previous antagonist experiment. In order to test whether R3-Fc or Wt-Fc affects Ang1-activation of Akt phosphorylation, HUVECs challenged with Ang1 showed the activation of Akt phosphorylation. R3-Fc or Wt-Fc ectodomain was added in cells stimulated with Ang1. As expected Akt phosphorylation was inhibited by Wt-Fc ectodomain while R3 did not affect the Akt phosphorylation stimulated by Ang1 (Figure 4.16).

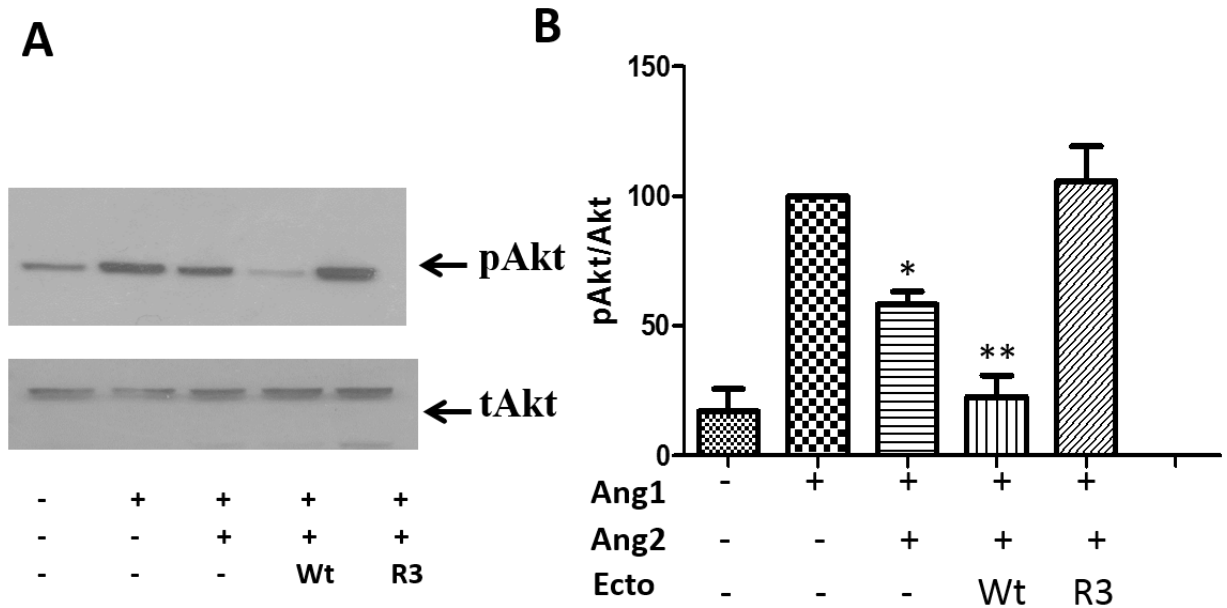


**Figure 4.13 Evolved ectodomain blocks the antagonistic effects of Ang2 in the endothelial cells line EA.hy926.**

A, The antagonistic effect of Ang2 on Ang1-induced Akt phosphorylation were tested. Cells were stimulated with 0.7nM Ang1 in the absence or presence of 3nM Ang2 with or without 25  $\mu$ g/ml wild-type or R3 ectodomain for 30 min prior to cell lysis. Equal amounts of cell lysates were resolved by SDS-PAGE and immunoblotted with antibodies recognizing Akt phosphorylated on S473 (pAkt) or total AKT (tAkt) as indicated. B, Akt phosphorylation was quantified by densitometric scanning of blots from three independent experiments, normalized to total Akt and expressed as % of Ang1 effect. Data are expressed as means and SEM (\* $P$ < 0.05, \*\* $P$ <0.01 vs Ang1, oneway ANOVA followed by Tukey's analysis).

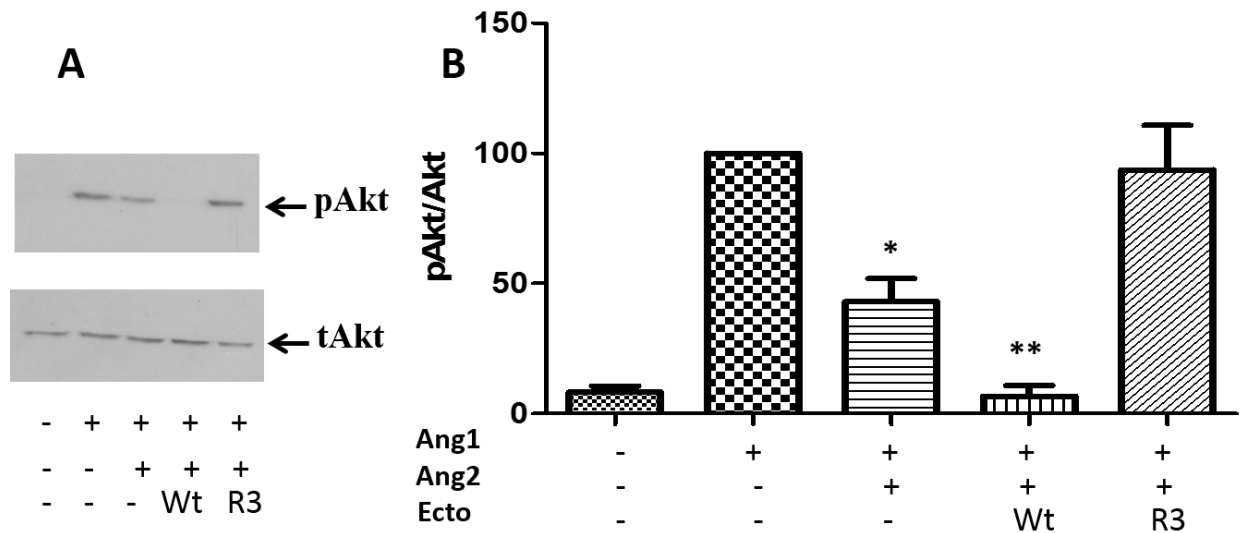


**Figure 4.14 Evolved ectodomain blocks the antagonistic effects of Ang2 in HUVECs.**

A, The antagonistic effect of Ang2 on Ang1-induced Akt phosphorylation were tested. Cells were stimulated with 0.7nM Ang1 in the absence or presence of 3nM Ang2 with or without 25  $\mu$ g/ml wild-type or R3 ectodomain for 30 min prior to cell lysis. Equal amounts of cell lysates were resolved by SDS-PAGE and immunoblotted with antibodies recognizing Akt phosphorylated on S473 (pAkt) or total AKT (tAkt) as indicated. B, Akt phosphorylation was quantified by densitometric scanning of blots from three independent experiments, normalized to total Akt and expressed as % of Ang1 effect. Data are expressed as means and SEM (\* $P$ < 0.05, \*\* $P$ <0.01 vs Ang1, oneway ANOVA followed by Tukey's analysis).

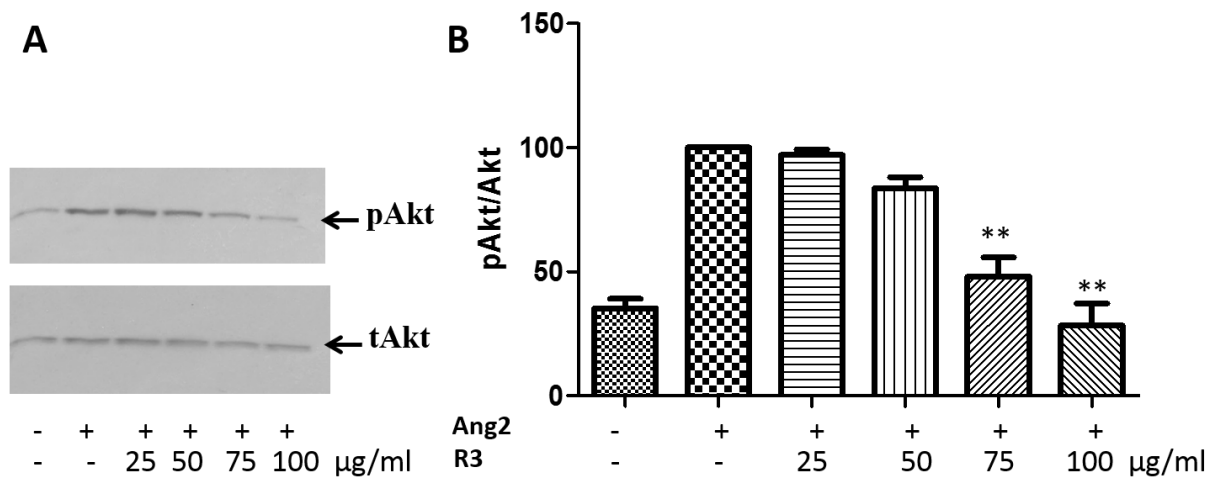


**Figure 4.15 Evolved ectodomain blocks the agonistic effects of Ang2 in HUVECs.**

A, The dose dependent of R3-Fc inhibited Ang2-activation of Akt phosphorylation were tested. Cells were stimulated with 6nM Ang2 with or without 25 to 100  $\mu\text{g/ml}$  R3-Fc for 30 min prior to cell lysis. Equal amounts of cell lysates were resolved by SDS-PAGE and immunoblotted with antibodies recognizing Akt phosphorylated on S473 (pAkt) or total AKT (tAkt) as indicated. B, Akt phosphorylation was quantified by densitometric scanning of blots from three independent experiments, normalized to total Akt and expressed as % of Ang2 effect. Data are expressed as means and SEM (\* $P < 0.05$ , \*\* $P < 0.01$  vs Ang2, oneway ANOVA followed by Tukey's analysis)..

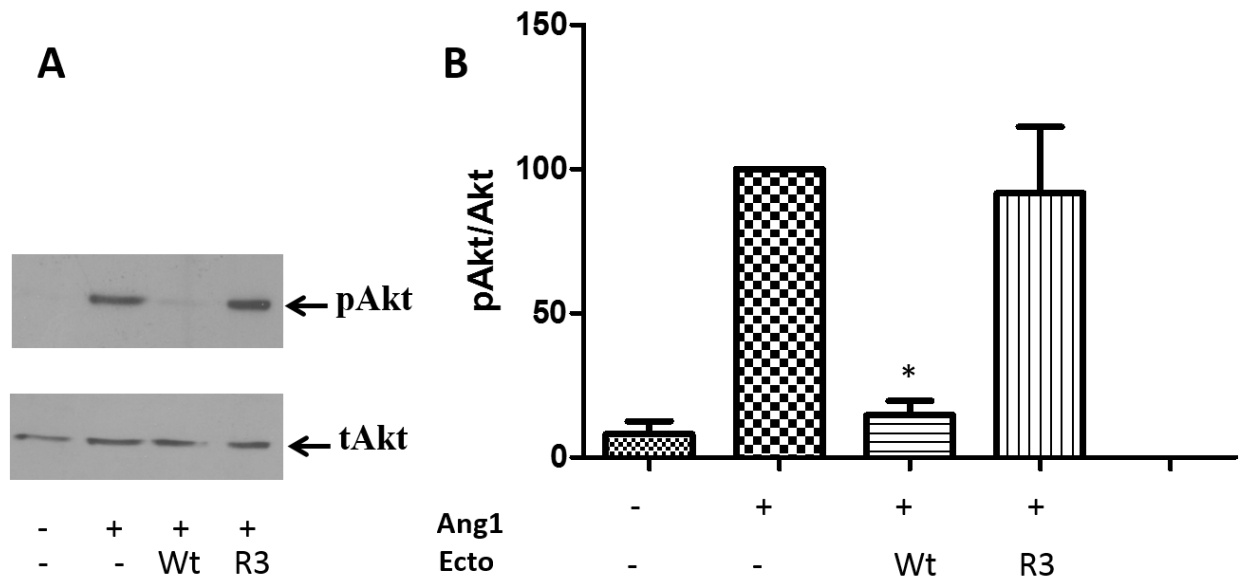


**Figure 4.16 Effect of R3-Fc and Wt-Fc on Ang1-activation of Akt phosphorylation in HUVECs.**

A, The effect of R3-Fc and Wt-Fc on Ang1-activation of Akt phosphorylation were tested. Cells were stimulated with 0.7nM Ang1 with or without 25 µg/ ml R3-Fc or Wt-Fc ectodomain for 30 min prior to cell lysis. Equal amounts of cell lysates were resolved by SDS/PAGE and immunoblotted with antibodies recognizing Akt phosphorylated on S473 (pAkt) or total AKT (tAkt) as indicated. B, Akt phosphorylation was quantified by densitometric scanning of blots from three independent experiments, normalized to total Akt and expressed as % of Ang1 effect. Data are expressed as means and SEM (\*P< 0.05, \*\*P<0.01 vs Ang1, oneway ANOVA followed by Tukey's analysis).

#### **4.6 Effect of evolved ectodomain on endothelial function regulated by angiopoietin**

The effects of evolved ectodomain was further examined in another cellular context. An endothelial migration assay was used to test the action of the R3 ectodomain on functional activity in endothelial cells. A previous study reported high concentration of Ang2 stimulated endothelial migration (Yuan et al., 2009). Endothelial cells (EA.hy926) were tested to their ability to migrate through a porous transwell membrane in response to Ang1 (0.7nM) or Ang2 (12nM) in the absence or presence of R3-Fc. Angiopoietin and R3–Fc were added to the lower chambers. As shown in Figure 4.17 and Figure 4.18 Ang1 caused an increase in endothelial migration to 150% of that seen with control treatment (no angiopoietin). Adding R3-Fc did not affect Ang1 stimulation of migration. This is consistent with R3 not being able to bind Ang1. High concentration of Ang2 also stimulated endothelial migration. When R3-Fc was added in these experiments it blocked Ang2-stimulated migration but had a lower effect than on cell signalling. This is consistent with Ang2 being bound by R3 preventing its action on endothelial cells.

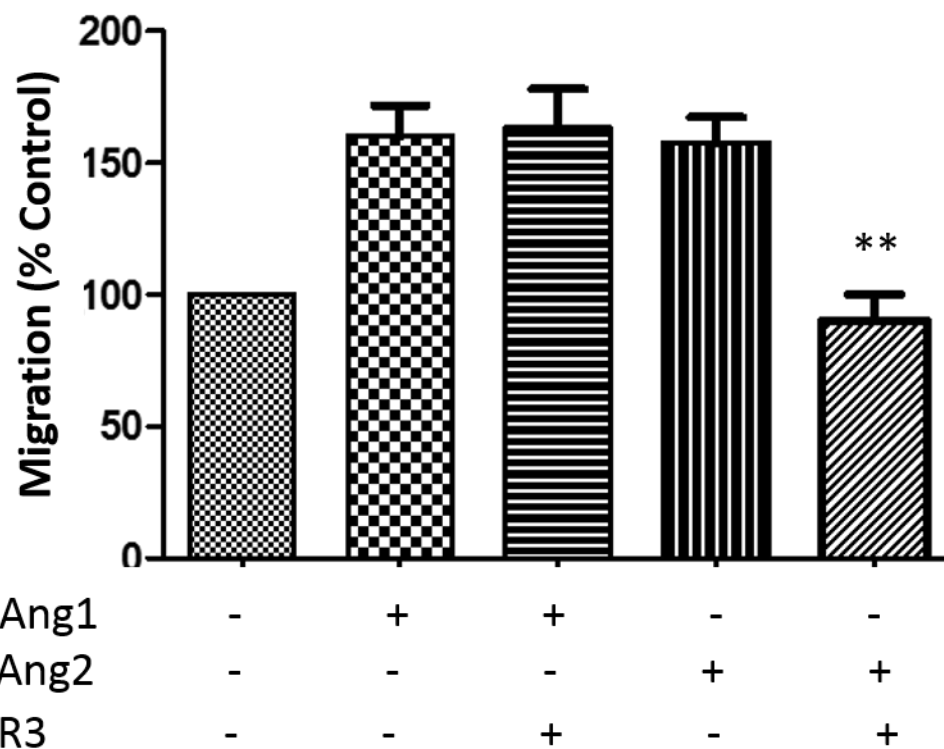


**Figure 4.17 Effect of evolved ectodomain on migration induced by angiopoietins in the endothelial cells line EA.hy926.**

Migration assays were performed in Transwell tissue culture well containing 8µm pore size inserts. Serum-free medium containing 250µg/ml BSA together with Ang1 (0.7nM) or Ang2 (12nM), in the absence or presence of R3-Fc, was placed in the lower chamber of the wells. 10<sup>5</sup> cells, in serum-free medium containing 250µg/ml BSA, were placed in the upper chambers and cells were allowed to migrate for 4h at 37°C. Cells on the upper surface were gently removed with a cotton bud and membrane fixed in 4% formaldehyde. Membranes were washed in PBS and nuclei stained with 4, 6-diamidino-2-phenylindole (0.1µg/ml). Membranes were mounted in glycerol and the numbers of cells migrating through the membrane were counted in 5 random fields on the underside of each insert membrane. Data are expressed as means and SEM for three independent experiments (\*\*p<0.01, one way ANOVA followed by Turkey's analysis).

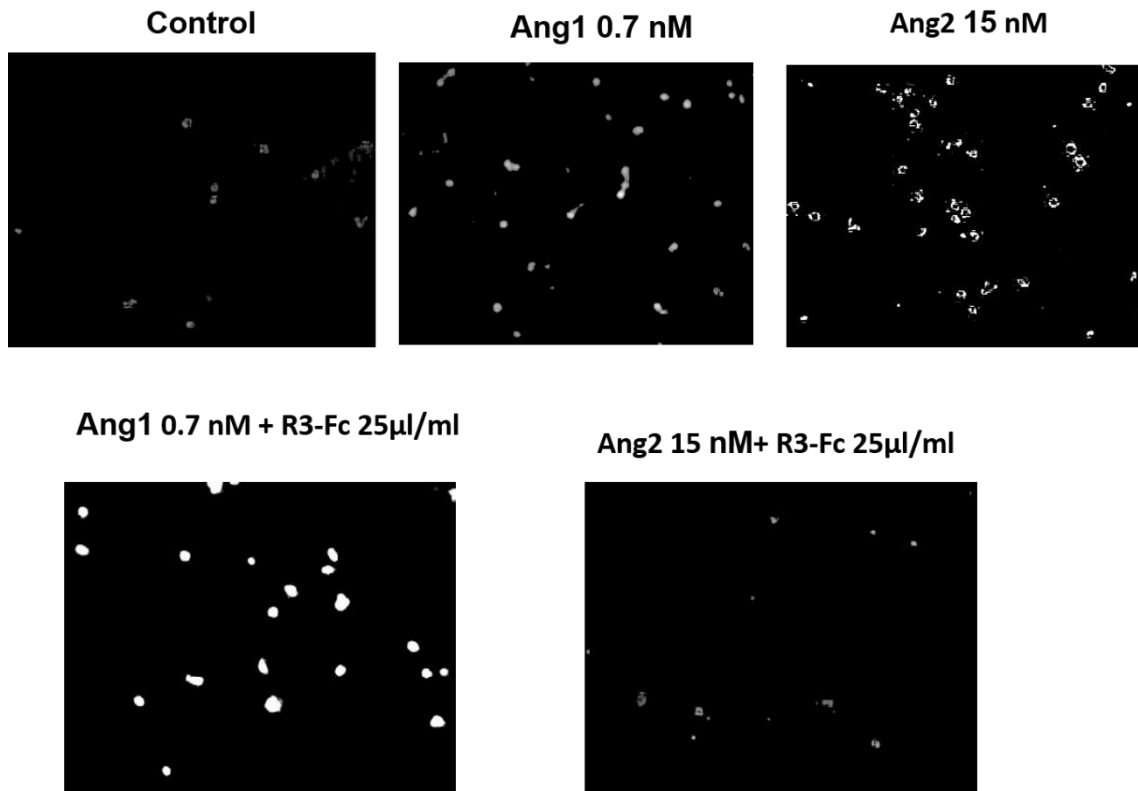


**Figure 4.18 Example of effects of evolved ectodomain on migration induced by angiopoietins in the endothelial cells line EA.hy926.**

Migration assays were performed as described in Section 2.10. Membranes were mounted in glycerol and the numbers of cells migrating through the membrane were counted in 5 random fields on the underside of each insert membrane. Cells undergoing migration were captured using a light microscope at x20 magnification

## 4.7 Discussion

In this study, the evolved ectodomain was engineered from the wild-type Tie2 ectodomain by directed evolution strategy producing a specific Ang2 binding protein form. This form switches binding specificity by a combination of three amino acid changes at the receptor binding interface. Generally, wild-type Tie2 ectodomain binds to Ang1 and Ang2 with the same site of the receptor binding domain and Ang2 binds Tie2 but with lower affinity than Ang1 (Yuan et al., 2009). Therefore it has been difficult to modify those properties of a non-specific angiopoietin receptor to specific Ang2 binding, but this can be done by using cell surface display in combination with somatic hypermutation-driven gene diversification. In order to characterise the mutant protein, the soluble recombinant proteins were produced in mammalian cells system because these cells have the necessary posttranslational modifications. Glycosylation is one of the most common posttranslational modifications of proteins. Glycosylation may affect protein stability, solubility, antigenicity, folding, localization, biological activity, and circulation half-life (Palomares et al., 2004). Based on amino acid sequence, the predicted molecular mass of R3-Fc is 75 kDa. SDS/PAGE (Figure 4.3) estimates the mass at approximately 100 kDa. It is likely to additional mass due to glycosylation of the ectodomain.

Although recombinant protein production in HEK293 cells produced soluble ectodomain-Fc fusion proteins the yields of the mutants were still low, at levels of 1.2 mg/L. To further improve yields and quality for production of these proteins, the system requires further optimisation.

The data demonstrate the ability of the evolved ectodomain to bind Ang2 but not Ang1 in BLI analysis and ELISA assays. As expected wild-type ectodomain was able to bind both ligands. R3-Fc preferentially bound to Ang2 and had negligible Ang1 binding. However, R3-Fc has lower maximal binding for Ang2 binding compared to Wt-Fc. These results indicate the changes of three residues make a dramatic switch in the binding characteristics of the evolved ectodomain. To further explore the individual effects of the F161I substitution and double deletion of R167 and H168, these substitutions were tested for Ang1 and Ang2 binding in

ELISA. It was found that angiopoietin-binding ability between wild-type and F161I-ectodomain were similar, while angiopoietin-binding ability of double deletion of R167 and H168 was abolished. The crystal structures of the Ang2-Tie2 complex, and the Ang1-Tie2 complex have been reported (Barton et al., 2006, Yu et al., 2013). It is known that the first 210 amino acids of the Tie2 receptor is important to bind both Ang1 and Ang2 (Barton et al., 2006) and the mutations of R3-Fc occur at the binding interface of the receptor. Nonetheless, the finding by the ELISA binding assay showed mutation of I for F161 in Tie2 ectodomain did not alter binding to both ligands. This mutation is unlikely to affect binding affinity to angiopoietin ligands. As determined from the crystal structure of Ang2 in complex with Tie2, F161 of Tie2 contacts with F469 in Ang2 (Barton et al., 2006). Substitution of I for F does not change the hydrophobic character of this position but this mutation may alter stacking interactions with non-protein ligand that contain aromatic groups at this position. The phenylalanine and isoleucine are closely related (Betts and Russell, 2003). They often play a roles in binding recognition.

Double deletion of R167 and H168 ectodomain lost the ability of Ang1 and Ang2 binding in ELISA assay, demonstrating a major role of these residues in binding. Crystal structure showed R167 and H168 form a salt bridge with the D448 in Ang2 and the D450 in Ang1. Additionally, H168 forms a hydrogen bond with Y476 in Ang2 and also interacts with P452 (Barton et al., 2006). In general, the formation of salt-bridges creates stabilizing hydrogen bonds that are important for protein stability. Both Y476 and P452 are conserved in Ang1 and Ang2. Hence it would be anticipated that deletion of RH affected both Ang1 and Ang2 binding. It is concluded that specific Ang2 binding was seen only when the presence of three residues mutation and this was not seen in either individual F161I ectodomain or deletion of R167/H168 ectodomain. An understanding of the mechanism for specific Ang2 binding of R3 will require determination of R3 structure.

The evolved molecule was tested for inhibitory effect on Ang2 at cellular and functional levels in endothelial cells. It is known Ang2 exhibits context-dependent behaviour. Ang2 can inhibit or stimulate Tie2 receptor phosphorylation under

different experimental conditions. Examination of the effects of R3-Fc on Ang1 and Ang2 effects on Akt phosphorylation was performed. The evolved ectodomain was found to inhibit both agonist and antagonist effects of Ang2 on Akt signaling. Importantly, R3-Fc did not inhibit Ang1 signaling. In addition to blocking the effects of Ang2 on signaling, R3 also inhibited Ang2 effects on endothelial migration. These data are consistent with the ability of R3-Fc to bind specifically to Ang2 and block the Ang2 binding to cellular Tie2 receptor.

In our present study, the evolved ectodomain is able to interfere the agonistic and antagonist effects of Ang2. It was interesting that higher concentrations of R3 were needed to inhibit Ang2 effects on signalling in HUVECs (Figure 4.15) than to inhibit migration effects in EA.hy926 cells (Figure 4.17). The reason for this cell-specific difference is not known and requires further investigation. Increasing evidence suggests Ang2 is associated with number of diseases (Lind et al., 2005, Bhandari et al., 2006, Fiedler and Augustin, 2006). Recently, many studies reported that elevated Ang2 can promote the tumour angiogenesis and metastasis (Albini and Noonan, 2012, Mazzieri et al., 2011). Therefore, blocking of Ang2-Tie2 receptor interaction mediated anti-angiogenesis, thereby inhibiting of tumour proliferation. This evolved protein therefore is a possibly attractive therapeutic agent for cancer and other pathological conditions that have elevated Ang2, including inflammation, tumour angiogenesis and sepsis.

## **Chapter 5: Modification of R3, Integrin binding and *in vivo* activity**

This chapter describes work aimed at decreasing the molecular size of R3 and testing whether R3 affects the interaction of Ang2 with integrins. In addition, the effects of R3 *in vivo* are examined.

### **5.1 Decreasing R3 Size**

R3-Fc is approximately 80 kDa. Whilst this is smaller than therapeutics such as antibodies, a further decrease in R3 size may increase functionality of the protein as it is likely to improve tissue penetration. The angiopoietin binding site in wild-type Tie2 lies on the second Ig domain (Barton et al., 2006). In deletion studies the minimum size of Tie2 to retain angiopoietin-binding has been reported as residues 1-210 (Macdonald et al., 2006). As the three amino acids responsible for Ang2 specific binding of R3 are at position 161, 167 and 168. It is likely that a smaller version of R3 encompassing residues 1-210 would also be capable of binding Ang2 and retaining its specificity. To create this truncated form of R3, site directed mutagenesis was used. pCEP-Wt-Tie2-Fc (Appendix 7.3) which comprises of 1-210 Tie2 with C-terminal human Fc and His6 tag was kindly supplied by Dr Richard Kammerer (Paul Scherrer Institute, Switzerland). Primers were designed to introduce the F161I and R167, H168 deletion into the wild-type sequence by site directed mutagenesis. Site directed mutagenesis was performed using the QuickChange protocol. In order to produce R3-210 a two-stage strategy was used. Firstly, F161I was introduced the F161 into this sequence prior to transformation into competent cells. The sequence was subsequently confirmed by sequencing. Following generation of F/I pCEP-Fc, this plasmids further required to introduce RH deletion mutation into F/I pCEP-Fc. Sequencing was again utilized as confirmation of mutation of the R167, H168 deletion into R31-210 F161I pCEP-Fc.

In order to characterise the R3-210 protein, this plasmid construct was transiently transfected and expressed into HEK293 cells before purification as a soluble fusion protein. His-tagged R3-210 was purified by nickel affinity chromatography as a soluble recombinant form. After the purification steps, fractions of eluted protein of R3-210 were stained with Coomassie blue dye following gel electrophoresis as shown in

Figure 5.1. Three faint bands were observed at around 70 kDa on the gel and a single band is seen in each fraction. The concentration of purified protein was below that detectable using the Bradford protein assay. This probably was due to the yields of protein being very low and out of working range of detection that should be within range 20-2000  $\mu\text{g/ml}$ . To detect fractions of soluble R3-210 following protein purification the fractions were subjected to SDS/PAGE followed by immunoblotting with anti-Tie2 ectodomain antibody as shown in Figure 5.2. In order to maximize yields of soluble protein, scaling up the initial volume of cell culture was optimised for transfection. The yields obtained after optimisation did not improve. These experiments were repeated several times and ended up with the same outcomes. It was not possible to obtain enough purified R3-210 to allow characterisation in binding and cellular assay. These experiments were suggestive for optimizing the development of R3 in the future.

## **5.2 The effects of R3 on Ang2 integrin binding**

Recently Felcht (Felcht et al., 2012) reported that Ang2 bound to integrins  $\alpha\beta3$ ,  $\alpha\beta5$ , and  $\alpha5\beta1$  in a subpopulation of TIE2-negative endothelial cells. Integrins are heterodimeric cell surface molecules composed of alpha and beta subunits that are involved in angiogenesis and cancer. Interestingly,  $\alpha\beta3$  integrin has been shown to be abundantly expressed on angiogenic endothelial cells (Kim et al., 2000b, Weis and Cheresh, 2011a). The binding site for integrins on Ang2 is not known. It is also not known whether binding of Tie2 ectodomain affects Ang2 binding to integrins. However, the ability of ectodomain to block integrin binding may be useful for suppressing integrin mediated Ang2 effects. Experiments were therefore designed to test the effects of R3 on Ang2 binding to integrins.

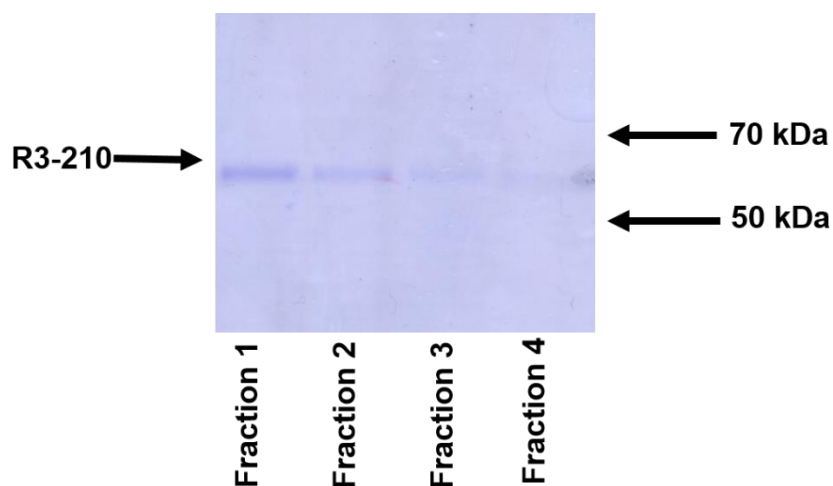


**Figure 5.1** Coomassie stained SDS gels of protein fraction of soluble R3-210.

Soluble R3-210 ectodomains were purified with Ni-NTA chromatography following expression in HEK293 cells. Fractions 1-4 were resolved by SDS/PAGE followed by staining with Coomassie blue. The position of R3-210 is indicated.

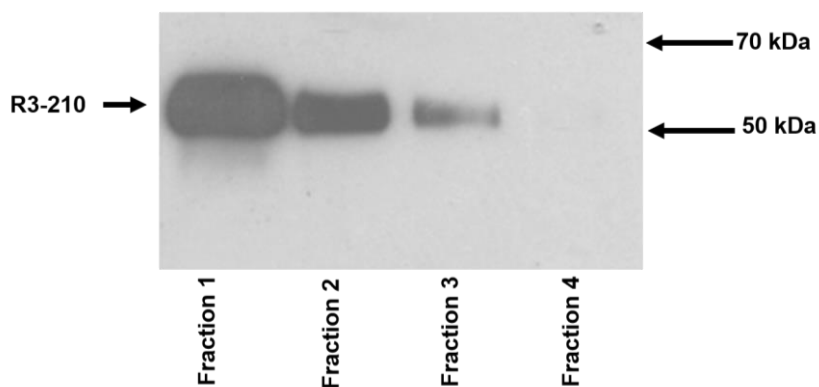


**Figure 5.2** Blot expressions of protein fraction of soluble R3-210 probed for Tie2.

Fractions of soluble R3-210 were purified with Ni-NTA chromatography following expression in HEK293 cells. Fractions 1-4 were further resolved by SDS/PAGE and Western blot followed by immunoblotting with Tie2 ectodomain antibody as described in Section 2.5. The positions of molecular weight marker are indicated. Protein bands, between 50-70 kDa, were observed in fractions 1-3.

### ***5.2.1 Effects of pH on ectodomain Ang2 binding***

To test the ability of R3-Fc to bind Ang2 and block Ang2 bound to integrin as initial test, binding of R3 or Wt ectodomain to Ang2 was examined using ELISA binding assay under the conditions reported for Ang2 binding to integrins (Felcht et al., 2012). Ang2 was immobilized overnight at 4°C. Following blocking with TBS, 25 µg/ml R3-Fc and Wt-Fc were added to bind for 2 hour prior to detection with anti-Tie2 ectodomain antibody followed by peroxidase-conjugated secondary antibody and colorimetric quantification. Since  $\alpha\beta3$  integrin requires acidic extracellular pH for binding (Paradise et al., 2011), this binding assay was performed at different pH values of 4.5 and 7.5. As shown in Figure 5.3 R3-bound Ang2 in acidic pH was higher as compared with wild-type Tie2 ectodomain bound Ang2 in physiologic pH. Although it looked like the wild-type bound to Ang2 was more increased at low pH than physiologic pH, but there was no significant difference in ability of the wild-type ectodomain to bind Ang2 upon the change of pH. Interestingly, the ability of R3 to bind Ang2 was significantly higher than that of the wild-type in neutral pH. These experiments confirmed that R3 could be able to bind Ang2 at pH 4.5, the pH at which Ang2-integrin binding has been examined by Felcht (Felcht et al., 2012).

### ***5.2.2 Ang2 integrin binding***

To examine Ang2 binding to integrin, an ELISA was established under conditions previously reported (Felcht et al., 2012). 2 µg/ml  $\alpha\beta3$  integrin was immobilized overnight at 4°C. Following blocking with TBS containing BSA, 2 µg/ml biotinylated-Ang2 were added to bind integrin for 2 hour prior to detection with Streptavidin-HRP followed by peroxidase-conjugated secondary antibody and colorimetric quantification.

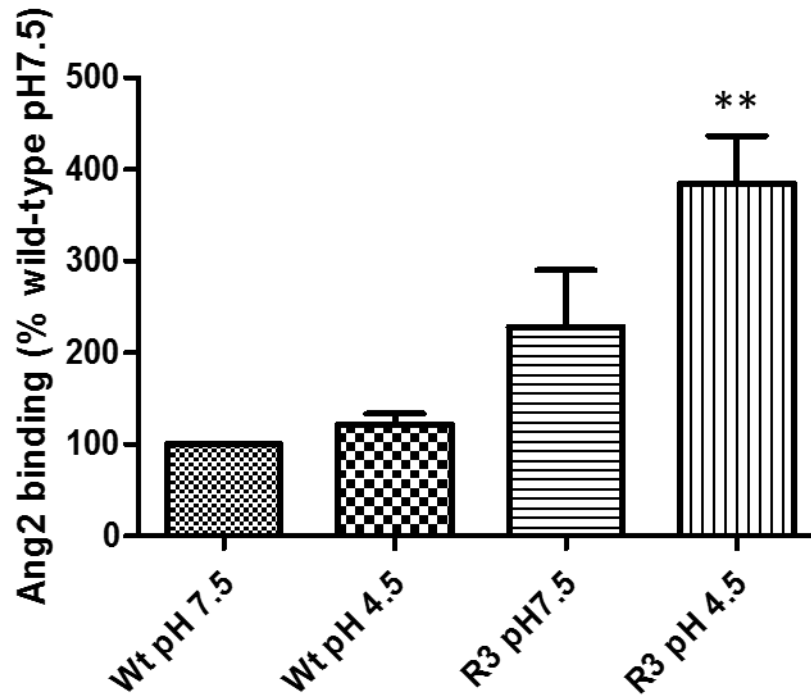


**Figure 5.3 The ability of R3 to bind Ang2 in pH 4.5 and pH 7.5.**

Binding of R3-Fc or Wt-Fc to Ang2 was examined using ELISA binding assay in which 2  $\mu\text{g/ml}$  Ang2 was immobilized overnight at 4°C. Following blocking with TBS 1% BSA with 1 mM  $\text{Mn}^{2+}$ , 25  $\mu\text{g/ml}$  R3-Fc or Wt Fc was added to bind Ang2 for 1 hour. Following washing with TBS at the indicated pH, the binding was detected with Tie2 ectodomain antibodies followed by peroxidase-conjugated secondary antibody and colorimetric quantification. The experiment was performed at three independent times. Data are expressed as mean  $\pm$  SEM related to wild-type binding at pH 7.5 (\* $P < 0.05$ ; \*\* $P < 0.01$ , One-way ANOVA and performing all the pairwise comparisons using Tukey's Test).

Three independent experiments of ELISA were performed and data showed very low binding signal between Ang2 and integrin at pH 4.5 and pH 7.5 as shown in Figure 5.4 and Figure 5.5. There was no significant difference between BSA and integrin for Ang2 binding, Therefore, it was not possible to test the ability of R3-Fc for blocking Ang2 binding to integrin by this method.

Alternative way to test the effect of R3-Fc on integrin-Ang2 binding was therefore tried. For a preliminary experiment, co-immunoprecipitation assay using anti-integrin together with integrin and Ang2 was performed and co-immunoprecipitation of Ang2 with integrin was tested. Ang2,  $\alpha\beta3$  integrin and human anti-integrin  $\alpha\beta3$  antibody (R&D) was incubated with protein G-Sepharose beads. Ang2 incubated with nonspecific IgG was used as negative control. Ang2 incubated with integrin and G-Sepharose beads was also used as control. Following incubation overnight at 4°C, the immunoprecipitate samples were resolved by SDS/PAGE prior to immunoblotting with anti-His tag antibody to detect Ang2. As shown in Figure 5.6, one single sharp band was observed at around 50 kDa correspond to the molecular mass of Ang2 and this was stronger in the presence of  $\alpha\beta3$  and anti- $\alpha\beta3$ . This suggests binding of Ang2 and  $\alpha\beta5$  integrin in this assay.

Experiments were performed in the presence of R3-Fc to test whether it inhibits Ang2 binding. However, the R3 construct contains a His tag. His tag bound blots were difficult to interpret due to a strong background signal for the R3 (data not shown). This immunoprecipitation assay was therefore adapted further monitoring binding of biotinylated-Ang2 to integrin with and without R3-Fc and recovering Ang2 with streptavidin beads. The activity of  $\alpha\beta3$  integrin to bind Ang2 was tested by integrin antibody. Integrin  $\alpha\beta3$  and streptavidin beads was incubated and used as negative control. Following incubation overnight at 4°C, the immunoprecipitate were resolved by SDS/PAGE followed by immunoblotting with human integrin  $\alpha\beta3$  antibody (R&D).

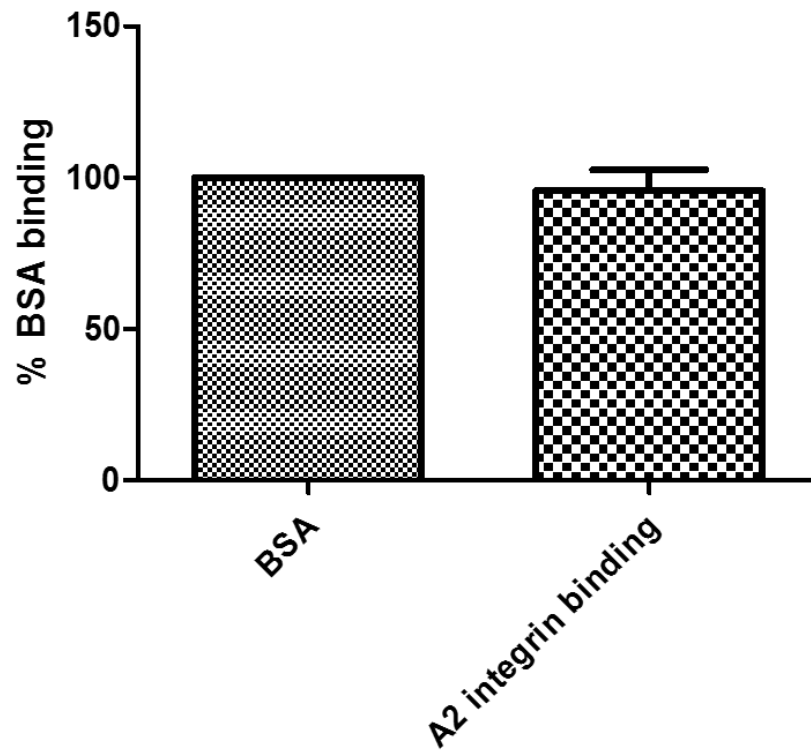


**Figure 5.4 The ability of Ang2 to bind  $\alpha\beta 3$  integrin in pH 7.5.**

Ang2 integrin binding ELISA was performed. 2  $\mu\text{g/ml}$   $\alpha\beta 3$  integrin was immobilized for overnight at 4°C. Following blocking with TBS (1% BSA) with 1 mM  $\text{Mn}^{2+}$ , 2 $\mu\text{g/ml}$  biotynalated Ang2 were added to bind integrin with indicated pH for 2 hour prior to detection with Streptavidin-HRP followed by peroxidase-conjugated secondary antibody and colorimetric quantification. Student's t-test was performed but there was no significant difference between BSA and Ang2-integrin binding. The experiment was performed at three independent times. Data are expressed as mean  $\pm$  SEM related to %BSA binding.

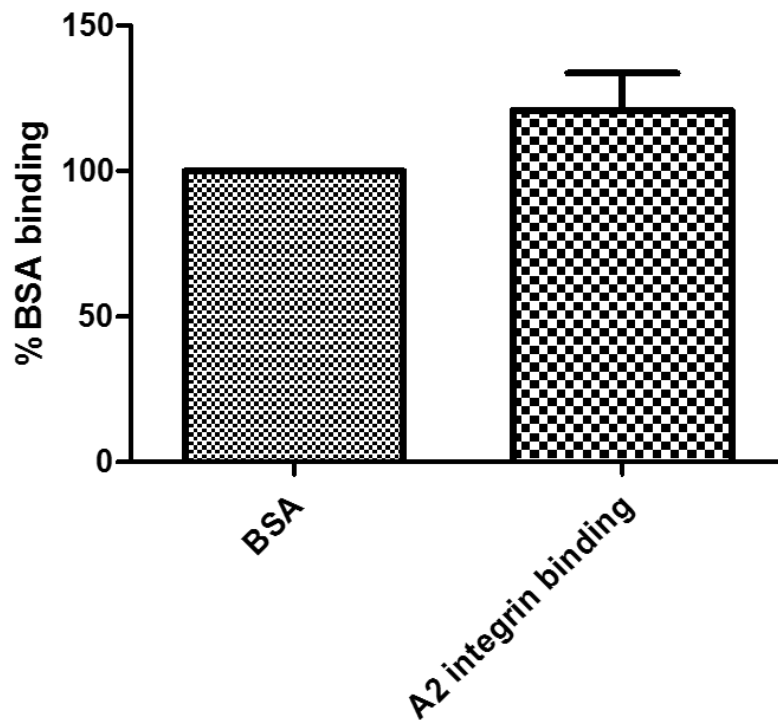


**Figure 5.5 The ability of Ang2 to bind  $\alpha\beta 3$  integrin in pH 4.5.**

Ang2 integrin binding ELISA was performed. 2  $\mu\text{g/ml}$   $\alpha\beta 3$  integrin was immobilized for overnight at 4°C. Following blocking with TBS (1% BSA) with 1 mM  $\text{Mn}^{2+}$ , 2  $\mu\text{g/ml}$  biotynalated-Ang2 were added to bind integrin with indicated pH for 2 hour prior to detection with Streptavidin-HRP followed by peroxidase-conjugated secondary antibody and colorimetric quantification. Data are represented as mean  $\pm$  SEM compared to % BSA binding. Student's t-test was performed but there was no significant difference between BSA and Ang2-integrin binding. The experiment was performed at three independent times. Data are expressed as mean  $\pm$  SEM related to %BSA binding.

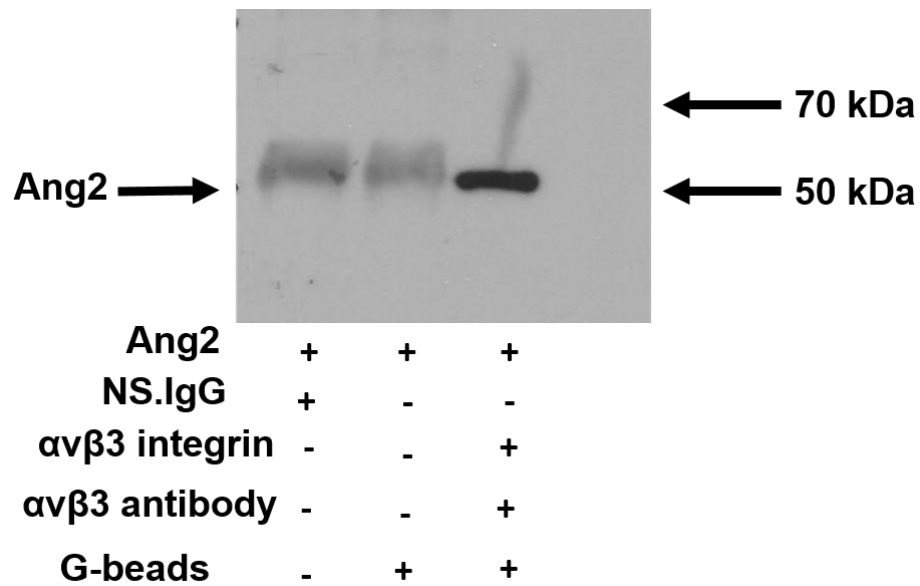


**Figure 5.6 The ability of Ang2 to bind  $\alpha\beta 3$  integrin in immunoprecipitation assay for Ang2 in a cell-free system.**

300ng Ang2, 500 ng integrin  $\alpha\beta 3$  and 2  $\mu\text{g}$  integrin  $\alpha\beta 3$  antibody was incubated with protein G-Sepharose beads. Ang2 incubated with G sepharose beads was used as control. Ang2 incubated with nonspecific IgG was used as negative control. Following incubation overnight at 4°C, the immunoprecipitate samples was resolved by SDS/PAGE and Western blot followed by immunoblotting with anti-His tag antibody against Ang2. The position of Ang2 is indicated by arrow. This experiment was performed two times.

In all blots there were no immunoreactive bands detected (data not shown). Possible reasons could be that the anti-integrin antibody was not sensitive enough to detect the integrin bound to Ang2, or alternatively there was no binding between Ang2 and integrin. The membrane was stripped and re-probed with streptavidin HRP antibody to confirm binding of Ang2 and streptavidin beads. As shown in Figure 5.7, Ang2 bound to streptavidin beads is indicated. This experiment was repeated 2 times with the same result. In addition the membrane was stripped and re-probed with two further different  $\alpha\beta3$  integrin antibodies. However again no immunoreactive bands were detected (data not shown). As these experiments were being performed parallel studies were done in which Ang2 was pre-incubated with R3-Fc for 20 minutes on ice, then anti-his tag antibody was added and preincubated with integrin followed by incubation with protein G-sepharose beads in indicated buffer overnight at 4°C. Following incubation, the immunoprecipitate was subjected to SDS/PAGE and Western blot followed by immunoblotting with the rabbit monoclonal antibody to integrin beta3. Integrin incubated with anti-his tag antibody and protein G-sepharose beads was used as negative control. As shown in Figure 5.8 again no bands were corresponding to integrin. Importantly, the antibody also failed to detect  $\alpha\beta3$  integrin on the blot. Due to time constraints, therefore, it was not possible to establish a satisfactory assay.

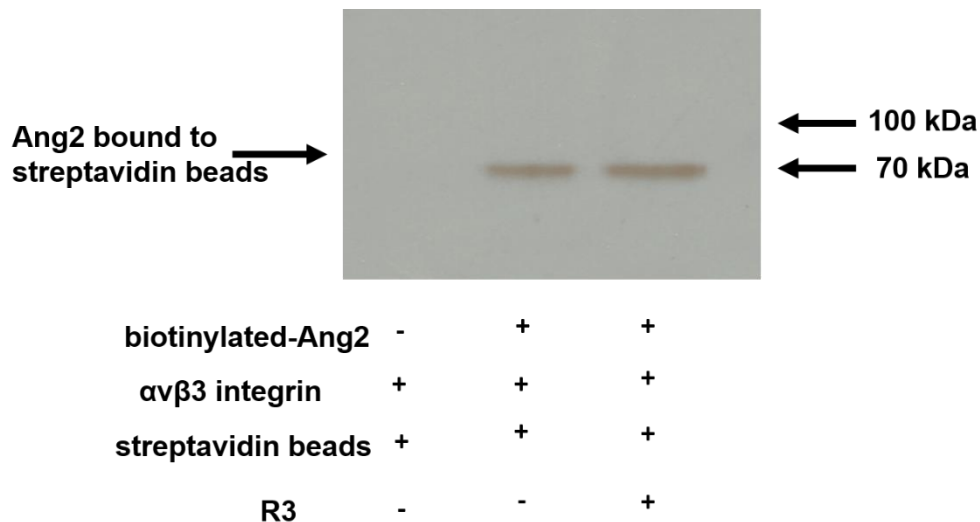


**Figure 5.7 The ability of Ang2 to bind  $\alpha\beta 3$  integrin in immunoprecipitation assay for  $\alpha\beta 3$  integrin in a cell-free system.**

Immunoprecipitation assay for Ang2-integrin binding was performed. 25 $\mu$ g/ml R3-Fc was preincubated with 300 ng biotinylated Ang2 for allowing R3-Fc bound to Ang2. Twenty minutes later, biotinylated Ang2 with and without R3-Fc was further preincubated with 500 ng  $\alpha\beta 3$  integrin on ice for 10 minutes to form the Ang2- $\alpha\beta 3$  integrin complex before adding streptavidin beads into each sample. Integrin  $\alpha\beta 3$  and streptavidin beads was incubated and used as negative control. Following incubation overnight at 4°C, the immunoprecipitate were resolved by SDS/PAGE and Western blot followed by immunoblotting with human integrin  $\alpha\beta 5$  antibody (R&D). The signal of Ang2-integrin binding was not visible on blot. The membrane was stripped and re-probed for streptavidin HRP antibody to confirm the generation of Ang2 and streptavidin beads. The Ang2 bound to streptavidin bead are indicated as molecular marker around 66 kDa. This experiment was performed two times.

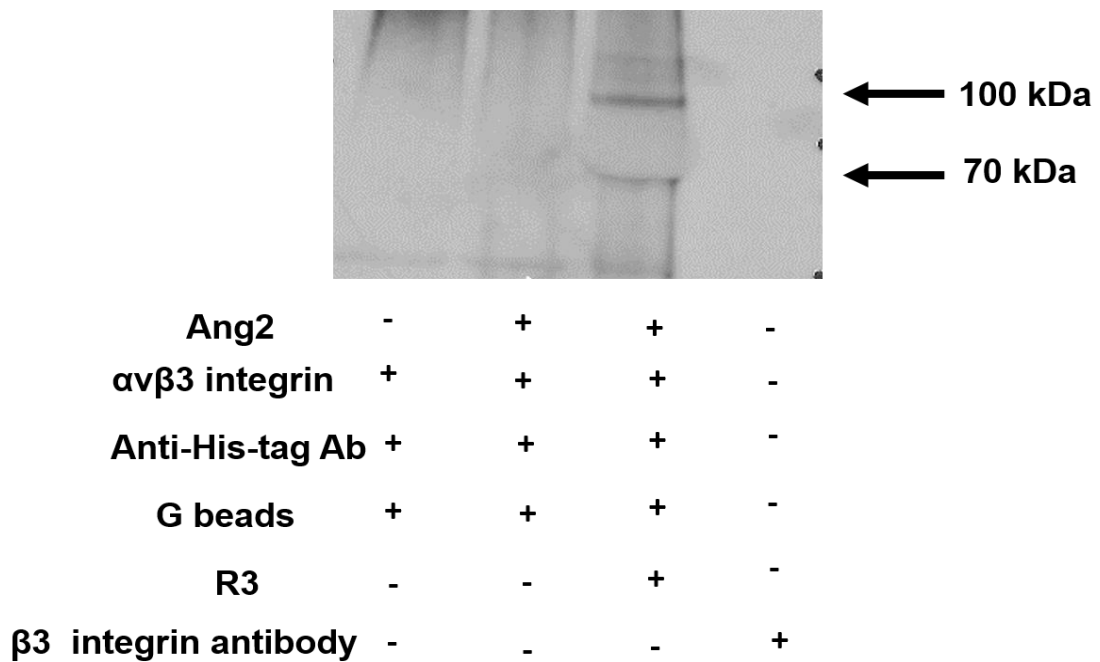


**Figure 5.8 The ability of Ang2 to bind  $\alpha\text{v}\beta\text{3}$  integrin in immunoprecipitation assay for  $\alpha\text{v}\beta\text{3}$  integrin in a cell-free system.**

300 ng Ang2 was preincubated with 25 $\mu\text{g}/\text{ml}$  R3-Fc for 20 minutes on ice. Then anti-his tag antibody was added and preincubated with  $\alpha\text{v}\beta\text{3}$  integrin followed by incubation with protein G-sepharose beads in indicated buffer overnight at 4°C. Following incubation the immunoprecipitates were subjected to SDS/PAGE and Western blot followed by immunoblotting with the rabbit monoclonal antibody to integrin beta 3 antibody. Integrin and anti-his tag antibody was used as negative control. The positions of protein markers are indicated.

## **5.3 Test of R3 activity in vivo**

### ***5.3.1 Effects on local oedema***

The Angiopoietins have been proved to play a role in regulating vascular permeability. Ang1 has anti-inflammatory properties by inhibiting vascular permeability and oedema in response to lipopolysaccharide (LPS), VEGF and other inflammatory agents (Yao et al., 2014). Conversely, Ang2 promotes inflammation and vascular leakage and mediates the pro-leakage effects of LPS (Mofarrahi et al., 2008). Therefore, initial testing for the potential of evolved ectodomain in vivo activity was examined. To test in vivo activity of R3-Fc, its ability to inhibit localized oedema formation induced by LPS was determined. Mice were injected subcutaneously in the hock with control vehicle, or LPS with or without evolved ectodomain (R3-Fc) or the non-binding RH deletion ectodomain. One and two hours later, mice were culled by cervical dislocation. Blood was collected and mouse hocks were prepared for histological analysis. As shown in Figure 5.9 subcutaneous oedema was produced by LPS as demonstrated by increased subcutis thickness, measured from the distance of the tibia periost to epidermis. This effect was blocked by R3-Fc. Subcutaneous thickness and the data are provided in Figure 5.10 and Figure 5.11. Additional experiments were performed in which Dr. Cordula Stover (University of Leicester) analysed hocks are shown in Figure 5.12. Overall these data suggest R3 inhibited activity of LPS to induce oedema in this model. However additional numbers of mice will be needed to confirm this statistically.

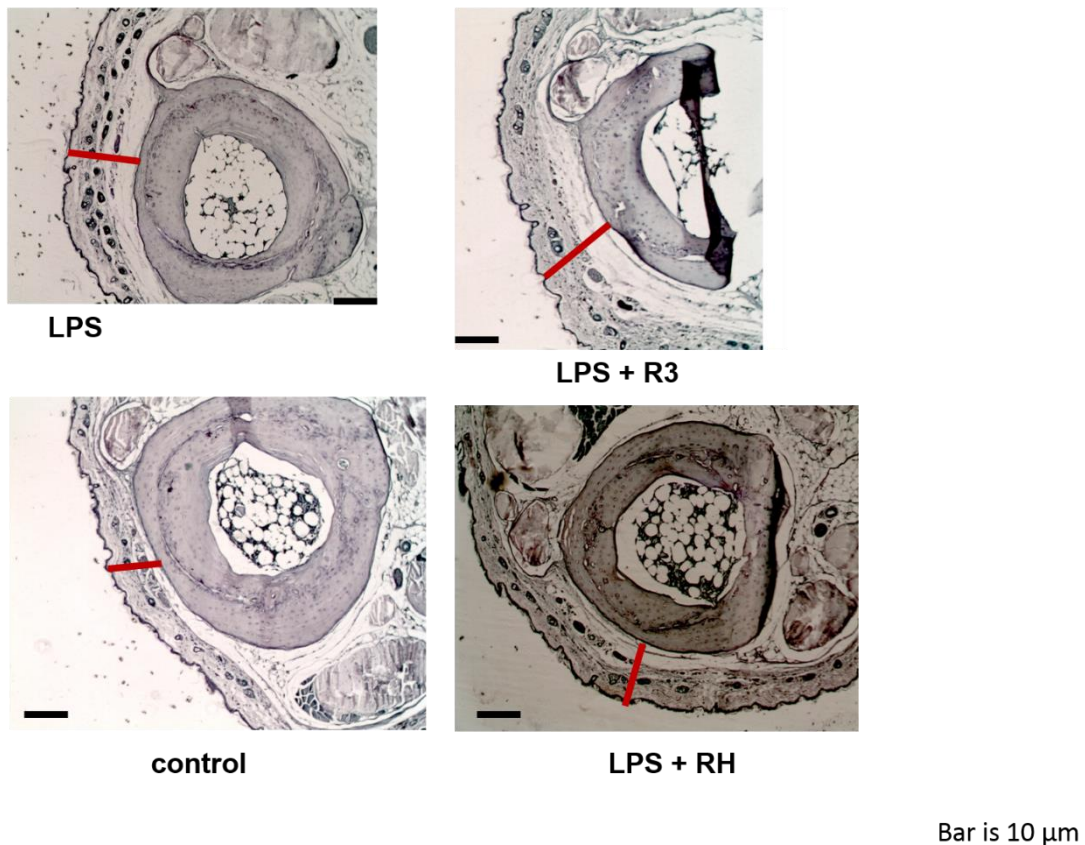


**Figure 5.9 Examples of measurement of subcutis thickness in various mice hock sections.**

Mice were received 5 $\mu\text{g}$  LPS with and without 15  $\mu\text{g}$  R3-Fc. After 2 hours, mice were sacrificed and hocks were prepared for histological analysis. 5  $\mu\text{m}$  sections were stained with Wright's stain. The distances of the tibia periost to epidermis were measured using Delta Pix InSight (v.3.3.1) image software. These images were done using magnification of x 20. Red lines indicate subcutical thickness.

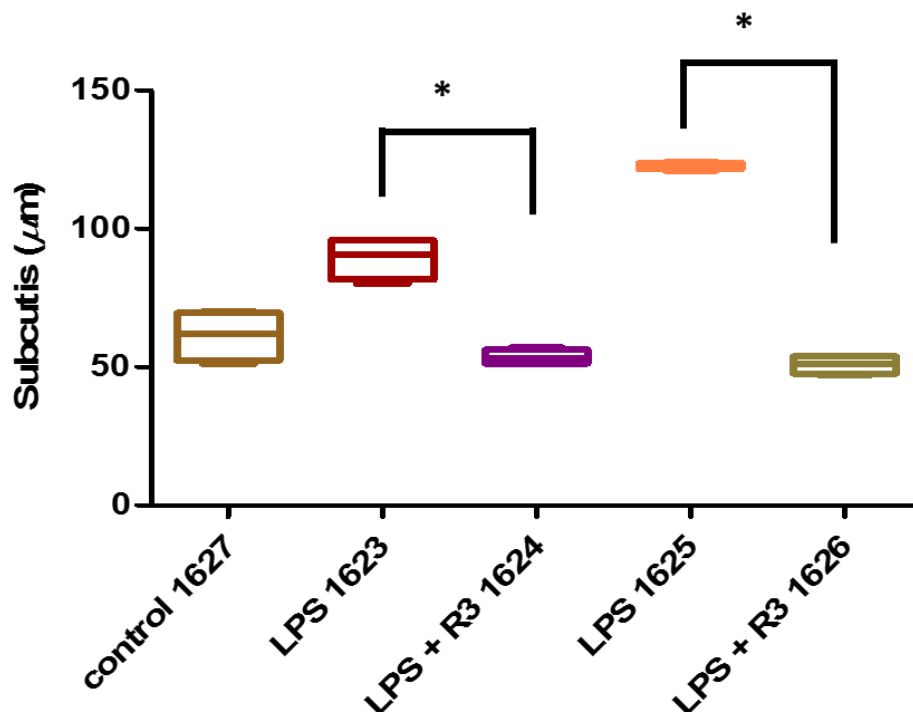


**Figure 5.10 Quantitative analysis of local oedema formation in mice after 1 hour injection.**

Mice injected with control carrier, 5µg LPS, 5µg LPS with 15µg R3-Fc. After 1 hour mice were sacrificed and hock prepared for histological analysis. 5µm sections were stained by Wright's stain. Data from individual mouse hocks are presented as mean subcutis thickness (distance between tibial periost and epidermis). Mean ± SEM for at least five measurements/section are shown and compared to the matched controls (\*P<0.05; \*\*P<0.01, Students't' test). All samples were blinded.

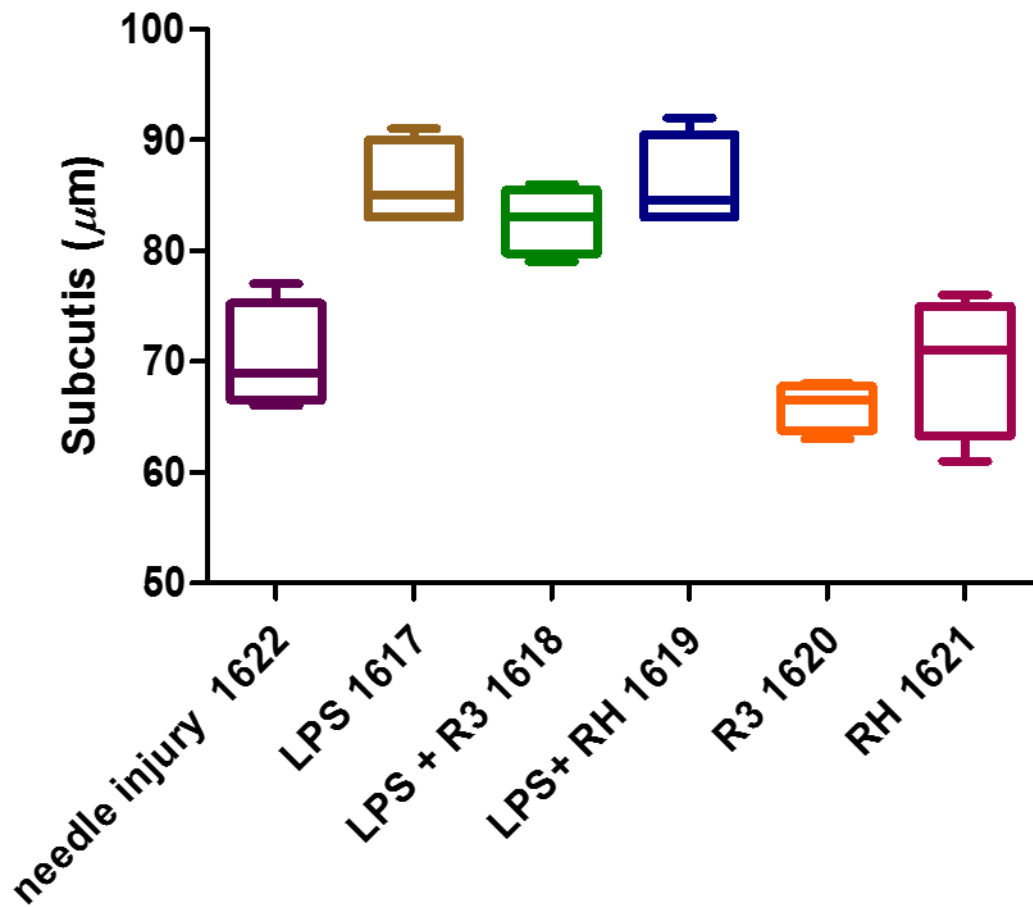


**Figure 5.11 Quantitative analysis of local oedema formation in mice after 2 hour injection.**

Mice injured with needle as control, mice injected with 5 µg LPS, LPS with 15 µg R3-Fc, LPS with 15 µg RH ectodomain, 15 µg R3-Fc and 15 µg RH ectodomain. Data from individual mouse hocks are presented as mean subcutis thickness (distance between tibial periost and epidermis). Mean ± SEM for at least 5 measurements/section are shown and compared to the matched controls (\*P<0.05; \*\*P<0.01, Students't' test). All samples were blinded.

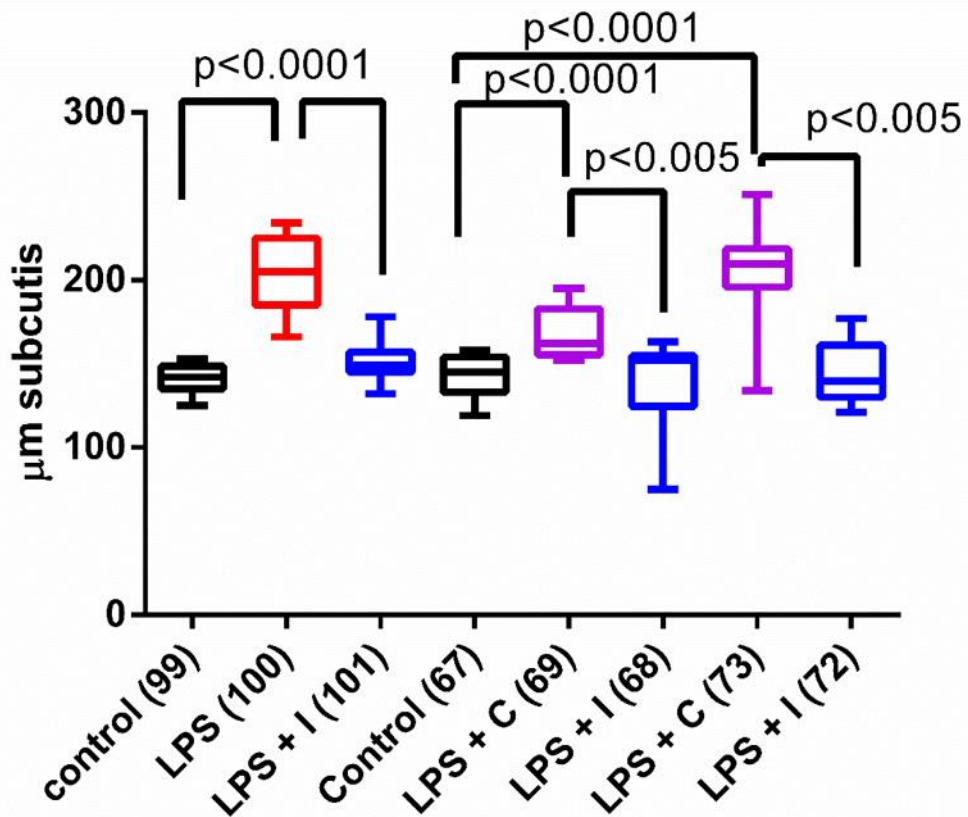


**Figure 5.12 Evolved ectodomain suppresses localized oedema in vivo.**

Quantitative analysis of local oedema formation in mice injected with control carrier, LPS, LPS with R3-Fc or LPS with  $\Delta$ R16, H168 ectodomain or C. Data from individual mouse hocks taken two hours post-injection are presented as mean subcutis thickness (distance between tibial periost and epidermis), minimum and maximum values  $\pm$  SD and compared to the matched controls (\* $P < 0.005$ ; \*\* $P < 0.0001$ , Students 't' test). The experiment was performed at two independent times (mice 99-101 and 67-69, 72,73) with the same stock of LPS.

### **5.3.2 Effects on Factor B**

Complement factor B is part of the alternative pathway of the complement activation and has a role to protect host cells from pathogen (Markiewski and Lambris, 2007). It normally circulates in the blood as non-activated form. The single polypeptide chain of factor B get cleaved into Bb and Ba by complement factor D upon the activation of the alternative pathway. Activation of factor B mediates inflammatory processes which results in the production of C3bBb. It also becomes activated by LPS (Prakash and Hellman, 2010). Factor B is used as indicator of inflammation.

Therefore, the effects of R3 on factor B were also tested. To do this serum from mice that had been injected with LPS with or without R3 were subjected to SDS/PAGE followed by immunoblotting with goat anti Complement Factor B detected with donkey anti goat (Fab') 2. As shown in Figure 5.13, LPS caused loss of intact factor B. This was blocked by R3. Additional experiments will be required to test reproducibility.

### **5.3.3 Effects on Mast cell degranulation**

Mast cells are involved in oedema, itchiness, innate and adaptive immune responses, and wound healing (Stone et al., 2010). Degranulation of mast cells occur following mast cell activation results in the release of many pro-inflammatory mediators such histamine and heparin (Iuvone et al., 1999).

To test the effects of LPS and R3 on degranulation, 5 µm sections from the hocks were stained with Wright's stain and morphology of mast cells examined. Typical appearance of intact and degranulation mast cells as well as hair follicle, neutrophil and vessels are shown in Figure 5.14, Figure 5.15. Mast cell granules are oval-shaped with purplish cytoplasm, ranging from 6 to 12 µm in diameter and the nuclei of mast cells appear oval or round (Stone et al., 2010).

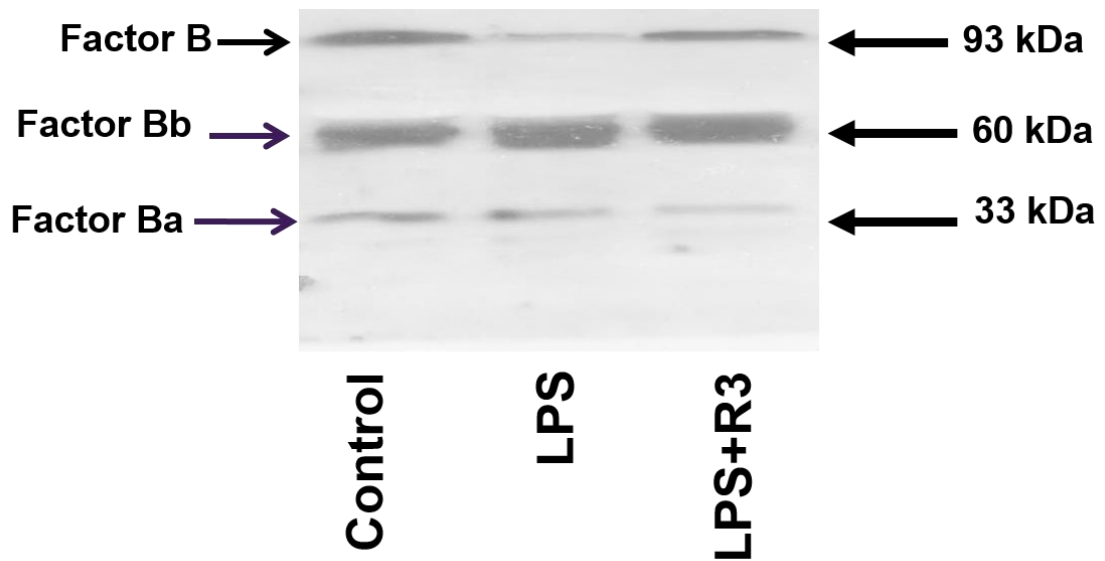


**Figure 5.13 The ability of R3-Fc for inhibiting complements Factor B that was activated by LPS.**

Mouse were injected with 5  $\mu$ g LPS with and without 15  $\mu$ g R3-Fc before collection of blood for serum. Mice sera were subjected to SDS/PAGE and Western blot before immunoblotting with anti-complement Factor B antibody. Molecular mass of factor B and its fragments are indicated by the arrow.

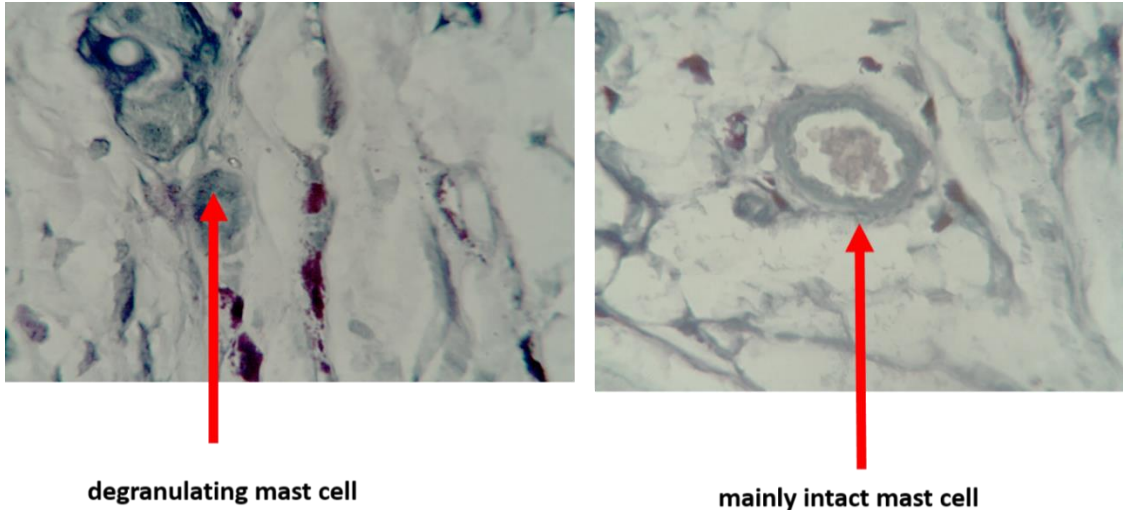


**Figure 5.14 Section of histological analysis of Mast cells.**

Mouse hocks were shaved, marked and removed prior to fixation at 4 °C for decalcification. 5 µm sections were stained with Wright's stain. These images were done using magnification of x100. The intact mast cell and degranulating mast cell are indicated by the arrow.

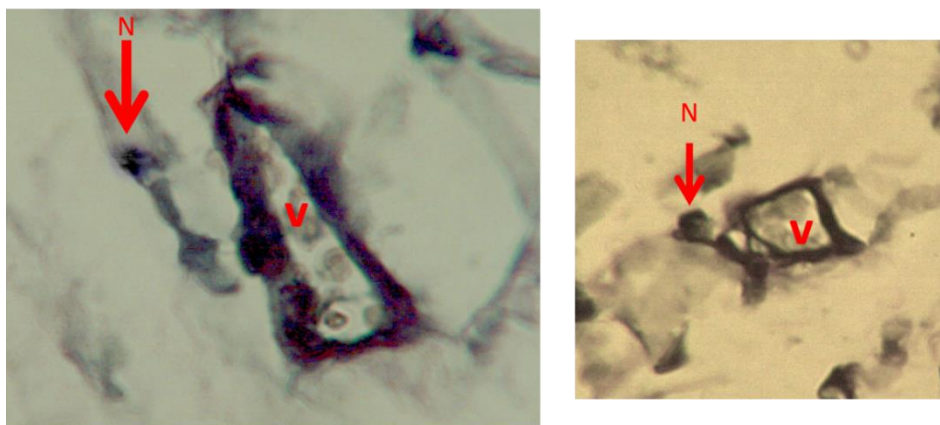


**Figure 5.15 Section of histological analysis for neutrophils.**

These images were taken from mouse injected with 5 µg LPS. After 2 hours, Mouse hocks were prepared and fixed before section was stained with Wright's stain. The neutrophils are indicated by the arrow and the vessels are indicated as v. These images were done using magnification of x100.

They are packed with 50-100 coarse granules. Based on the intensity of metachromasia, intact mast cells exhibit intense metachromasia and dense granules obscuring the nucleus while degranulated mast cells with less intense metachromasia and clear outline of the nucleus (Sharma et al., 2011). Intact and degranulated mast cells were counted in the skin sections under the light microscope to see whether R3 was able to affect LPS-induced degranulation. Mast cells were counted for both one and two hour experiments. For the one-hour group there was no significant difference in the total number of mast cells or the percentage of degranulated mast cells between LPS plus R3 and LPS. For another pair of mice, there was greater percentage of degranulated mast cells in the mouse treated with LPS plus R3 compared to the mouse receiving just LPS. Surprisingly, the untreated mouse showed a greater percent degranulated mast cells compared to treated mice as shown in Table 5.1. Unlike in the one-hour group (Table 5.2), there was difference in the total number of mast cells in the two-hour treated mice. The total number of mast cell looked higher in mice injected with RH ectodomain with or without LPS. The results demonstrated the percentage of degranulated mast cells was lower in mouse injected with LPS and R3 compared to mice injected with LPS with or without RH. Interesting, the lower percentage of degranulated mast cells was found in the needle injured mouse as well as mice injected with the RH deletion or R3 ectodomain. The data suggests more experiments are needed to clarify these effects.

**Table 5.1 the percentage of degranulated mast cells relate to the treatment (R3) for the one-hour group.**

<b>Treatment</b>	<b>Degranulated mast cells per cm<sup>2</sup></b>	<b>Total Mast cells per cm<sup>2</sup></b>	<b>Percentage of degranulated mast cells</b>
<b>LPS, n=1</b>	<b>7</b>	<b>85</b>	<b>8</b>
<b>LPS+R3, n=1</b>	<b>15</b>	<b>67</b>	<b>22</b>
<b>LPS, n=1</b>	<b>10</b>	<b>97</b>	<b>10</b>
<b>LPS+R3, n=1</b>	<b>9</b>	<b>95</b>	<b>9</b>
<b>no treatment, n=1</b>	<b>33</b>	<b>83</b>	<b>35</b>
<b>LPS (propKo), n=1</b>	<b>24</b>	<b>44</b>	<b>55</b>
<b>LPS, n=1</b>	<b>20</b>	<b>57</b>	<b>35</b>

Mice were injected with control carrier, LPS, LPS with R3 ectodomain. After 1 hour mouse hocks were prepared prior to fixation at 4 °C for decalcification. 5 µm sections were stained with Wright's stain. Intact and degranulated mast cells were counted in each section and shown in percentage. The mast cells were counted 2 times with magnification of x 40 per cm<sup>2</sup>.

**Table 5.2 The percentage of degranulated mast cells relate to the treatment (R3) for the two-hour group.**

<b>Treatment</b>	<b>Degranulated mast cells per cm<sup>2</sup></b>	<b>Total Mast cells per cm<sup>2</sup></b>	<b>Percentage of degranulated mast cells</b>
<b>LPS, n=1</b>	<b>13</b>	<b>49</b>	<b>27</b>
<b>LPS + R3, n=1</b>	<b>10</b>	<b>49</b>	<b>20</b>
<b>LPS +RH, n=1</b>	<b>18</b>	<b>74</b>	<b>24</b>
<b>R3, n=1</b>	<b>6</b>	<b>58</b>	<b>10</b>
<b>RH, n=1</b>	<b>7</b>	<b>66</b>	<b>11</b>
<b>needle injury as control, n=1</b>	<b>3</b>	<b>44</b>	<b>7</b>

Mice were injected with control carrier, LPS, LPS with R3 ectodomain or LPS with  $\Delta$ R167, H168 ectodomain. After 2 hours mouse hocks were prepared prior to fixation at 4 °C for decalcification. 5  $\mu$ m sections were stained with Wright's stain. Intact and degranulated mast cells were counted in individual section and shown in percentage. The mast cells were counted 2 times with magnification of x 40 per cm<sup>2</sup>.

## **5.4 Discussion**

This chapter aimed to examine the possibility of decreasing R3 size and its potential effects on Ang2 integrin interaction. In addition preliminary assessment of *in vivo* activity was performed

### **5.4.1 Producing 1-210 R3**

In Chapter 3 the ability of R3-Fc to neutralize Ang2 to bind Tie2 in cell signaling analysis as well as cellular functional assay was tested. The evolved ectodomain achieved the Ang2 binding specificity. As described above R3 carried the Tie2 ectodomain (442 amino acid) while R3-210 carried the shorter lengths fragment (210 amino acid) of Tie2 ectodomain. cDNA of wild-type Tie2 ectodomain was produced with three mutations corresponding to R3 by site directed mutagenesis. The smaller 210 sequence of Tie2 ectodomain should retain Ang2 binding specificity but may have better tissue penetration. To test this 1-210 Wt Tie2 ectodomain was mutated to generate R3-210 and R3-210 was transiently transfected into HEK293 cells followed by purification of soluble R3-210. However, problems were encountered producing high yields of purified product of R3-210 recombinant protein as compared to R3-Fc. The reason for poor yields is not known. R3 is cloned into pcDNA™3.1 while R3-210 is cloned into pCEP4. Both vectors have CMV promoters and SV40 transcriptional terminators. pcDNA™3.1 is 5.4 kb vector, but PCEP4 is 10.1 kb vector. It may be that vector size influences expression. To test if expression was affected by vector R3-210 should be re-cloned into pcDNA™3.1. Due to time constraints it was not possible to proceed any further with R3-210 optimisation.

### **5.4.2 Ang2 integrin binding**

Integrins are cell adhesion receptor that is involved in pathological angiogenesis. Integrins are overexpressed on blood vessel of several types of tumour (Weis and Cheresh, 2011b). Among all integrins,  $\alpha\beta3$  integrin plays an important role during tumor angiogenesis (Weis and Cheresh, 2011a). Therefore,  $\alpha\beta3$  intergrin

is an attractive target for the treatment of cancer. Ang2 regulate angiogenesis through Tie2 and integrin signaling (Felcht et al., 2012). Tie2 expression is down-regulated on endothelial cells during angiogenesis (Felcht et al., 2012), while integrins are overexpressed (Weis et al. 2011). Felcht (Felcht et al., 2012) reported that Ang2 bound directly to  $\alpha v \beta 3$  integrin and other integrins and demonstrated Ang2 antibody interfered with integrin signaling (Felcht et al., 2012), resulting in the inhibition of FAK signaling pathway that mediates cell migration and angiogenesis (Zhao and Guan, 2011). It was of interest to test whether R3-Fc would affect Ang2 binding to integrins. To do this initial experiments were performed to ensure R3-Fc was able to bind Ang2 under the acidic conditions reported by Felcht that are needed for Ang2 integrin binding. Therefore, the ability of R3-Fc to bind Ang2 was tested compared to the wild-type at pH 4.5 and pH 7.5. Our finding demonstrated the Ang2 binding of R3-Fc was higher than that of the wild-type at both normal and acidic pH. R3-Fc binding to Ang2 at pH 4.5 was higher than R3-Fc bound to Ang2 at pH 7.5. The Ang2 binding property of R3-Fc in acidic conditions may be beneficial for anti-angiogenesis in tumours where the pH is decreased (Felcht et al., 2012). The ability of Ang2 to bind integrins at different pH was next examined in the ELISA binding study prior to adding R3 for inhibiting this interaction. The binding between Ang2 and integrin was very low even at pH 4.5 in an ELISA-type format. The ability to bind in solution was therefore further tested. Immunoprecipitation assay in a cell-free system was applied to test Ang2 integrin binding as well as the effect of R3-Fc on Ang2-integrin binding. The immunoprecipitation data indicated Ang2 directly bound to the integrin in the first experiment consistent with reports of other researchers (Felcht et al., 2012). However, the data in Figure 5.6 are not clear. Ang2 has a molecular mass of 70kDa and the main band in Figure 5.6 is around 50 kDa. This band therefore may be antibody heavy chain, Additional experiments will be required to clarify this. However, it was not possible to extend this experiment to incorporate R3 due to background staining of blots with His-tagged R3. Additional immunoprecipitation formats were attempted, however they were not successful, probably due to problems detecting integrin with the available antibodies. To perform this experiment it will be necessary to obtain antibody that could detect low levels of  $\alpha v \beta 3$  intergrin on blots. This suggests repeating immunoprecipitation assay using anti-integrin together with

integrin and Ang2 should be performed. Then, signal of Ang2 integrin binding should be detected with anti-Ang2 antibody instead of anti His tag antibody. This may help to decrease the background from His-tagged R3. Also it would be possible to use anti-Ang2 antibody for detection in place of anti-His in experiment with anti-integrin co-immunoprecipitation. In this case, large amount of anti-integrin antibody IgG was present that migrates similar to alpha subunit of integrin around 150 kDa, thereby interfering with detection of integrin subunit. To test this and prevent such interference additional experiments will be performed in which the samples are resolved under reducing conditions to cleave IgG. In the future, it may be possible to detect integrins on a blot using a nonreducing SDS/PAGE sample buffer compared to a reducing SDS/PAGE sample buffer.

#### ***5.4.3 In vivo activity studies***

To test the ability of R3-Fc *in vivo*, a mouse model of LPS-induced localized oedema was performed. Previous studies have provided evidence that circulating levels of Ang2 are elevated in various inflammatory conditions (Kumpers et al., 2009). Ang2 is released from Weibel–Palade bodies in endothelial cells upon stimulation with pro-inflammatory stimuli thereby contributing to vascular leakage and oedema (Benest et al., 2013). In mice, Ang2 blocking antibody inhibits LPS-induced vascular permeability (Ziegler et al., 2013). To test the effect of R3-Fc on LPS-induced oedema, subcutis thickness of mouse hock sections was measured. As expected the increased of subcutaneous thickness was found in mice injected with LPS. Interestingly, the subcutis oedema of mice was reduced by the co-administration with R3-Fc. This suggests R3-Fc inhibits LPS-induced localized oedema in a pathway involving Ang2. Therefore, R3-Fc might block Ang2, leading to reduction of inflammation. However, more experiments were needed to demonstrate this effect with statistical significant. Additional mice controls could examine if any inhibitory effect of R3-Fc can be reversed by giving high Ang2 concentrations.

It was of interest to test whether R3-Fc had any effects on markers of inflammation. Therefore, another set of experiments was performed. The

activation of the alternative pathway of the complement system was evaluated by measuring complement protein B and its fragments. Factor B was activated in response to LPS (Gardiner et al., 1991, Prakash and Hellman, 2010). Fragments Bb and Ba of factor B were reported to be increased following activation of factor B. In this experiment, after 2 hours of LPS challenged with and without R3, mouse sera were analysed by SDS/PAGE followed by immunoblotting for Factor B and its fragments. The blot showed the intact factor B of mouse injected LPS was decreased compared to the control mouse, whereas the factor B from the mouse injected with LPS and R3 was equivalent to the control. The results suggest that the activation of the alternative pathway was activated by LPS and R3 inhibited this effect. Surprisingly, the levels of fragment production were not marked difference among treated and untreated mice. It is possible that Bb fragment might interact and form a complex with other proteins in mouse sera. It will be important to repeat this experiment on additional animals in order to test the statistical significance of the data.

In a further experiment, the effect of LPS and R3-Fc on the degranulation of mast cells was tested. Mast cells play a role in inflammation process (Amin, 2012). Activation of mast cells leads to mast cells degranulation, thereby releasing of inflammatory mediators from the granules (Theoharides, 2014). Degranulation of mast cells can be evaluated as a measure of inflammatory response. After LPS stimulation, the largest percentage of degranulated mast cells was expected to find in LPS injected mouse hocks. Therefore, quantitation and characterisation of mast cells in mouse hock sections was performed by immunohistological study. Wright's staining showed the presence of the degranulation of mast cells in inflamed tissue among mice in the one-hour group. Unexpectedly, the greater percentage of mast cell degranulation was noted in untreated mouse compared to other. This may mean simply that the cells degranulated upon skin injury. Surprisingly, a high percentage of mast cell degranulation was observed in mouse injected with LPS together with R3 as compared to the matched control. For the two-hour group, mast cells of mice injected with LPS degranulated more than that of mice injected with LPS plus R3. There was no clear difference in the percentage of mast cell degranulation among mice who received R3 or RH ectodomain alone or in the needle injured control. The results indicated the extent

of mast cell infiltration and degranulation was not correlated with LPS-inflamed tissue in the first hour. In contrast in the two-hour group the degranulation of mast cells correlated well with tissue exposure to LPS. This suggests that the degranulation of mast cells occurred after two hours of applying LPS. It will be interesting to test another mast cell stain which picks up other types of mast cells. Another reason is the R3 treatment has no effect on the percentage of degranulated mast cells that do not express Tie2 receptor. Further experiments will be needed to test whether R3 affects mast cells degranulation.

## Chapter 6: General Discussion

The activation of Ang1/Tie2 signalling is important for the maintenance of vessel function (Brindle et al., 2006, Augustin et al., 2009). Ang2 acts on Tie2 as a competitive antagonist for the Ang1 binding site causing attenuation of the action of Ang1. As a consequence of Ang2 up-regulation in the number of diseases, the vascular protective effects of Ang1 decreases, causing increased vessel permeability and destabilizing quiescent endothelial cells. Accumulating evidence report that the up-regulation of Ang2 is deleterious, and Ang2 has been found to be involved in pathological processes in several diseases such as inflammation, vascular remodelling and tumour angiogenesis (Davis et al., 1996, Chong et al., 2004, Maisonpierre et al., 1997). Therefore, various therapeutic molecules that inhibit Ang2 have been proposed as potential candidates for blocking the action of Ang2 such as Ang2 targeting peptides and Ang2 antibody (Hashizume et al., 2010, Holopainen et al., 2012). A complementary approach to peptides and antibodies for blocking ligands is the ligand trap. This study has attempted to create an Ang2-ligand trap by directed evolution of Tie2 ectodomain and characterise its binding, cellular and *in vivo* effects

### 6.1 Evolution of Tie2 ectodomain

In the work presented in this thesis, Tie2 extracellular domain (residues 1-442), was used to evolve the Ang2 trap that bound specifically to Ang2. The directed evolution of Tie2 ectodomain used SHM-mediated mutagenesis in DT40 B cells to diversify the rearranged gene by random mutation, producing a library of mutant Tie2 molecules. This method allows linking of a genotype plus a potentially easier approach to multiple rounds of library development. Furthermore, as the method used higher eukaryotic cells it is readily applied to mammalian proteins. In experiments described in Chapter 3 attempts were made to utilize this SHM-driven mutagenesis evolving ectodomain. However, despite several attempts, variants with improved specific binding to Ang2 were not obtained. It is possible that this screening flow cytometric selection was not

sensitive enough to resolve population discrimination. The sort window of Ang2 binding versus Tie2 expression was used to screen and select high Ang2 binding populations. This suggests the screening and conditions that was established is not optimal for evolution of mutant Tie2.

Directed evolution of Tie2 ectodomain was performed in parallel by others in the group using the same DT40 approach, but a different type of screening was used. They used as initial sort window of Ang1 binding versus Tie2 expression to screen and select low Ang1 binding population. After 3 iterations the selection strategy was changed to obtain cells with the highest Ang2 binding whilst maintaining low Ang1 binding. After 4 rounds of sorting, significant diversity of population were generated between rounds of sorting with lower Ang1 binding but high Ang2 binding. The ectodomain that preferentially binds to Ang2 was successfully evolved. It suggests that the probability of selecting a cell with reduced Ang1 binding as initial followed by selecting population with highest Ang2 binding together with low Ang1 binding may be more potential than selecting population with improved Ang2 binding.

## **6.2 Characterisation of evolved Tie2 ectodomain**

As described above, an evolved Tie2 ectodomain was not produced. However, in parallel experiments performed by others in the group a specific Ang2 binding of Tie2 ectodomain was evolved and designated R3. R3 is identical to wild-type Tie2 ectodomain (Wt), but has 3 mutations, consisting of Isoleucine in place of Phenylalanine 161. In addition Arginine 167 and Histidine 168 are deleted. The binding characteristics of R3 were analysed by using soluble evolved Tie2 ectodomain.

The binding ability of R3-Fc were tested in BLI analysis and ELISA assay. The results demonstrate R3-Fc was able to bind Ang2 but not Ang1. Nonetheless, R3-Fc has lower maximal binding for Ang2 compared to Wt-Fc. These results indicate the three residues changes make a dramatic switch in the binding characteristics of R3. Barton et al. (2006) revealed that Ang2 binds and interact

at the interface of the Ig2 binding domain (residues 122 -209) by analysing the crystal structure of the Ang2-Tie2 complex. This is consistent with the location of the mutations of R3 at Ig2 binding domain of the Tie2 receptor.

The receptor-binding interfaces of Ang1 and Ang2 are related. Examination of crystal structures have been reported, Ang2 in complex with Tie2 and Ang1 in complex with Tie2 are very similar. Ang2 binds Ig2 domain of Tie2 without major conformational changes or domain rearrangement in either receptor or ligand utilizing a lock and key mode for receptor-ligand binding.

To gain further insight into the contribution of each mutation, individual binding effects of the F161I substitution and double deletion of R167 and H168, ELISA was used to test for Ang1 and Ang2 binding. It has been found that angiotensin-binding ability between the F161I substitution and Wt-Fc was similar, whereas angiotensin-binding ability of the double deletion of R167 and H168 was abolished. Generally, the replacement of Phenylalanine with Isoleucine is unlikely to substantially change properties as they are structurally similar being relatively large and hydrophobic. In addition, they often play a major role in binding recognition. As determined from the crystal structure of the Ang2-Tie2 complex, the F161I substitution conserves the hydrophobic character of this position but this mutation may alter aromatic stacking between Phe-161 in Tie2 and Phe-469 in Ang2. Thus, this mutation is unlikely to affect binding affinity to angiotensin ligands (Barton et al., 2006, Brindle et al., 2013).

Double deletion of R167 and H168 blocked binding of ectodomain to Ang1 and Ang2, demonstrating a major impact of these binding residues on receptor-ligand binding domain. The crystal structure shows R167 in Tie2 forms a salt bridge with Ang2 and Ang1, whereas H168 in Tie2 forms a hydrogen bond with Ang2, and also interacts with another residue in ANG2 (Barton et al., 2006). The formation of hydrogen bonds and salt bridges between Tie2 and Ang1 as well as Ang2 create a stabilization of the ligand-receptor complex that is efficient for Ang1 and Ang2 binding (Barton et al., 2006, Yu et al., 2013, Brindle et al., 2013). The possibility of the double deletion of R167 and H168 affects the binding of Ang1 as well as Ang2. It is concluded that specific Ang2 binding requires the

combination of mutation of three residues. An understanding of the mechanism for specific Ang2 binding of R3 will be important to determine the structure of R3 in the future.

The potential of R3-Fc was tested for inhibitory effects on Ang2 in endothelial cells using cellular and functional assay. Examination of the effect of R3 on Ang1 and Ang2 effects on Akt phosphorylation was performed. The R3-Fc has been found to inhibit both agonist and antagonist effects of Ang2 on Akt signalling. Importantly, R3-Fc did not interfere Ang1 signalling. In addition to blocking the effects of Ang2 on signalling, R3-Fc also inhibited Ang2 effects on endothelial migration. These data are consistent with the ability of R3-Fc to bind specifically to Ang2 and block the Ang2 binding to cellular Tie2 receptor.

In order to characterise R3-Fc effects more comprehensively it will be necessary to perform additional experiments on cell signalling and function. These experiments should include complete concentration dependent effects on the ability of Ang2 to antagonize Ang1 as well as Ang2 agonist effects on other endothelial signalling pathways such as Erk1/2, Dok2. Similarly, it will be important to test its effects on other endothelial functions such as permeability and apoptosis. In this study, effects on non-endothelial cells were not test. It would be of interest to examine effects of R3-Fc on Ang2 stimulated function in Tie2 expressing monocytes for example.

### **6.3 Modification of R3, Integrin binding and *in vivo* activity**

#### **6.3.1 Decreasing R3 size**

Although 80 kDa of R3, consisting of Tie2 receptor binding domain that contains residues 1-442 with three mutation changes, is smaller than full-length antibodies (150 kDa), it may be possible to further decrease the size of R3 for improving tissue penetration. The truncated form of R3 with residues 1-210, comprising Ig1 and Ig2 was created since the binding site of the receptor-ligand interaction

locates on Ig2 binding domain (Barton et al 2006). pCEP-Wt-Fc containing residues 1-210 was used to introduce mutations according to the mutation of R3 by site directed mutagenesis. Following the creation of R3-210, R3-210 soluble form was produced after transfection and purification. The characterisation of R3-210 did not proceed due to the amount of protein produced being very low. Previously, the product yield of R3 has been consistently obtained by the same protocol as described in Section 2.5. R3-210 and R3 were expressed from different vectors. The larger size of R3-210 expression vector may affect the expression of the R3-210 in HEK293 cells. The effects of the vector on the production of secreted soluble R3-210-Fc could be proved by re-cloning R3-210 into the same vector of R3 (pcDNA 3.1) vector. Then the protein production both full size and truncated could be compared. However, work to decrease the size of R3 and its characterisation will need to be continued.

### **6.3.2 Ang2 integrin binding**

Ang2 has been reported to bind integrins (Felcht et al., 2012). It has been found that integrin  $\alpha v\beta 3$  is exclusively expressed on angiogenic endothelial cells and It is also expressed by platelets (Cowden Dahl et al., 2005). A recent study reported Ang2 also bind directly to  $\alpha v\beta 3$  integrin (Felcht et al., 2012). In this study, the ability of R3 for blocking Ang2 binding to integrin was tested by ELISA binding assay. This assay was found to be insufficiently sensitive to measure integrin-Ang2 binding. Therefore, the determination of the ability of R3 to interfere with integrin signalling was not possible. These results are in contrast to those of Felcht et al. (2013) that showed Ang2-integrin binding by ELISA assay under the same condition. Optimisation of the ELISA assay condition further is required to confirm this binding activity in the future. However, our ELISA results indicate the Ang2 binding of R3 in pH 4.5 was significantly higher than that of the wild-type. This suggests the Ang2 binding of R3 is higher in low pH, enhancing the potential of R3 for therapeutic exploitation in inhibition of Ang2 under acidic circumstances, such as in tumour growth.

As an alternative strategy, an immunoprecipitation assay in a cell-free system was applied to test the ability of R3 to inhibit Ang2-integrin binding. Our finding demonstrated that Ang2 was able to bind to the  $\alpha v\beta 3$  integrin in a co-immunoprecipitation assay using an anti-integrin immunoprecipitating antibodies together with Ang2 detection, but this assay could not be extended to determine the effect of R3 on Ang2-integrin binding because of high background staining of blots with His-tagged R3 when probing for His-tagged Ang2. Whilst additional immunoprecipitation experiments were attempted to probe for Ang2-integrin binding with 3 different integrin antibodies, none of the antibodies was able to detect the integrin in blots. If a suitable anti-integrin antibody for blotting cannot be found it may be possible to immunoprecipitate with anti-integrin and detect Ang2 with an anti-Ang2 antibody.

### **6.3.3 *In vivo activities study***

The *in vivo* activity of R3 *in vivo* was examined by using a mouse model of LPS-induced localized oedema. Ang2 has been shown to mediate LPS-induced vascular leakage (Mofarrahi et al., 2008). The results suggested that R3 was able to inhibit the formation of oedema compared to control using the measurement of subcutis thickness of mouse hock sections. Despite the consistent effects of R3 for its inhibitory actions on local oedema in two independent times with the same stock of LPS, more experiments are needed for statistical analysis. Additional mice controls in these experiments could examine if any inhibitory effect of R3 can be reversed by giving high Ang2 concentration.

Other set of experiments were performed to measure the effects on markers of inflammation in mouse serum using immunoblotting analysis for Factor B. Factor B was selected to test the inhibitory effect of R3 on inflammation. It is known that complement protein B is cleaved into its fragment in response to the activation of alternative pathway of complement system (Gardiner et al., 1991, Prakash and Hellman, 2010). In general, cleavage of Factor B is not a marker of inflammation. However, as shown in Figure 5.13 LPS did stimulate cleavage of Factor B in this

study. The results show the degradation of the intact Factor B induced by LPS can be reversed by co-injection with R3. However, if this was due to decreased cleavage it would be expected that Bb levels should also decrease and this was not found. It is possible that complexes of Bb fragment with other proteins in mouse sera occurred after the cleavage of the intact factor B. However, R3 is likely to have an inhibitory effect on local oedema in vivo model. Again, these findings should be confirmed by adding more experiments with more mice to each group.

The effect of R3 and LPS on the degranulation of mast cells was examined using Wright's staining of mouse hock sections. The results indicate intact and degranulated mast cells infiltration was not correlated with inflamed tissues after one hour of injection of LPS, while in two-hour group the extent of mast cells correlated well with tissue exposure to LPS. These consistent to Qiao et al. (2006) that demonstrated the acute effect of LPS was not related to mast cell degranulation within one hour after applied LPS (Qiao et al., 2006). Therefore, it may be possible to confirm this finding by designing the measurement of inflammation with many time points and these will compare each time point with the 0 point. Alternatively, another mast cell stain should be used to confirm the results. Importantly, the effects of R3 on mast cells degranulation with more samples should be investigated in the future.

#### **6.4 Conclusion**

The work presented in this thesis demonstrates SHM-driven directed evolution combined with cell surface display enables evolution of a mutant of Tie2 ectodomain with specific binding of Ang2. This evolved ectodomain was produced as a soluble fusion protein and demonstrate to bind Ang2 but not Ang1 and Ang4. Moreover, this mutant ectodomain had lower maximal binding for Ang2 compared to Wt-Fc. In addition, the evolved Tie2 ectodomain could inhibit Ang2 action on endothelial cell signalling and inhibit functional effects of Ang2 without interfering with Ang1. The preliminary work with an *in vivo* model demonstrated the evolved Tie2 ectodomain was able to inhibit the formation of local oedema.

## Appendices

Appendix One	List of Primers
Appendix Two	Amplification conditions
Appendix Three	Set up reactions for site directed mutagenesis into pCEP-Wt-Tie2-Fc
Appendix Four:	Reaction components for amplification
Appendix Five	Reaction components for site directed mutagenesis
Appendix Six	Nucleotide and Amino Acid sequence alignment of AID
Appendix Seven	Vectors

## Appendix One: List of Primers

### Primers for Chick AID (ggAID)

Primer	Sequence (5' -> 3')	Tm (C°)
Forward	AGAAGATCTATGGACAGCCTCTTGATGAAGAGG	68.2
Reverse	GCAGAATTCTCAAAGTCCCAGAGTTTTAAAGGC	67

### Primers for Tie2

Primer	Sequence (5' -> 3')	Tm (C°)
Forward	CACCGCTAGCATGGACTCTTTAGCCAGCTT	69.5
Reverse	GGAATTCTTAACAGAAATGTTGAAGGGCT	62.94

### Primers for F/I mutation

Primer	Sequence (5' -> 3')	Tm (C°)
Forward	GATTTACAAAAATGGTTCCATCATCCATTCAGTGCCCC G	66
Reverse	CGGGGCACTGAATGGATGGATGATGGAACCATTTTTG TAAATC	67

**Primers for RH deletion**

<b>Primer</b>	<b>Sequence (5' -&gt; 3')</b>	<b>Tm (C°)</b>
Forward	CCTTCATCCATTCAGTGCCTGAAGTACCTGATATTCTA	78.37
Reverse	TAGAATATCAGGTACTTCAGGCACTGAATGGATGAAG G	78.37

**Appendix Two: Amplification conditions**

Primers		Tie2	ggAID
Initial duration	Temp(°C)	94	95
	Duration (min)	3	3
Denaturation	Temp(°C)	94	95
	Duration (min)	1	1
Annealing	Temp(°C)	60	55
	Duration (min)	1	1
Extension	Temp(°C)	72	72
	Duration (min)	1	1
	Cycles	30	30
Final extension	Temp(°C)	72	72
	Duration (min)	10	10

**Appendix Three:** Set up reactions for site directed mutagenesis into pCEP-Wt-Tie2-Fc

Primers		F/I mutation	RH mutation
Initial duration	Temp(°C)	95	95
	Duration (min)	5	5
Denaturation	Temp(°C)	95	95
	Duration (min)	0.5	0.5
Annealing	Temp(°C)	60	60
	Duration (min)	0.5	0.5
Extension	Temp(°C)	68	68
	Duration (min)	5.5	5.5
	Cycles	18	18
Final extension	Temp(°C)	72	72
	Duration (min)	7	7

Cool for 2 mins on ice then add 10 units DPN1 below the oil and incubate for 1-2 hour at 37°C

Transform 10 µl into competent cells

PCEP stock concentration= 158 ng/ µl; so 0.5 µl + 15.3 µl water

**Appendix Four:** Reaction components for amplification

	Fwd primer	Tie2	ggAID
	Rev primer	Tie2	ggAID
	BIOTAQ 10x NH4 buffer	-	2.5µl
	50mM MgCl <sub>2</sub>	-	2.0µl
	Biotaq	-	0.25µl
Phusion	5xHF buffer	10µl	-
	Phusion	0.5µl	-
All	10mM dNTPs	1µl	0.5µl
	Primer	0.5µl	0.5µl
	Primer	0.5µl	0.5µl
	100% DMSO	0.5µl	0.5µl
	DNA	30ng, 5µl	5µl
	H <sub>2</sub> O	to 50µl	to 25µl

**Appendix Five:** Reaction components for site directed mutagenesis

Make up oligo's: make to 100pmol/  $\mu\text{l}$  as per sheet in 10mM T/E, then dilute 1.25  $\mu\text{l}$  and 48.75  $\mu\text{l}$  water

Components	F/I mutation	RH mutation
Fwd primer	1 $\mu\text{l}$	1 $\mu\text{l}$
Rev primer	1 $\mu\text{l}$	1 $\mu\text{l}$
dNTP mix(10 mM)	0.4 $\mu\text{l}$ 50mM	0.4 $\mu\text{l}$ 50mM
PCR buffer(5x)	5 $\mu\text{l}$	5 $\mu\text{l}$
water	14.85 $\mu\text{l}$	14.85 $\mu\text{l}$
DMSO (5%)	1.25 $\mu\text{l}$	1.25 $\mu\text{l}$
template DNA	1 $\mu\text{l}$ (5ng)	1 $\mu\text{l}$ (5ng)
Phusion high fidelity Taq polymerase	0.5 $\mu\text{l}$	0.5 $\mu\text{l}$

## **Appendix Six: Nucleotide and Amino Acid sequence alignment of AID**

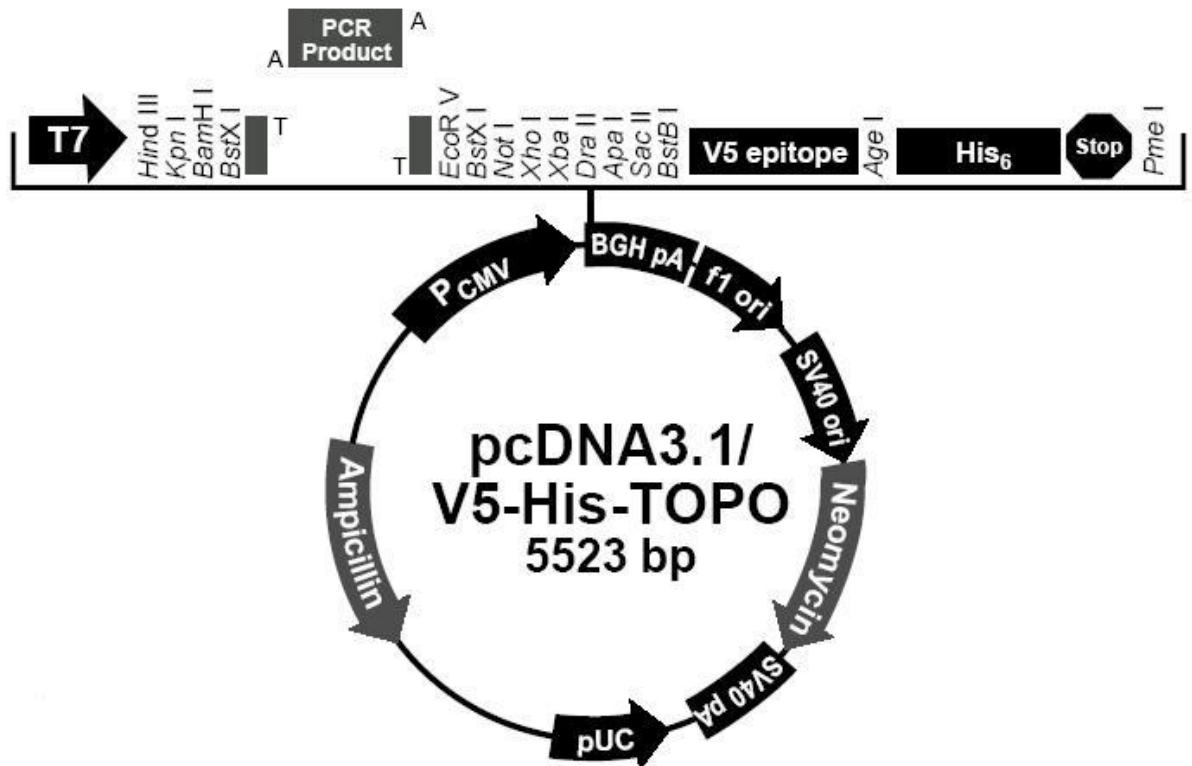
### **Cloning AID in the PEF6/V5 His TOPO vector**

atg gac agc ctc ttg atg aac cgg agg aag ttt ctt tac caa ttc aaa aat gtc cgc tgg gct  
aag ggt cgg cgt gag acc tac ctg tgc tac gta gtg aag agg cgt gac agt gct aca tcc  
ttt tca ctg gac ttt ggt tat ctt cgc aat aag aac ggc tgc cac gtg gaa ttg ctc ttc ctc  
cgc tac atc tcg gac tgg gac cta gac cct ggc cgc tgc tac cgc gtc acc tgg ttc acc  
tcc tgg agc ccc tgc tac gac tgt gcc cga cat gtg gcc gac ttt ctg cga ggg aac ccc  
aac ctc agt ctg agg atc ttc acc gcg cgc ctc tac ttc tgt gag gac cgc aag gct gag  
ccc gag ggg ctg cgg cgg ctg cac cgc gcc ggg gtg caa ata gcc atc atg acc ttc aaa  
gat tat ttt tac tgc tgg aat act ttt gta gaa aac cac gaa aga act ttc aaa gcc tgg gaa  
ggg ctg cat gaa aat tca gtt cgt ctc tcc aga cag ctt cgg cgc atc ctt ttg ccc ctg tat  
gag gtt gat gac tta cga gac gca ttt cgt act ttg gga ctt tga

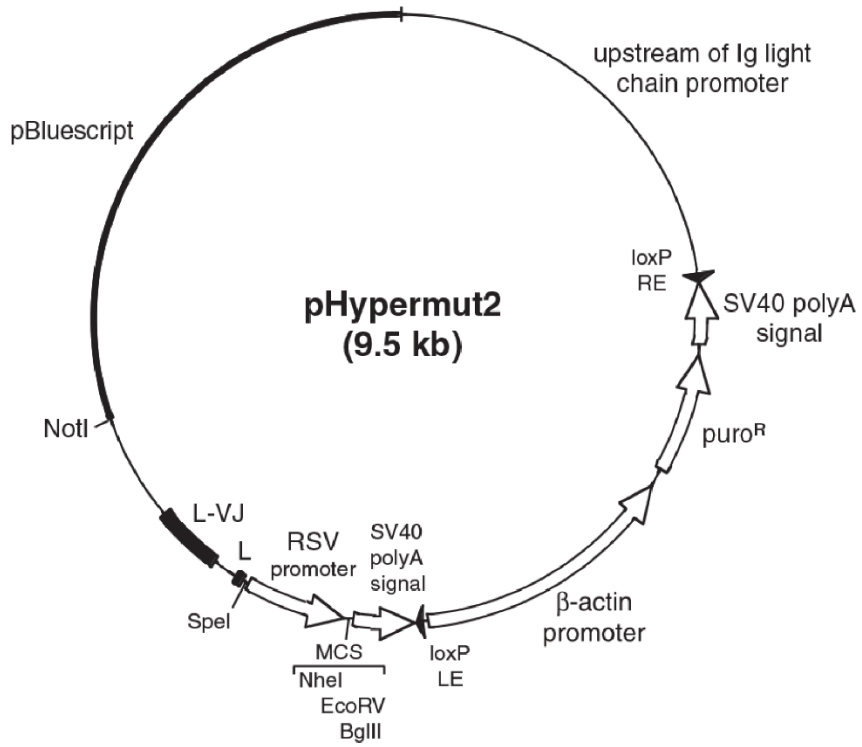
MDSLLMNRRKFLYQFKNVRWAKGRRETYLCYVVKRRDSATSFSLDFGYLRN  
KNGCHVELLFLRYISDWDLDPGRRCYRVTWFTSWSPCYDCARHVADFLRGNP  
NSLRIFTARLYFCEDRKAEPGLRRLHRAGVQIAIMTFKDYFYCWNTFVENHE  
RTFKAWEGLHENSVRLSRQLRRILLPLYEVDDLRFDAFRTLGL

## Appendix Seven: Cloning

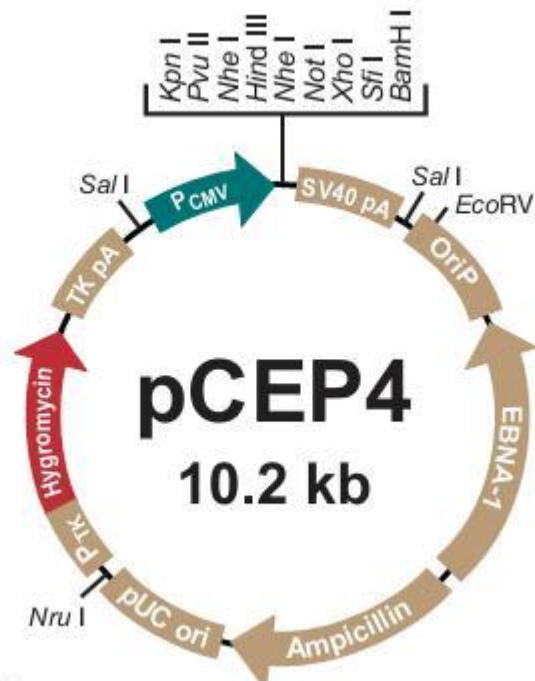
### 7.1 pcDNA™3.1D/V5-His-TOPO® expression vector



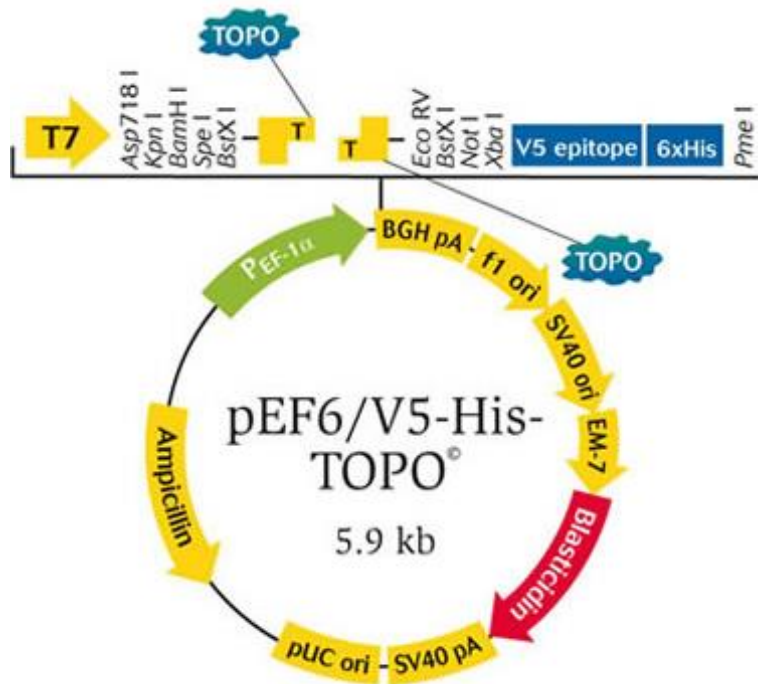
## 7.2 pHypermur2 vector



### 7.3 pCEP4



## 7.4 pEF6/V5-His-TOPO®



## Bibliography

- ALBERTS, B., JOHNSON, A., LEWIS, J., RAFF, M., ROBERTS, K. & WALTER, P. 2002. *Molecular Biology of the Cell*. New York: Garland Science.
- ALBINI, A. & NOONAN, D. M. 2012. Angiopoietin2 and tie2: tied to lymphangiogenesis and lung metastasis. New perspectives in antimetastatic antiangiogenic therapy. *J Natl Cancer Inst*, 104, 429-31.
- AMIN, K. 2012. The role of mast cells in allergic inflammation. *Respir Med*, 106, 9-14.
- ARAKAWA, H. & BUERSTEDDE, J. M. 2009. Activation-induced cytidine deaminase-mediated hypermutation in the DT40 cell line. *Philos Trans R Soc Lond B Biol Sci*, 364, 639-44.
- ARAKAWA, H., HAUSCHILD, J. & BUERSTEDDE, J. M. 2002. Requirement of the activation-induced deaminase (AID) gene for immunoglobulin gene conversion. *Science*, 295, 1301-6.
- ARAKAWA, H., KUDO, H., BATRAK, V., CALDWELL, R. B., RIEGER, M. A., ELLWART, J. W. & BUERSTEDDE, J. M. 2008. Protein evolution by hypermutation and selection in the B cell line DT40. *Nucleic Acids Res*, 36, e1.
- ARAKAWA, H., SARIBASAK, H. & BUERSTEDDE, J. M. 2004. Activation-induced cytidine deaminase initiates immunoglobulin gene conversion and hypermutation by a common intermediate. *PLoS Biol*, 2, E179.
- AUDERO, E., CASCONI, I., MANIERO, F., NAPIONE, L., ARESE, M., LANFRANCONE, L. & BUSSOLINO, F. 2004. Adaptor ShcA protein binds tyrosine kinase Tie2 receptor and regulates migration and sprouting but not survival of endothelial cells. *J Biol Chem*, 279, 13224-33.
- AUGUSTIN, H. G., KOH, G. Y., THURSTON, G. & ALITALO, K. 2009. Control of vascular morphogenesis and homeostasis through the angiopoietin-Tie system. *Nat Rev Mol Cell Biol*, 10, 165-77.
- BARTON, W. A., TZVETKOVA-ROBEV, D., MIRANDA, E. P., KOLEV, M. V., RAJASHANKAR, K. R., HIMANEN, J. P. & NIKOLOV, D. B. 2006. Crystal structures of the Tie2 receptor ectodomain and the angiopoietin-2-Tie2 complex. *Nat Struct Mol Biol*, 13, 524-32.

- BARTON, W. A., TZVETKOVA, D. & NIKOLOV, D. B. 2005. Structure of the angiopoietin-2 receptor binding domain and identification of surfaces involved in Tie2 recognition. *Structure*, 13, 825-32.
- BENEST, A. V., KRUSE, K., SAVANT, S., THOMAS, M., LAIB, A. M., LOOS, E. K., FIEDLER, U. & AUGUSTIN, H. G. 2013. Angiopoietin-2 is critical for cytokine-induced vascular leakage. *PLoS One*, 8, e70459.
- BETTS, M. J. & RUSSELL, R. B. 2003. Amino Acid Properties and Consequences of Substitutions, in *Bioinformatics for Geneticists*. Chichester, John Wiley & Sons, Ltd.
- BHANDARI, V., CHOO-WING, R., LEE, C. G., ZHU, Z., NEDRELOW, J. H., CHUPP, G. L., ZHANG, X., MATTHAY, M. A., WARE, L. B., HOMER, R. J., LEE, P. J., GEICK, A., DE FOUGEROLLES, A. R. & ELIAS, J. A. 2006. Hyperoxia causes angiopoietin 2-mediated acute lung injury and necrotic cell death. *Nat Med*, 12, 1286-93.
- BLAGODATSKI, A. & KATANAEV, V. L. 2011. Technologies of directed protein evolution in vivo. *Cell Mol Life Sci*, 68, 1207-14.
- BLUNDELL, T. L., ELLIOTT, G., GARDNER, S. P., HUBBARD, T., ISLAM, S., JOHNSON, M., MANTAFOUNIS, D., MURRAY-RUST, P., OVERINGTON, J., PITTS, J. E. & ET AL. 1989. Protein engineering and design. *Philos Trans R Soc Lond B Biol Sci*, 324, 447-60.
- BODER, E. T. & WITTRUP, K. D. 1997. Yeast surface display for screening combinatorial polypeptide libraries. *Nat Biotechnol*, 15, 553-7.
- BOGDANOVIC, E., NGUYEN, V. P. & DUMONT, D. J. 2006. Activation of Tie2 by angiopoietin-1 and angiopoietin-2 results in their release and receptor internalization. *J Cell Sci*, 119, 3551-60.
- BRINDLE, N. P., SAHARINEN, P. & ALITALO, K. 2006. Signaling and functions of angiopoietin-1 in vascular protection. *Circ Res*, 98, 1014-23.
- BRINDLE, N. P., SALE, J. E., ARAKAWA, H., BUERSTEDDE, J. M., NUAMCHIT, T., SHARMA, S. & STEELE, K. H. 2013. Directed evolution of an angiopoietin-2 ligand trap by somatic hypermutation and cell surface display. *J Biol Chem*, 288, 33205-12.
- CAMPBELL, I. D. & HUMPHRIES, M. J. 2011. Integrin structure, activation, and interactions. *Cold Spring Harb Perspect Biol*, 3.

- CAO, Y., SONVEAUX, P., LIU, S., ZHAO, Y., MI, J., CLARY, B. M., LI, C. Y., KONTOS, C. D. & DEWHIRST, M. W. 2007. Systemic overexpression of angiopoietin-2 promotes tumor microvessel regression and inhibits angiogenesis and tumor growth. *Cancer Res*, 67, 3835-44.
- CHEN, H. H., WENG, B. Q., CHENG, K. J., LIU, H. Y., WANG, S. Q. & LU, Y. Y. 2014. Effect of the vascular endothelial growth factor expression level on angiopoietin-2-mediated nasopharyngeal carcinoma growth. *Vasc Cell*, 6, 4.
- CHO, C. H., KAMMERER, R. A., LEE, H. J., YASUNAGA, K., KIM, K. T., CHOI, H. H., KIM, W., KIM, S. H., PARK, S. K., LEE, G. M. & KOH, G. Y. 2004. Designed angiopoietin-1 variant, COMP-Ang1, protects against radiation-induced endothelial cell apoptosis. *Proc Natl Acad Sci U S A*, 101, 5553-8.
- CHONG, A. Y., CAINE, G. J. & LIP, G. Y. 2004. Angiopoietin/tie-2 as mediators of angiogenesis: a role in congestive heart failure? *Eur J Clin Invest*, 34, 9-13.
- COFFELT, S. B., TAL, A. O., SCHOLZ, A., DE PALMA, M., PATEL, S., URBICH, C., BISWAS, S. K., MURDOCH, C., PLATE, K. H., REISS, Y. & LEWIS, C. E. 2010. Angiopoietin-2 regulates gene expression in TIE2-expressing monocytes and augments their inherent proangiogenic functions. *Cancer Res*, 70, 5270-80.
- COLBY, D. W., KELLOGG, B. A., GRAFF, C. P., YEUNG, Y. A., SWERS, J. S. & WITTRUP, K. D. 2004. Engineering antibody affinity by yeast surface display. *Methods Enzymol*, 388, 348-58.
- COWDEN DAHL, K. D., ROBERTSON, S. E., WEAVER, V. M. & SIMON, M. C. 2005. Hypoxia-inducible factor regulates alphavbeta3 integrin cell surface expression. *Mol Biol Cell*, 16, 1901-12.
- DALLABRIDA, S. M., ISMAIL, N., OBERLE, J. R., HIMES, B. E. & RUPNICK, M. A. 2005. Angiopoietin-1 promotes cardiac and skeletal myocyte survival through integrins. *Circ Res*, 96, e8-24.
- DALLABRIDA, S. M., ISMAIL, N. S., PRAVDA, E. A., PARODI, E. M., DICKIE, R., DURAND, E. M., LAI, J., CASSIOLA, F., ROGERS, R. A. & RUPNICK, M. A. 2008. Integrin binding angiopoietin-1 monomers reduce cardiac hypertrophy. *Faseb j*, 22, 3010-23.

- DALY, C., EICHTEN, A., CASTANARO, C., PASNIKOWSKI, E., ADLER, A., LALANI, A. S., PAPADOPOULOS, N., KYLE, A. H., MINCHINTON, A. I., YANCOPOULOS, G. D. & THURSTON, G. 2013. Angiopoietin-2 functions as a Tie2 agonist in tumor models, where it limits the effects of VEGF inhibition. *Cancer Res*, 73, 108-18.
- DALY, C., WONG, V., BUROVA, E., WEI, Y., ZABSKI, S., GRIFFITHS, J., LAI, K. M., LIN, H. C., IOFFE, E., YANCOPOULOS, G. D. & RUDGE, J. S. 2004. Angiopoietin-1 modulates endothelial cell function and gene expression via the transcription factor FKHR (FOXO1). *Genes Dev*, 18, 1060-71.
- DAVIS, S., ALDRICH, T. H., JONES, P. F., ACHESON, A., COMPTON, D. L., JAIN, V., RYAN, T. E., BRUNO, J., RADZIEJEWSKI, C., MAISONPIERRE, P. C. & YANCOPOULOS, G. D. 1996. Isolation of angiopoietin-1, a ligand for the TIE2 receptor, by secretion-trap expression cloning. *Cell*, 87, 1161-9.
- DAVIS, S., PAPADOPOULOS, N., ALDRICH, T. H., MAISONPIERRE, P. C., HUANG, T., KOVAC, L., XU, A., LEIDICH, R., RADZIEJEWSKA, E., RAFIQUE, A., GOLDBERG, J., JAIN, V., BAILEY, K., KAROW, M., FANDL, J., SAMUELSSON, S. J., IOFFE, E., RUDGE, J. S., DALY, T. J., RADZIEJEWSKI, C. & YANCOPOULOS, G. D. 2003. Angiopoietins have distinct modular domains essential for receptor binding, dimerization and superclustering. *Nat Struct Biol*, 10, 38-44.
- DIMARCHI, R. D., CHANCE, R. E., LONG, H. B., SHIELDS, J. E. & SLIEKER, L. J. 1994. Preparation of an insulin with improved pharmacokinetics relative to human insulin through consideration of structural homology with insulin-like growth factor I. *Horm Res*, 41 Suppl 2, 93-6.
- DIXIT, M., BESS, E., FISSLTHALER, B., HARTEL, F. V., NOLL, T., BUSSE, R. & FLEMING, I. 2008. Shear stress-induced activation of the AMP-activated protein kinase regulates FoxO1a and angiopoietin-2 in endothelial cells. *Cardiovasc Res*, 77, 160-8.
- DUMONT, D. J., YAMAGUCHI, T. P., CONLON, R. A., ROSSANT, J. & BREITMAN, M. L. 1992. tek, a novel tyrosine kinase gene located on mouse chromosome 4, is expressed in endothelial cells and their presumptive precursors. *Oncogene*, 7, 1471-80.

- ECONOMIDES, A. N. & STAHL, N. 2013. Receptor-Fc and Ligand Traps as High-Affinity Biological Blockers: Development and Clinical Applications, in Fusion Protein Technologies for Biopharmaceuticals: Applications and Challenges. Hoboken, John Wiley & Sons, Inc.
- ELLIS, L. M., LIU, W., AHMAD, S. A., FAN, F., JUNG, Y. D., SHAHEEN, R. M. & REINMUTH, N. 2001. Overview of angiogenesis: Biologic implications for antiangiogenic therapy. *Semin Oncol*, 28, 94-104.
- FALCON, B. L., HASHIZUME, H., KOUMOUTSAKOS, P., CHOU, J., BREADY, J. V., COXON, A., OLINER, J. D. & MCDONALD, D. M. 2009. Contrasting actions of selective inhibitors of angiopoietin-1 and angiopoietin-2 on the normalization of tumor blood vessels. *Am J Pathol*, 175, 2159-70.
- FELCHT, M., LUCK, R., SCHERING, A., SEIDEL, P., SRIVASTAVA, K., HU, J., BARTOL, A., KIENAST, Y., VETTEL, C., LOOS, E. K., KUTSCHERA, S., BARTELS, S., APPAK, S., BESEMFELDER, E., TERHARDT, D., CHAVAKIS, E., WIELAND, T., KLEIN, C., THOMAS, M., UEMURA, A., GOERDT, S. & AUGUSTIN, H. G. 2012. Angiopoietin-2 differentially regulates angiogenesis through TIE2 and integrin signaling. *J Clin Invest*, 122, 1991-2005.
- FELMEDEN, D. C., BLANN, A. D. & LIP, G. Y. 2003. Angiogenesis: basic pathophysiology and implications for disease. *Eur Heart J*, 24, 586-603.
- FIEDLER, U. & AUGUSTIN, H. G. 2006. Angiopoietins: a link between angiogenesis and inflammation. *Trends Immunol*, 27, 552-8.
- FIEDLER, U., KRISSEL, T., KOIDL, S., WEISS, C., KOBLIZEK, T., DEUTSCH, U., MARTINY-BARON, G., MARME, D. & AUGUSTIN, H. G. 2003. Angiopoietin-1 and angiopoietin-2 share the same binding domains in the Tie-2 receptor involving the first Ig-like loop and the epidermal growth factor-like repeats. *J Biol Chem*, 278, 1721-7.
- FIEDLER, U., REISS, Y., SCHARPFENECKER, M., GRUNOW, V., KOIDL, S., THURSTON, G., GALE, N. W., WITZENRATH, M., ROSSEAU, S., SUTTORP, N., SOBKE, A., HERRMANN, M., PREISSNER, K. T., VAJKOCZY, P. & AUGUSTIN, H. G. 2006. Angiopoietin-2 sensitizes endothelial cells to TNF-alpha and has a crucial role in the induction of inflammation. *Nat Med*, 12, 235-9.

- GALLAGHER, D. C., PARIKH, S. M., BALONOV, K., MILLER, A., GAUTAM, S., TALMOR, D. & SUKHATME, V. P. 2008. Circulating angiopoietin 2 correlates with mortality in a surgical population with acute lung injury/adult respiratory distress syndrome. *Shock*, 29, 656-61.
- GAMBLE, J. R., DREW, J., TREZISE, L., UNDERWOOD, A., PARSONS, M., KASMINKAS, L., RUDGE, J., YANCOPOULOS, G. & VADAS, M. A. 2000. Angiopoietin-1 is an antipermeability and anti-inflammatory agent in vitro and targets cell junctions. *Circ Res*, 87, 603-7.
- GARDINER, J. S., KEIL, L. B. & DEBARI, V. A. 1991. In vitro formation of complement activation products by lipopolysaccharide chemotypes of *Salmonella minnesota*. *Int Arch Allergy Appl Immunol*, 96, 51-4.
- GIULIANO, J. S., JR., LAHNI, P. M., HARMON, K., WONG, H. R., DOUGHTY, L. A., CARCILLO, J. A., ZINGARELLI, B., SUKHATME, V. P., PARIKH, S. M. & WHEELER, D. S. 2007. Admission angiopoietin levels in children with septic shock. *Shock*, 28, 650-654.
- GRAY, S. J., BLAKE, B. L., CRISWELL, H. E., NICOLSON, S. C., SAMULSKI, R. J., MCCOWN, T. J. & LI, W. 2010. Directed evolution of a novel adeno-associated virus (AAV) vector that crosses the seizure-compromised blood-brain barrier (BBB). *Mol Ther*, 18, 570-8.
- GU, J., YAMAMOTO, H., OGAWA, M., NGAN, C. Y., DANNO, K., HEMMI, H., KYO, N., TAKEMASA, I., IKEDA, M., SEKIMOTO, M. & MONDEN, M. 2006. Hypoxia-induced up-regulation of angiopoietin-2 in colorectal cancer. *Oncol Rep*, 15, 779-83.
- HANSEN, T. M., SINGH, H., TAHIR, T. A. & BRINDLE, N. P. 2010. Effects of angiopoietins-1 and -2 on the receptor tyrosine kinase Tie2 are differentially regulated at the endothelial cell surface. *Cell Signal*, 22, 527-32.
- HASHIMOTO, T. & PITTET, J. F. 2006. Angiopoietin-2: modulator of vascular permeability in acute lung injury? *PLoS Med*, 3, e113.
- HASHIZUME, H., FALCON, B. L., KURODA, T., BALUK, P., COXON, A., YU, D., BREADY, J. V., OLINER, J. D. & MCDONALD, D. M. 2010. Complementary actions of inhibitors of angiopoietin-2 and VEGF on tumor angiogenesis and growth. *Cancer Res*, 70, 2213-23.

- HELLINGA, H. W. 1997. Rational protein design: combining theory and experiment. *Proc Natl Acad Sci U S A*, 94, 10015-7.
- HOLOPAINEN, T., SAHARINEN, P., D'AMICO, G., LAMPINEN, A., EKLUND, L., SORMUNEN, R., ANISIMOV, A., ZARKADA, G., LOHELA, M., HELOTERA, H., TAMMELA, T., BENJAMIN, L. E., YLA-HERTTUALA, S., LEOW, C. C., KOH, G. Y. & ALITALO, K. 2012. Effects of angiopoietin-2-blocking antibody on endothelial cell-cell junctions and lung metastasis. *J Natl Cancer Inst*, 104, 461-75.
- HORNER, A., BORD, S., KELSALL, A. W., COLEMAN, N. & COMPSTON, J. E. 2001. Tie2 ligands angiopoietin-1 and angiopoietin-2 are coexpressed with vascular endothelial cell growth factor in growing human bone. *Bone*, 28, 65-71.
- HUANG, H., BHAT, A., WOODNUTT, G. & LAPPE, R. 2010. Targeting the ANGPT-TIE2 pathway in malignancy. *Nat Rev Cancer*, 10, 575-85.
- IUVONE, T., DEN BOSSCHE, R. V., D'ACQUISTO, F., CARNUCCIO, R. & HERMAN, A. G. 1999. Evidence that mast cell degranulation, histamine and tumour necrosis factor alpha release occur in LPS-induced plasma leakage in rat skin. *Br J Pharmacol*, 128, 700-4.
- KAIPAINEN, A., VLAYKOVA, T., HATVA, E., BOHLING, T., JEKUNEN, A., PYRHONEN, S. & ALITALO, K. 1994. Enhanced expression of the tie receptor tyrosine kinase messenger RNA in the vascular endothelium of metastatic melanomas. *Cancer Res*, 54, 6571-7.
- KALLI, A. C., WEGENER, K. L., GOULT, B. T., ANTHIS, N. J., CAMPBELL, I. D. & SANSOM, M. S. 2010. The structure of the talin/integrin complex at a lipid bilayer: an NMR and MD simulation study. *Structure*, 18, 1280-8.
- KIM, H. & KOH, G. Y. 2011. Ang2, the instigator of inflammation. *Blood*, 118, 4767-8.
- KIM, I., KIM, H. G., SO, J. N., KIM, J. H., KWAK, H. J. & KOH, G. Y. 2000a. Angiopoietin-1 regulates endothelial cell survival through the phosphatidylinositol 3'-Kinase/Akt signal transduction pathway. *Circ Res*, 86, 24-9.
- KIM, I., MOON, S. O., PARK, S. K., CHAE, S. W. & KOH, G. Y. 2001. Angiopoietin-1 reduces VEGF-stimulated leukocyte adhesion to

- endothelial cells by reducing ICAM-1, VCAM-1, and E-selectin expression. *Circ Res*, 89, 477-9.
- KIM, K. T., CHOI, H. H., STEINMETZ, M. O., MACO, B., KAMMERER, R. A., AHN, S. Y., KIM, H. Z., LEE, G. M. & KOH, G. Y. 2005. Oligomerization and multimerization are critical for angiotensin-1 to bind and phosphorylate Tie2. *J Biol Chem*, 280, 20126-31.
- KIM, S., HARRIS, M. & VARNER, J. A. 2000b. Regulation of integrin alpha vbeta 3-mediated endothelial cell migration and angiogenesis by integrin alpha5beta1 and protein kinase A. *J Biol Chem*, 275, 33920-8.
- KOCKS, C. & RAJEWSKY, K. 1989. Stable expression and somatic hypermutation of antibody V regions in B-cell developmental pathways. *Annu Rev Immunol*, 7, 537-59.
- KOGA, N., TATSUMI-KOGA, R., LIU, G., XIAO, R., ACTON, T. B., MONTELIONE, G. T. & BAKER, D. 2012. Principles for designing ideal protein structures. *Nature*, 491, 222-7.
- KOUTROUBAKIS, I. E., XIDAKIS, C., KARMIRIS, K., SFIRIDAKI, A., KANDIDAKI, E. & KOUROUMALIS, E. A. 2006. Potential role of soluble angiotensin-2 and Tie-2 in patients with inflammatory bowel disease. *Eur J Clin Invest*, 36, 127-32.
- KUMPERS, P., VAN MEURS, M., DAVID, S., MOLEMA, G., BIJZET, J., LUKASZ, A., BIERTZ, F., HALLER, H. & ZIJLSTRA, J. G. 2009. Time course of angiotensin-2 release during experimental human endotoxemia and sepsis. *Crit Care*, 13, R64.
- LEE, H. J., CHO, C. H., HWANG, S. J., CHOI, H. H., KIM, K. T., AHN, S. Y., KIM, J. H., OH, J. L., LEE, G. M. & KOH, G. Y. 2004. Biological characterization of angiotensin-3 and angiotensin-4. *FASEB J*, 18, 1200-8.
- LEE, S. Y., CHOI, J. H. & XU, Z. 2003. Microbial cell-surface display. *Trends Biotechnol*, 21, 45-52.
- LI, Z., WOO, C. J., IGLESIAS-USSEL, M. D., RONAI, D. & SCHARFF, M. D. 2004. The generation of antibody diversity through somatic hypermutation and class switch recombination. *Genes Dev*, 18, 1-11.
- LIND, A. J., WIKSTROM, P., GRANFORS, T., EGEVAD, L., STATIN, P. & BERGH, A. 2005. Angiotensin 2 expression is related to histological

- grade, vascular density, metastases, and outcome in prostate cancer. *Prostate*, 62, 394-9.
- LIP, P. L., CHATTERJEE, S., CAINE, G. J., HOPE-ROSS, M., GIBSON, J., BLANN, A. D. & LIP, G. Y. 2004. Plasma vascular endothelial growth factor, angiopoietin-2, and soluble angiopoietin receptor tie-2 in diabetic retinopathy: effects of laser photocoagulation and angiotensin receptor blockade. *Br J Ophthalmol*, 88, 1543-6.
- LOUGHNA, S. & SATO, T. N. 2001. Angiopoietin and Tie signaling pathways in vascular development. *Matrix Biol*, 20, 319-25.
- MACDONALD, P. R., PROGIAS, P., CIANI, B., PATEL, S., MAYER, U., STEINMETZ, M. O. & KAMMERER, R. A. 2006. Structure of the extracellular domain of Tie receptor tyrosine kinases and localization of the angiopoietin-binding epitope. *J Biol Chem*, 281, 28408-14.
- MAISONPIERRE, P. C., GOLDFARB, M., YANCOPOULOS, G. D. & GAO, G. 1993. Distinct rat genes with related profiles of expression define a TIE receptor tyrosine kinase family. *Oncogene*, 8, 1631-7.
- MAISONPIERRE, P. C., SURI, C., JONES, P. F., BARTUNKOVA, S., WIEGAND, S. J., RADZIEJEWSKI, C., COMPTON, D., MCCLAIN, J., ALDRICH, T. H., PAPADOPOULOS, N., DALY, T. J., DAVIS, S., SATO, T. N. & YANCOPOULOS, G. D. 1997. Angiopoietin-2, a natural antagonist for Tie2 that disrupts in vivo angiogenesis. *Science*, 277, 55-60.
- MAKINDE, T. & AGRAWAL, D. K. 2008. Intra and extravascular transmembrane signalling of angiopoietin-1-Tie2 receptor in health and disease. *J Cell Mol Med*, 12, 810-28.
- MARKIEWSKI, M. M. & LAMBRIS, J. D. 2007. The role of complement in inflammatory diseases from behind the scenes into the spotlight. *Am J Pathol*, 171, 715-27.
- MARRON, M. B., HUGHES, D. P., EDGE, M. D., FORDER, C. L. & BRINDLE, N. P. 2000. Evidence for heterotypic interaction between the receptor tyrosine kinases TIE-1 and TIE-2. *J Biol Chem*, 275, 39741-6.
- MARRON, M. B., SINGH, H., TAHIR, T. A., KAVUMKAL, J., KIM, H. Z., KOH, G. Y. & BRINDLE, N. P. 2007. Regulated proteolytic processing of Tie1 modulates ligand responsiveness of the receptor-tyrosine kinase Tie2. *J Biol Chem*, 282, 30509-17.

- MASTER, Z., JONES, N., TRAN, J., JONES, J., KERBEL, R. S. & DUMONT, D. J. 2001. Dok-R plays a pivotal role in angiopoietin-1-dependent cell migration through recruitment and activation of Pak. *EMBO J*, 20, 5919-28.
- MAZZIERI, R., PUCCI, F., MOI, D., ZONARI, E., RANGHETTI, A., BERTI, A., POLITI, L. S., GENTNER, B., BROWN, J. L., NALDINI, L. & DE PALMA, M. 2011. Targeting the ANG2/TIE2 axis inhibits tumor growth and metastasis by impairing angiogenesis and disabling rebounds of proangiogenic myeloid cells. *Cancer Cell*, 19, 512-26.
- MCKEAN, D., HUPPI, K., BELL, M., STAUDT, L., GERHARD, W. & WEIGERT, M. 1984. Generation of antibody diversity in the immune response of BALB/c mice to influenza virus hemagglutinin. *Proc Natl Acad Sci U S A*, 81, 3180-4.
- MOFARRAHI, M., NOUH, T., QURESHI, S., GUILLOT, L., MAYAKI, D. & HUSSAIN, S. N. 2008. Regulation of angiopoietin expression by bacterial lipopolysaccharide. *Am J Physiol Lung Cell Mol Physiol*, 294, L955-63.
- MULLIS, K. B. & FALOONA, F. A. 1987. Specific synthesis of DNA in vitro via a polymerase-catalyzed chain reaction. *Methods Enzymol*, 155, 335-50.
- MURAMATSU, M., SANKARANAND, V. S., ANANT, S., SUGAI, M., KINOSHITA, K., DAVIDSON, N. O. & HONJO, T. 1999. Specific expression of activation-induced cytidine deaminase (AID), a novel member of the RNA-editing deaminase family in germinal center B cells. *J Biol Chem*, 274, 18470-6.
- NADAR, S. K., KARALIS, I., AL YEMENI, E., BLANN, A. D. & LIP, G. Y. 2005. Plasma markers of angiogenesis in pregnancy induced hypertension. *Thromb Haemost*, 94, 1071-6.
- ODEGARD, V. H. & SCHATZ, D. G. 2006. Targeting of somatic hypermutation. *Nat Rev Immunol*, 6, 573-83.
- ORFANOS, S. E., KOTANIDOU, A., GLYNOS, C., ATHANASIOU, C., TSIGKOS, S., DIMOPOULOU, I., SOTIROPOULOU, C., ZAKYNTHINOS, S., ARMAGANIDIS, A., PAPAPETROPOULOS, A. & ROUSSOS, C. 2007. Angiopoietin-2 is increased in severe sepsis: correlation with inflammatory mediators. *Crit Care Med*, 35, 199-206.

- PALOMARES, L. A., ESTRADA-MONDACA, S. & RAMIREZ, O. T. 2004. Production of recombinant proteins: challenges and solutions. *Methods Mol Biol*, 267, 15-52.
- PAPAPETROPOULOS, A., FULTON, D., MAHBOUBI, K., KALB, R. G., O'CONNOR, D. S., LI, F., ALTIERI, D. C. & SESSA, W. C. 2000. Angiopoietin-1 inhibits endothelial cell apoptosis via the Akt/survivin pathway. *J Biol Chem*, 275, 9102-5.
- PARADISE, R. K., LAUFFENBURGER, D. A. & VAN VLIET, K. J. 2011. Acidic extracellular pH promotes activation of integrin alpha(v)beta(3). *PLoS One*, 6, e15746.
- PARTANEN, J., ARMSTRONG, E., MAKELA, T. P., KORHONEN, J., SANDBERG, M., RENKONEN, R., KNUUTILA, S., HUEBNER, K. & ALITALO, K. 1992. A novel endothelial cell surface receptor tyrosine kinase with extracellular epidermal growth factor homology domains. *Mol Cell Biol*, 12, 1698-707.
- PELED, J. U., KUANG, F. L., IGLESIAS-USSEL, M. D., ROA, S., KALIS, S. L., GOODMAN, M. F. & SCHARFF, M. D. 2008. The biochemistry of somatic hypermutation. *Annu Rev Immunol*, 26, 481-511.
- PETERS, K. G., KONTOS, C. D., LIN, P. C., WONG, A. L., RAO, P., HUANG, L., DEWHIRST, M. W. & SANKAR, S. 2004. Functional significance of Tie2 signaling in the adult vasculature. *Recent Prog Horm Res*, 59, 51-71.
- PRAKASH, A. & HELLMAN, J. 2010. Editorial: Pattern recognition receptors and factor B: "complement"ary pathways converge. *J Leukoc Biol*, 88, 605-7.
- PURI, M. C. & BERNSTEIN, A. 2003. Requirement for the TIE family of receptor tyrosine kinases in adult but not fetal hematopoiesis. *Proc Natl Acad Sci U S A*, 100, 12753-8.
- PURI, M. C., ROSSANT, J., ALITALO, K., BERNSTEIN, A. & PARTANEN, J. 1995. The receptor tyrosine kinase TIE is required for integrity and survival of vascular endothelial cells. *Embo j*, 14, 5884-91.
- QIAO, H., ANDRADE, M. V., LISBOA, F. A., MORGAN, K. & BEAVEN, M. A. 2006. FcepsilonR1 and toll-like receptors mediate synergistic signals to markedly augment production of inflammatory cytokines in murine mast cells. *Blood*, 107, 610-8.

- RAJEWSKY, K., FORSTER, I. & CUMANO, A. 1987. Evolutionary and somatic selection of the antibody repertoire in the mouse. *Science*, 238, 1088-94.
- RASUL, S., REITER, M. H., ILHAN, A., LAMPICHLER, K., WAGNER, L. & KAUTZKY-WILLER, A. 2011. Circulating angiopoietin-2 and soluble Tie-2 in type 2 diabetes mellitus: a cross-sectional study. *Cardiovasc Diabetol*, 10, 55.
- REYNOLDS, L. E., CONTI, F. J., LUCAS, M., GROSE, R., ROBINSON, S., STONE, M., SAUNDERS, G., DICKSON, C., HYNES, R. O., LACY-HULBERT, A. & HODIVALA-DILKE, K. 2005. Accelerated re-epithelialization in beta3-integrin-deficient mice is associated with enhanced TGF-beta1 signaling. *Nat Med*, 11, 167-74.
- SALE, J. E., CALANDRINI, D. M., TAKATA, M., TAKEDA, S. & NEUBERGER, M. S. 2001. Ablation of XRCC2/3 transforms immunoglobulin V gene conversion into somatic hypermutation. *Nature*, 412, 921-6.
- SALE, J. E. & NEUBERGER, M. S. 1998. TdT-accessible breaks are scattered over the immunoglobulin V domain in a constitutively hypermutating B cell line. *Immunity*, 9, 859-69.
- SATO, T. N., QIN, Y., KOZAK, C. A. & AUDUS, K. L. 1993. Tie-1 and tie-2 define another class of putative receptor tyrosine kinase genes expressed in early embryonic vascular system. *Proc Natl Acad Sci U S A*, 90, 9355-8.
- SCHNURCH, H. & RISAU, W. 1993. Expression of tie-2, a member of a novel family of receptor tyrosine kinases, in the endothelial cell lineage. *Development*, 119, 957-68.
- SCHOLZ, A., LANG, V., HENSCHLER, R., CZABANKA, M., VAJKOCZY, P., CHAVAKIS, E., DRYNSKI, J., HARTER, P. N., MITTELBRONN, M., DUMONT, D. J., PLATE, K. H. & REISS, Y. 2011. Angiopoietin-2 promotes myeloid cell infiltration in a beta(2)-integrin-dependent manner. *Blood*, 118, 5050-9.
- SCHOLZ, A., REHM, V. A., RIEKE, S., DERKOW, K., SCHULZ, P., NEUMANN, K., KOCH, I., PASCU, M., WIEDENMANN, B., BERG, T. & SCHOTT, E. 2007. Angiopoietin-2 serum levels are elevated in patients with liver cirrhosis and hepatocellular carcinoma. *Am J Gastroenterol*, 102, 2471-81.

- SCHRADER, C. E., BRADLEY, S. P., VARDO, J., MOCHEGOVA, S. N., FLANAGAN, E. & STAVNEZER, J. 2003. Mutations occur in the Ig Smu region but rarely in Sgamma regions prior to class switch recombination. *Embo j*, 22, 5893-903.
- SEEGAR, T. C., ELLER, B., TZVETKOVA-ROBEV, D., KOLEV, M. V., HENDERSON, S. C., NIKOLOV, D. B. & BARTON, W. A. 2010. Tie1-Tie2 interactions mediate functional differences between angiopoietin ligands. *Mol Cell*, 37, 643-55.
- SHARMA, R., SIRCAR, K., SINGH, S. & RASTOGI, V. 2011. Role of mast cells in pathogenesis of oral lichen planus. *J Oral Maxillofac Pathol*, 15, 267-71.
- STEMMER, W. P. 1994. DNA shuffling by random fragmentation and reassembly: in vitro recombination for molecular evolution. *Proc Natl Acad Sci U S A*, 91, 10747-51.
- STONE, K. D., PRUSSIN, C. & METCALFE, D. D. 2010. IgE, mast cells, basophils, and eosinophils. *J Allergy Clin Immunol*, 125, S73-80.
- TANAKA, S., MORI, M., SAKAMOTO, Y., MAKUUCHI, M., SUGIMACHI, K. & WANDS, J. R. 1999. Biologic significance of angiopoietin-2 expression in human hepatocellular carcinoma. *J Clin Invest*, 103, 341-5.
- THEOHARIDES, T. C. 2014. Mast cells in irritable bowel syndrome and ulcerative colitis: function not numbers is what makes all the difference. *Dig Dis Sci*, 59, 897-8.
- THOMAS, M. & AUGUSTIN, H. G. 2009. The role of the Angiopoietins in vascular morphogenesis. *Angiogenesis*, 12, 125-37.
- THOMAS, M., FELCHT, M., KRUSE, K., KRETSCHMER, S., DEPPERMAN, C., BIESDORF, A., ROHR, K., BENEST, A. V., FIEDLER, U. & AUGUSTIN, H. G. 2010. Angiopoietin-2 stimulation of endothelial cells induces alphavbeta3 integrin internalization and degradation. *J Biol Chem*, 285, 23842-9.
- TIWARI, M. K., SINGH, R., SINGH, R. K., KIM, I. W. & LEE, J. K. 2012. Computational approaches for rational design of proteins with novel functionalities. *Comput Struct Biotechnol J*, 2, e201209002.
- TSIGKOS, S., ZHOU, Z., KOTANIDOU, A., FULTON, D., ZAKYNTHINOS, S., ROUSSOS, C. & PAPAPETROPOULOS, A. 2006. Regulation of Ang2

- release by PTEN/PI3-kinase/Akt in lung microvascular endothelial cells. *J Cell Physiol*, 207, 506-11.
- VALENZUELA, D. M., GRIFFITHS, J. A., ROJAS, J., ALDRICH, T. H., JONES, P. F., ZHOU, H., MCCLAIN, J., COPELAND, N. G., GILBERT, D. J., JENKINS, N. A., HUANG, T., PAPADOPOULOS, N., MAISONPIERRE, P. C., DAVIS, S. & YANCOPOULOS, G. D. 1999. Angiopoietins 3 and 4: diverging gene counterparts in mice and humans. *Proc Natl Acad Sci U S A*, 96, 1904-9.
- WANG, C. L., HARPER, R. A. & WABL, M. 2004a. Genome-wide somatic hypermutation. *Proc Natl Acad Sci U S A*, 101, 7352-6.
- WANG, L., JACKSON, W. C., STEINBACH, P. A. & TSIEN, R. Y. 2004b. Evolution of new nonantibody proteins via iterative somatic hypermutation. *Proc Natl Acad Sci U S A*, 101, 16745-9.
- WEBER, C. C., CAI, H., EHRBAR, M., KUBOTA, H., MARTINY-BARON, G., WEBER, W., DJONOV, V., WEBER, E., MALLIK, A. S., FUSSENEGGER, M., FREI, K., HUBBELL, J. A. & ZISCH, A. H. 2005. Effects of protein and gene transfer of the angiopoietin-1 fibrinogen-like receptor-binding domain on endothelial and vessel organization. *J Biol Chem*, 280, 22445-53.
- WEBER, G. F., BJERKE, M. A. & DESIMONE, D. W. 2011. Integrins and cadherins join forces to form adhesive networks. *J Cell Sci*, 124, 1183-93.
- WEIS, S. M. & CHERESH, D. A. 2011a.  $\alpha_V$  integrins in angiogenesis and cancer. *Cold Spring Harb Perspect Med*, 1, a006478.
- WEIS, S. M. & CHERESH, D. A. 2011b. Tumor angiogenesis: molecular pathways and therapeutic targets. *Nat Med*, 17, 1359-70.
- WOO, C. J., MARTIN, A. & SCHARFF, M. D. 2003. Induction of somatic hypermutation is associated with modifications in immunoglobulin variable region chromatin. *Immunity*, 19, 479-89.
- WOO, K. V. & BALDWIN, H. S. 2011. Role of Tie1 in shear stress and atherosclerosis. *Trends Cardiovasc Med*, 21, 118-23.
- WOOLF, A. S., GNUDI, L. & LONG, D. A. 2009. Roles of angiopoietins in kidney development and disease. *J Am Soc Nephrol*, 20, 239-44.
- YAO, J. H., CUI, M., LI, M. T., LIU, Y. N., HE, Q. H., XIAO, J. J. & BAI, Y. 2014. Angiopoietin1 inhibits mast cell activation and protects against anaphylaxis. *PLoS One*, 9, e89148.

- YU, X., SEEGAR, T. C., DALTON, A. C., TZVETKOVA-ROBEV, D., GOLDGUR, Y., RAJASHANKAR, K. R., NIKOLOV, D. B. & BARTON, W. A. 2013. Structural basis for angiotensin-1-mediated signaling initiation. *Proc Natl Acad Sci U S A*, 110, 7205-10.
- YUAN, H. T., KHANKIN, E. V., KARUMANCHI, S. A. & PARIKH, S. M. 2009. Angiotensin 2 is a partial agonist/antagonist of Tie2 signaling in the endothelium. *Mol Cell Biol*, 29, 2011-22.
- YUAN, H. T., TIPPING, P. G., LI, X. Z., LONG, D. A. & WOOLF, A. S. 2002. Angiotensin correlates with glomerular capillary loss in anti-glomerular basement membrane glomerulonephritis. *Kidney Int*, 61, 2078-89.
- YUAN, H. T., VENKATESHA, S., CHAN, B., DEUTSCH, U., MAMMOTO, T., SUKHATME, V. P., WOOLF, A. S. & KARUMANCHI, S. A. 2007. Activation of the orphan endothelial receptor Tie1 modifies Tie2-mediated intracellular signaling and cell survival. *Faseb j*, 21, 3171-83.
- YUAN, L., KUREK, I., ENGLISH, J. & KEENAN, R. 2005. Laboratory-directed protein evolution. *Microbiol Mol Biol Rev*, 69, 373-92.
- ZHANG, W., BARDWELL, P. D., WOO, C. J., POLTORATSKY, V., SCHARFF, M. D. & MARTIN, A. 2001. Clonal instability of V region hypermutation in the Ramos Burkitt's lymphoma cell line. *Int Immunol*, 13, 1175-84.
- ZHAO, J. & GUAN, J. L. 2009. Signal transduction by focal adhesion kinase in cancer. *Cancer Metastasis Rev*, 28, 35-49.
- ZHAO, X. & GUAN, J. L. 2011. Focal adhesion kinase and its signaling pathways in cell migration and angiogenesis. *Adv Drug Deliv Rev*, 63, 610-5.
- ZIEGLER, T., HORSTKOTTE, J., SCHWAB, C., PFETSCH, V., WEINMANN, K., DIETZEL, S., ROHWEDDER, I., HINKEL, R., GROSS, L., LEE, S., HU, J., SOEHNLEIN, O., FRANZ, W. M., SPERANDIO, M., POHL, U., THOMAS, M., WEBER, C., AUGUSTIN, H. G., FASSLER, R., DEUTSCH, U. & KUPATT, C. 2013. Angiotensin 2 mediates microvascular and hemodynamic alterations in sepsis. *J Clin Invest*.
- ZWAAGSTRA, J. C., SULEA, T., BAARDSNES, J., LENFERINK, A. E., COLLINS, C., CANTIN, C., PAUL-ROC, B., GROTHE, S., HOSSAIN, S., RICHER, L. P., L'ABBE, D., TOM, R., CASS, B., DUROCHER, Y. & O'CONNOR-MCCOURT, M. D. 2012. Engineering and therapeutic

application of single-chain bivalent TGF-beta family traps. *Mol Cancer Ther*, 11, 1477-87.